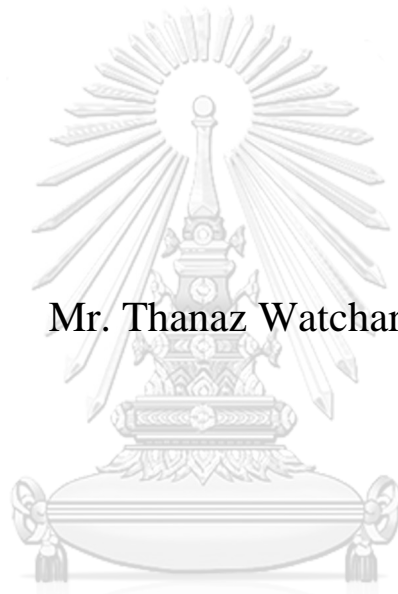


**PETROCHEMISTRY OF INTRUSIVE ROCKS IN THA  
TAKIAP DISTRICT, CHACHOENGSAO PROVINCE**



**Mr. Thanaz Watcharamai**

จุฬาลงกรณ์มหาวิทยาลัย  
**CHULALONGKORN UNIVERSITY**

**A Thesis Submitted in Partial Fulfillment of the Requirements  
for the Degree of Master of Science in Geology  
Department of Geology  
FACULTY OF SCIENCE  
Chulalongkorn University  
Academic Year 2020  
Copyright of Chulalongkorn University**

ศิลาเคมีของหินอัคนีแทรกซอนในบริเวณอำเภอท่าตะเียบ จังหวัดฉะเชิงเทรา



วิทยานิพนธ์นี้เป็นส่วนหนึ่งของการศึกษาตามหลักสูตรปริญญาวิทยาศาสตรมหาบัณฑิต

สาขาวิชาธรณีวิทยา ภาควิชาธรณีวิทยา

คณะวิทยาศาสตร์ จุฬาลงกรณ์มหาวิทยาลัย

ปีการศึกษา 2563

ลิขสิทธิ์ของจุฬาลงกรณ์มหาวิทยาลัย



รณัช วัชรมัย : ศิลาเคมีของหินอัคนีแทรกซอนในบริเวณอำเภอท่าตะเกียบ จังหวัดฉะเชิงเทรา. ( **PETROCHEMISTRY OF INTRUSIVE ROCKS IN THA TAKIAP DISTRICT, CHACHOENGSARO PROVINCE**) อ.ที่ปรึกษาหลัก : ดร.อภิสิทธิ์ ชาล่ำ

หินแกรนิตชนิดอัลคาไลน์มีการกระจายตัวไม่มากนักในประเทศไทย โดยจะพบในลักษณะเป็นพืดตอนขนาดเล็ก พื้นที่ศึกษาได้แก่ พื้นที่ท่าตะเกียบ และพื้นที่แม่ย่าน จัดอยู่ในแนวหินแกรนิตตะวันออกและแนวหินแกรนิตตอนกลางตามลำดับ ผลการศึกษาวิเคราะห์จากตัวอย่างหินของทั้งสองพื้นที่พบว่าประกอบด้วยแร่แอลคาไลเฟลด์สปาร์เป็นหลัก มีแร่ควอตซ์และเฟลกจิโอเคลสเล็กน้อย จึงสามารถจำแนกหินของทั้งสองพื้นที่ดังกล่าวได้เป็นหินแอลคาไลเฟลด์สปาร์ไซอีนิต (alkali-feldspar syenite) ถึงหินแอลคาไลเฟลด์สปาร์ควอตซ์ไซอีนิต (alkali-feldspar quartz syenite) ผลการศึกษารวมเคมีด้วยปริมาณผลรวมของโซเดียมออกไซด์กับโพแทสเซียมออกไซด์ ( $\text{Na}_2\text{O}+\text{K}_2\text{O}$ ) และอัตราส่วนของเหล็กออกไซด์ต่อผลรวมของเหล็กออกไซด์กับแมกนีเซียมออกไซด์ ( $\text{FeO}^{\text{tot}}/\text{FeO}^{\text{tot}}+\text{MgO}$ ) บ่งชี้ว่าหินดังกล่าวสามารถจำแนกได้เป็นหินไซอีนิต และหินแกรนิตชนิดเฟอร์โรน (ferroan granite) ตามลำดับ นอกจากนี้อัตราส่วนที่สูงของธาตุแกลเลียมต่อธาตุอะลูมิเนียม ( $\text{Ga}/\text{Al}$ ) และธาตุดีเทรียมต่อธาตุไนโอเบียม ( $\text{Y}/\text{Nb}$ ) ยังบ่งชี้ว่าหินจากทั้งสองพื้นที่เป็นหินแกรนิตชนิด A-type และสามารถแบ่งย่อยได้เป็นชนิดย่อย A<sub>2</sub> ซึ่งหินดังกล่าวมีความสัมพันธ์กับแมกมาชนิดอัลคาไลน์ และมีความสัมพันธ์กับลักษณะธรณีแปรสัณฐานแบบขยาย (extensional tectonic) จากลักษณะของกราฟสัดส่วนธาตุหายากต่อคอนไดรต์ (chondrite-normalized REE pattern) ที่ค่อนข้างราบ และมีค่าผิดปกติเชิงบวกที่ตำแหน่งของธาตุแทนทาลัม (Ta) ในกราฟสัดส่วนธาตุร่องรอยต่อเนื้อโลกแบบดั้งเดิม (primitive mantle normalized spider diagrams) บ่งชี้ว่าต้นกำเนิดแมกมาของหินไซอีนิตในพื้นที่ท่าตะเกียบได้รับอิทธิพลจากวัสดุที่กำเนิดจากเนื้อโลกเป็นหลัก และอนุมานได้ว่ามีการเกิดสัมพันธ์กับลักษณะธรณีแปรสัณฐานแบบขยายด้านหลังแนวภูเขาไฟ (back-arc) ซึ่งเทียบเคียงได้กับชุดหินแกรนิตเซี่ยวหลงเหอ (Xiaolonghe granite) ทางตะวันตกเฉียงใต้ของประเทศจีน ขณะที่หินไซอีนิตจากพื้นที่แม่ย่านแสดงลักษณะความสมบูรณ์ของธาตุหายากเบาในกราฟสัดส่วนธาตุหายากต่อคอนไดรต์ และแสดงค่าผิดปกติเชิงบวกที่ตำแหน่งของธาตุทอเรียม (Th) ยูเรเนียม (U) และตะกั่ว (Pb) และค่าผิดปกติเชิงลบของธาตุไนโอเบียม (Nb) และธาตุแทนทาลัม (Ta) ในกราฟสัดส่วนธาตุร่องรอยต่อเนื้อโลกแบบดั้งเดิมที่ เทียบเคียงได้กับชุดหินโพแทสเซียมสูง (potassic rock) บริเวณแอ่งขงบา (Xungba basin) ทางตอนใต้ของทิเบต ที่เกิดขึ้นภายหลังจากการชนกันของแผ่นเปลือกโลกทวีป ซึ่งบ่งบอกว่าหินไซอีนิตในพื้นที่แม่ย่านเกิดขึ้นหลังการชนกันของแผ่นเปลือกโลกทวีป และก่อกำเนิดจากการหลอมละลายบางส่วน (partial melting) ของแผ่นเปลือกโลกที่เกิดสัมพันธ์กับธรณีแปรสัณฐานแบบมุดตัว

จุฬาลงกรณ์มหาวิทยาลัย  
CHULALONGKORN UNIVERSITY

สาขาวิชา ธรณีวิทยา  
ปีการศึกษา 2563

ลายมือชื่อนิสิต .....  
ลายมือชื่อ อ.ที่ปรึกษาหลัก .....

## 6171964423 : MAJOR GEOLOGY

KEYWORD: Alkaline granite, A-type granite, Tha Takiap, Mae Yan

Thanaz Watcharamai : PETROCHEMISTRY OF INTRUSIVE ROCKS IN THE TAKIAP DISTRICT, CHACHOENGSAO PROVINCE. Advisor: ABHISIT SALAM, Ph.D.

In Thailand, alkaline granitoid rocks are less widespread and crop out in less extend as small stocks or plutons. The study areas are located in 2 vicinities of Tha Takiap and Mae Yan areas which respectively are a part of the eastern and central granite belts. Petrographic study of the rocks from both areas show that alkaline feldspar is the principal mineral phase with small amount of quartz and plagioclase. Compositionally, the investigated rocks fall in the range of alkali feldspar syenite to quartz-alkali feldspar syenite. High concentration of  $\text{Na}_2\text{O}+\text{K}_2\text{O}$  and high ratio of  $\text{FeO}^{\text{tot}}/(\text{FeO}^{\text{tot}}+\text{MgO})$  vs  $\text{SiO}_2$  indicate that most of the rocks from both areas are syenite and ferroan granite respectively. High ratio of Ga/Al and Y/Nb suggest that the rocks from both areas belong to  $A_2$  subtype of A-type granite category. These rocks originated from alkaline magmatism related to extensional tectonic setting. Flat chondrite-normalized REE pattern and positive anomaly of Ta on primitive mantle-normalized spider diagrams are resemble to those of Xiaolonghe granite, southwestern China. These similarities imply that the genesis of Tha Takiap syenitic rocks is related to back-arc extension tectonic setting and the magmatic source is mainly influenced by mantle-derived material. On the other hand, the enrichment of LREE on the chondrite-normalized REE patterns of Mae Yan syenitic rocks and positive anomalies of Th, U, and Pb as well as negative anomalies of Nb and Ta on the primitive mantle-normalized diagrams indicate that the dominant source of partial melting could be derived from continental crust related to subduction tectonic comparable to, post-collisional potassic rock in Xungba basin, southern Tibet.



Field of Study: Geology  
Academic Year: 2020

Student's Signature .....  
Advisor's Signature .....

## ACKNOWLEDGEMENTS

I would like to thank my supervisor, Dr. Abhisit Salam for his valuable supervision, encouragement, and critical reading on my thesis and manuscript. I would also like to thank my senior colleague, Dr. Tawatchai Chualaowanich who is one of the best teacher in my life, for his encouragement, and stimulated discussions.

I would also like to sincerely thank the Department of Mineral Resources for full financial support throughout my master's degree program at Chulalongkorn University, giving access to the drill core samples. I would also like to thank Mineral Resources Analysis and Identification Division for geochemical analysis knowledge and fully support for XRF analysis.

My appreciation is also extended to several people who has been assisted me during this study, in particular Dr. Takayuki Manaka for his suggestion and the manuscript revision; Dr. Punya Charusiri for his useful comments; as well as my classmates at Department of Geology, Chulalongkorn University, namely Miss Amporn Chaikham, Miss Maythira Sriwichai, Mr. Tanad Soisa and Mr. Sirawit Kaewpaluk for their supportive and encouragement. Many thanks also go to the staff at the Department of Geology, Chulalongkorn University, including Ms. Sopit Poompuang, Mr.Prajin Thongprachum, Mr. Suriya Chokmo, Ms. Jiraprapa Niampan and Ms. Bunjong Puangthong for their kind help on laboratory work.

Finally, I would like to express special thanks to my family, who provided moral support for my studies.

Thanaz Watcharamai

# TABLE OF CONTENTS

	<b>Page</b>
ABSTRACT (THAI) .....	iii
ABSTRACT (ENGLISH).....	iv
ACKNOWLEDGEMENTS .....	v
TABLE OF CONTENTS.....	vi
LIST OF TABLES .....	viii
LIST OF FIGURES .....	ix
CHAPTER 1 INTRODUCTION .....	1
1.1 Background.....	1
1.2 Location and Access .....	2
1.3 Purpose of study .....	3
1.4 Methodology.....	3
1.5 Thesis structure .....	6
CHAPTER 2 GEOLOGICAL SETTING.....	7
2.1 Regional Tectonic Setting.....	7
2.2 Granitic rock of Thailand.....	8
2.3 Regional Geology .....	12
CHAPTER 3 GEOLOGY AND PETROGRAPHY .....	16
3.1 Tha Takiap area .....	16
3.2 Mae Yan Area.....	21
3.3 Modal analysis .....	28
CHAPTER 4 GEOCHEMISTRY .....	33
4.1 Sampling and analytical methods .....	33
4.2 Major and minor element geochemistry .....	34
4.3 Trace element and REE geochemistry.....	40
4.4 Interpretation of whole-rock geochemistry .....	42

4.5 Mineral chemistry .....	44
CHAPTER 5 DISCUSSION AND CONCLUSION .....	56
5.1 Petrogenesis .....	56
5.2 Tectonic Implication .....	59
5.3 REE Potential.....	60
5.4 Conclusion .....	61
5.5 Recommendations for future works.....	63
REFERENCES .....	64
VITA.....	70





## LIST OF TABLES

	<b>Page</b>
Table 3.1 List of outcrops description of Tha Takiap area.....	18
Table 3.2 List of diamond-drilled cores samples from Tha Takiap area used for petrographic study, modal analysis, and geochemistry analysis. ....	21
Table 3.3 List of rock sample from Mae Yan Area that were collected for petrographic study, modal analysis, and geochemistry analysis.....	24
Table 3.4 Summary of petrography (modal analysis, texture and mineral).....	31
Table 4.1 Operating conditions for a PANalytical (Zetium) WDXRF spectrometer.....	34
Table 4.2 Whole-rock major and trace elements data of syenitic rock in Tha Takiap area. ....	35
Table 4.3 Whole-rock major and trace elements data of syenitic rock in Mae Yan area. ....	36
Table 4.4 Mineral chemistry of amphibole (hornblende) in syenitic rocks from the Tha Takiap area. ....	45
Table 4.5 Mineral chemistry of amphibole (hornblende) in syenitic rocks from the Mae Yan area.....	46
Table 4.6 Mineral chemistry of feldspar in syenitic rocks from the Tha Takiap area....	48
Table 4.7 Mineral chemistry of feldspar in syenitic rocks from the Mae Yan area.....	50
Table 4.8 Mineral chemistry of feldspar pairs in perthite of syenitic rocks from the Tha Takiap area. ....	52
Table 4.9 Mineral chemistry of feldspar pairs in perthite of syenitic rocks from the Mae Yan area.....	53

## LIST OF FIGURES

	<b>Page</b>
Fig. 1.1 Satellite image of Tha Takiap area (modified from Google satellite, 2020).....	3
Fig. 1.2 Satellite image of Mae Yan area (modified from Google satellite, 2020). .....	4
Fig. 1.3 Diagram of research methodology. ....	5
Fig. 2.1 Simplify granite belts of Thailand and neighboring Southeast Asia countries (Study area are showed in red square; granitic belt boundary are showed in red dashed line; and Nan-Uttaradit-Sa Kaeo suture are showed in blue line) (modified from Cobbing et al. (1992); Metcalfe (2011); Sone and Metcalfe (2008); Khin Zaw et al. (2014)).....	10
Fig. 2.2 Geological map of Tha Takiap area (modified from Department of Mineral Resources (2003); Tiya Piract (1996)). .....	13
Fig. 2.3 Geological map of Tha Takiap area (modified from Chauviroj and Chaturongkawanich (1985)). .....	15
Fig. 3.1 Field investigation of Tha Takiap area. a) Undulating plain landform with small hill at Ban Sam Ta Han. b) Photograph of plutonic rock from study point CS14. c) Photograph of low grade metamorphic rock from study point CS2. d) Photograph of Triassic granites nearby Tha Takiap area from study point CS11. e) Photograph of diamond-drilled core of mediun- to coarse-grained syenite (D12 at depth 23.6-23.8 m). f) Photograph of diamond-drilled core of volcanic rock (D11 at depth 44.8-45.0 m).....	17
Fig. 3.2 Simplified graphic log of diamond-drilled hole No. D11.....	19
Fig. 3.3 Simplified graphic log of diamond-drilled hole No. D12.....	20
Fig. 3.4 Petrographic characteristics of syenitic rocks from Tha Takiap area. a) Photomicrograph of syenite showing equigranular texture with K-feldspar showing perthitic texture and grid twin, hornblende, quartz and plagioclase. b) Photomicrograph of syenite, showing K-feldspar with perthitic texture and grid twin, quartz, plagioclase, and veinlet of chlorite. c) Photomicrograph of syenite, showing hornblende which is partly replaced by chlorite and K-feldspar. d) Photomicrograph of syenite, showing inclusion of apatite in hornblende which is replaced by chlorite, and K-feldspar which shows grid twin. Mineral abbreviations: Kfs (K-feldspar); Hbl (hornblende); Qtz (quartz); Pl (plagioclase);	

Px (pyroxene); Chl (chlorite); Ap (apatite). (left: plane polarized light, right: cross polarized light)..... 22

Fig. 3.5 Photograph of hand specimen sample of Mae Yan area. a) Photograph of fine- to medium-grained plutonic rock at Doi Kio Lom mountain (sample No. MH36-1). b) Photograph of medium- to coarse-grained plutonic rock of Doi Mae Yan (sample No. MH5-3). c) Photograph of fine- to medium-grained plutonic rock of Doi Mae Yan (sample No. MHPP5-1). d) Photograph of Triassic medium-grained porphyritic biotite granite in adjacent area of Mae Yan area. .... 23

Fig. 3.6 Petrographic characteristics of medium- to coarse-grained syenitic rocks from Mae Yan area. a) Photomicrograph of medium- to coarse-grained syenitic rock showing inequigranular with K-feldspar which shows perthitic texture. b) Photomicrograph of syenitic rock, showing K-feldspar which shows perthitic texture, hornblende, quartz, clinopyroxene, and apatite. c) Photomicrograph of medium- to coarse-grained syenitic rock, showing K-feldspar which shows perthitic texture, hornblende, quartz, sphene, and plagioclase. d) Photomicrograph of medium- to coarse-grained syenitic rock, showing zircon, sphene, K-feldspar which shows grid twin, and quartz. Mineral abbreviations: Kfs (K-feldspar); Hbl (hornblende); Qtz (quartz); Cpx (Clinopyroxene); Pl (plagioclase); Chl (chlorite); Ap (apatite); Sph (sphene); Zr (Zircon). (left: plane polarized light, right: cross polarized light). .... 25

Fig. 3.7 Petrographic characteristics of fine- to medium-grained syenitic rock from Mae Yan area. a) Photomicrograph of fine- to medium-grained syenitic rock with porphyritic texture, showing K-feldspar phenocrysts in perthitic texture and Carlsbad twin with finer-grained K-feldspar rich groundmass. b) Photomicrograph of fine- to medium-grained syenitic rock with equigranular texture, showing plagioclase with poikilitic texture, amphibole, K-feldspar, and quartz with monazite inclusion in plagioclase. c) Photomicrograph of fine- to medium-grained syenitic rock, showing amphibole with blue to greenish blue pleochroism that indicate riebeckite (Na-amphibole), K-feldspar, quartz, sphene, and apatite. d) Photomicrograph of fine- to medium-grained syenitic rock, showing monazite, amphibole and sphene assemblage. Mineral abbreviations: Kfs (K-feldspar); Hbl (hornblende); Qtz (quartz); Pl (plagioclase); Mz (monazite); Sph (sphene); Ap (apatite). (left: plane polarized light, right: cross polarized light). .... 27

Fig. 3.8 Photograph of unstained and stained hand specimen sample. a) Photograph medium-grained syenitic rock of Tha Takiap area. b) Photograph of medium- to coarse-grained syenitic rock of Mae Yan area. c) Photograph of fine- to medium-

- grained syenitic rock of Mae Yan area. (left: unstained sample, right: stained sample). .....29
- Fig. 3.9 Image of stained surface which were analyzed using Image Pro software. a) Photograph medium-grained syenitic rock of Tha Takiap area. b) Photograph of medium- to coarse-grained syenitic rock of Mae Yan area. c) Photograph of fine- to medium-grained syenitic rock of Mae Yan area. (left: unclassified by Image Pro software, right: classed by Image Pro software). ..... 30
- Fig. 3.10 Modal QAPF diagram (Streckeisen, 1976) of the syenitic rocks in the Tha Takiap and Mae Yan areas (Q=quartz; A=K-feldspar; P=plagioclase). (Red square is syenitic rocks from Tha Takiap area, green circle is medium- to coarse-grained syenitic rocks from Mae Yan area, blue circle is fine- to medium-grained syenitic rocks from Mae Yan area). ..... 32
- Fig. 4.1 Major and minor element bivariate diagrams plot against SiO<sub>2</sub> for syenitic rocks from the Tha Takiap and the Mae Yan areas; (a) SiO<sub>2</sub> versus TiO<sub>2</sub> (wt%); (b) SiO<sub>2</sub> versus Al<sub>2</sub>O<sub>3</sub> (wt%); (c) SiO<sub>2</sub> versus Fe<sub>2</sub>O<sub>3</sub><sup>(total)</sup> (wt%); (d) SiO<sub>2</sub> versus MgO (wt%); (e) SiO<sub>2</sub> versus CaO (wt%); (f) SiO<sub>2</sub> versus P<sub>2</sub>O<sub>5</sub> (wt%); (g) SiO<sub>2</sub> versus MnO (wt%); (h) SiO<sub>2</sub> versus Na<sub>2</sub>O (wt%); (i) SiO<sub>2</sub> versus K<sub>2</sub>O (wt%) (Red square is syenitic rocks from the Tha Takiap area, green circle is syenitic rocks from the Mae Yan area). ..... 37
- Fig. 4.2 Total-alkali versus silica (TAS) diagram of plutonic rock after (Cox et al., 1979) and adapted by (Wilson, 1989) for plutonic rocks showing rocks ranged in composition from syenite to granite within the field of alkaline, and differentiation trends. (Rock type symbols are same as Fig. 4.1). ..... 38
- Fig. 4.3 A/NK versus A/CNK diagram (after Shand (1943)) and I- and S-type granite classification boundary based on alumina saturation index (ASI) (gray line) (after Chappell and White (1974)). (Rock type symbols are same as Fig. 4.1).39
- Fig. 4.4 K<sub>2</sub>O versus Na<sub>2</sub>O (wt%) diagram subdividing the alkaline magma series (after Middlemost (1975)). (Rock type symbols are same as Fig. 4.1). ..... 39
- Fig. 4.5 Geochemical classification diagrams for syenitic rocks (after Frost et al. (2001)); (a) FeO<sup>tot</sup>/(FeO<sup>tot</sup>+MgO) versus SiO<sub>2</sub> (wt%) diagram classifies the studied syenitic rocks into ferroan granitoids; (b) Na<sub>2</sub>O+K<sub>2</sub>O-CaO versus SiO<sub>2</sub> (wt%) diagram classifies the studied syenitic rocks into alkalic affinity. (Rock type symbols are same as Fig. 4.1). ..... 40
- Fig. 4.6 Bivariate plots after Whalen et al. (1987) of syenitic rocks from the Tha Takiap and Mae Yan areas showing the enrichment of HFSEs indicate that syenitic rocks

of the both areas are A-type granite affinities; (a)  $\text{FeO}^{\text{tot}}/\text{MgO}$  versus  $\text{Zr}+\text{Nb}+\text{Ce}+\text{Y}$ ; (b)  $\text{Na}_2\text{O}+\text{K}_2\text{O}$  versus  $10000*\text{Ga}/\text{Al}$ ; (c)  $\text{Zr}$  versus  $10000*\text{Ga}/\text{Al}$ ; (d)  $\text{Nb}$  versus  $10000*\text{Ga}/\text{Al}$  (FG = field for fractionated felsic granites; OGT = field for unfractionated A-, I- and S-type granites; I=I-type; S=S-type; A=A-type) (Rock type symbols are same as Fig. 4.1)..... 41

- Fig. 4.7 Spider diagrams of syenitic rocks in the study areas plotted using normalized values of (Sun and McDonough, 1989). (a, b) Primitive mantle-normalized spider diagrams and chondrite-normalized REE patterns of the Tha Takiap syenitic rocks, respectively. (c, d) Primitive mantle-normalized spider diagrams and chondrite-normalized REE patterns of the Mae Yan syenitic rocks, respectively..... 42
- Fig. 4.8 Ternary plots of A-type granite discrimination after Eby (1992) of Tha Takiap syenitic rocks and Mae Yan syenitic rocks showing the most of sample were fall within  $A_2$  field (a) Y-Nb-Ce plot and (b) Y-Nb-3\*Ga plot (Rock type symbols are same as Fig. 4.1). ..... 44
- Fig. 4.9 Classification diagram for calcic amphibole (after Leake et al. (1997)) of syenitic rocks from the Tha Takiap and Mae Yan areas (Rock type symbols are same as Fig. 4.1). ..... 47
- Fig. 4.10 Ternary classification diagram Ab-An-Or for feldspar (after Smith and Brown (1988)) showing compositional variation in K-feldspar and plagioclase of syenitic rocks from the Tha Takiap and Mae Yan areas (Rock type symbols are same as Fig. 4.1). ..... 51
- Fig. 4.11 Ternary feldspar plot of feldspar pairs in perthite of syenitic rocks. Isotherms of the solvus were calculated with the Margules parameters of Elkins and Grove (1990) using SOLVCALC program (Wen and Nekvasil, 1994); (a) feldspar pairs in perthite of syenitic rocks from Tha Takiap area which were calculated by  $P=3.4$  kbar; (b) feldspar pairs in perthite of syenitic rocks from Tha Takiap area which were calculated by  $P=4.9$  kbar. .... 55
- Fig. 5.1 Discrimination diagrams for tectonic interpretation; (a) Rb versus (Y+Nb) bivariate plot after Pearce (1996) of Tha Takiap syenitic rocks and Mae Yan syenitic rocks; syn-COLG=syn-collisional granite; post-COLG=post-collisional granite; WPG=within-plate granite; VAG=volcanic arc granite; ORG=ocean ridge granite. (b) Rb-Hf-Ta triangular plot after Harris et al. (1986) of Tha Takiap syenite and Mae Yan syenite (Red square is syenitic rocks from Tha Takiap area, green circle is syenitic rocks from Mae Yan area)..... 58
- Fig. 5.2 Spider diagrams of syenitic rocks in the study areas plotted using normalized values of Sun and McDonough (1989). (a, b) Primitive mantle-normalized spider

diagrams and chondrite-normalized REE patterns of the Tha Takiap syenitic rocks, respectively, in comparison with data from Xiaolonghe granite which is extensional regime after microplate collision or back arc extension related A-type granite from Chen et al. (2015) presented as shade patterns. (c, d) Primitive mantle-normalized spider diagrams and chondrite-normalized REE patterns of the Mae Yan syenitic rocks, in comparison with data from post-collisional potassic rocks in southern Tibet from Liu et al. (2014) presented as shade patterns. ....59

Fig. 5.3 Schematic diagram showing reconstructed tectonic evolution and magmatism in the Tha Takiap and Mae Yan areas during Late Permian to Late Cretaceous (modified after Barber, Ridd, and Crow (2011); Salam et al. (2014); Sone and Metcalfe (2008)). ..... 61



# CHAPTER 1

## INTRODUCTION

### 1.1 Background

Granitic rocks in Thailand is a part of Southeast Asia granitic belt, one of the world largest historical tin producer that occupied about 60-65% of the world's annual production in 1980s (Beckinsale et al., 1979; Mitchell, 1977). The abundance of tin deposits led to intensive studies about granitic rock in this region, especially S-type granite. Unfortunately, tin crisis in 1990s rapidly collapsed the most of tin mining activities and significantly decreased the interest in granitic rock in the SE Asia region, including Thailand. However, some works with expectations of other mineralization types, especially copper-gold and base-metal that relate to I-type granite periodically conducted. Moreover, there are some possibility of rare earth elements (REEs) ion-adsorption type deposits that relate to weathering profile of granitic rock (Imai et al., 2013; Sanematsu et al., 2013) with the prototype of the Southern China (Bao and Zhao, 2008).

The distribution of granitic rocks in Thailand can be divided into three belts (Fig. 1.1) base on their specific characteristics; namely Eastern Granitic Belt (mainly I-type granite), Central Granitic Belt (mainly S-type granite), and Western Granitic Belt (S-type and I-type granite) (Charusiri et al., 1993; Cobbing, 2011; Cobbing et al., 1986; Nakapadungrat and Putthapiban, 1992; Department of Mineral Resources, 2014). Nevertheless some granitic bodies, especially alkaline affinities, cannot be classified properly neither as I- nor S-type according to the classification scheme proposed by Chappell and White (1974).

Alkaline rock which has been reported with limit exposure of small pluton in Thailand. This study focusses on petrography and geochemistry of alkaline granitic rock from two different granitic belts, (1) Tha Takiap area, reported in Mineral Resources Exploration and Evaluation Project: Area 4/2001 "Bo Thong" (Department of Mineral Resources, 2003), locates in Chachoengsao province, Central Thailand as a part of the Eastern Granitic Belt, and (2) Mae Yan area, the best well-known for alkaline granitoid complex in Thailand, locates in Mae Hong Son Province, the Northern Thailand as a part of Central Granitic Belt (Cobbing, 2011; Duangkhamawat and

Srichan, 2013; Pitfield, 1988). The study's result would improve understandings and develop concepts of tectonic settings of these two areas; moreover, alkaline igneous rocks have been interested in possibility of being an essential source from various types of mineral deposit which is important for modern industries, i.e. REE and High field-strength element (HFSE) (Salvi and Williams-Jones, 2005). Several REE deposits in the world have been found related to alkaline suites, i.e. carbonatite suite of the Bayan Obo deposit in China (Wu, 2008) and syenitic suite of the Thor Lake deposit in Canada. Also, the study's result would create preliminary data for the potential of REE deposits operations in the future.

## 1.2 Location and Access

In this study, the two areas are focused namely, 1) Tha Takiap area, and 2) Mae Yan area. Detail of each area is presented below:

**Tha Takiap area** is in Chachoengsao province, central Thailand, situated on SEE direction of Chachoengsao downtown (Fig. 1.1). It lies approximately between latitudes  $13^{\circ} 23' N$  and  $13^{\circ} 27' N$ , and longitudes  $101^{\circ} 40' E$  and  $101^{\circ} 43' E$ . The area appears on topographic maps at a scale of 1:50,000, series L7018, sheets 5335 IV (Amphoe Tha Takiap). This study area is accessible via many convenient routes. In the case of access from Chachoengsao downtown by car, is via Highway No. 304, No. 3551, No. 331 and No. 3259 approximately 95 km to Tha Takiap District. From Tha Takiap district the local road leads east 10 km to study area where nearby Khong Si Yad Reservoir. The landform of the study area is an undulating plain that mostly uses for agricultural activity.

**Mae Yan area** is in Mae Hong Son province, northern Thailand, located on NEE direction of Mae Hong Son downtown (Fig. 1.2). It lies approximately between latitudes  $19^{\circ} 10' N$  and  $19^{\circ} 30' N$ , and longitudes  $98^{\circ} 15' E$  and  $98^{\circ} 30' E$ . The area appears on topographic maps at a scale of 1:50,000, series L7018, sheets 4647 I (Amphoe Pai). By car accessing from the Mae Hong Son downtown is via Highway No. 1095 approximately 80 km to Doi Kiew Lom viewpoint where is northern part of Mae Yan area. From Doi Kiew Lom viewpoint leads to south east along Highway No. 1095 approximately 30 km pass Pai district to Thung Pong village. Southern part of Mae Yan area lies between 10 km and 20 km west of Thung Pong village. The landform



of the study area is the complex of high mountains ranges interspersed by deep valleys that are mostly covered with rain forest.

### 1.3 Purpose of study

This study focuses on petrography and geochemistry of syenite from two different granitic belts, (1) Tha Takiap Syenite, and (2) Mae Yan Alkaline Complex. The main purposes of this study are:

(1) To implement petrography and geochemistry of granitic rock from Tha Takiap area and Mae Yan area.

(2) To constrain the tectonic setting which related to petrogenesis of granitic rock from two study areas.



**Fig. 1.1** Satellite image of Tha Takiap area (modified from Google satellite, 2020).

### 1.4 Methodology

The diagram of research methodology was shown in Fig. 1.3

#### Field work

Samples of Mae Yan area used in this study were provided by Department of Mineral Resources (DMR) from its reconnaissance/regional exploration projects on REE in northern Thailand. Diamond-drilled cores of Tha Takiap granitic rocks were

also provide by DMR. These cores were stored at Rayong Rocks and Minerals Research Center. At least two drilled holes intersected granitic rocks whereas, the rest intersected only volcanic rocks. In addition, fieldworks survey has been conducted to obtain additional samples and important field geological information. Drilled-core logging has been conducted during the first and second fieldworks from 26 to 30 September 2018 and 23 to 27 February 2019 and the third fieldwork from 25 to 28 October 2019 mainly focused on field investigation. Eleven rock samples were collected from outcrops of Mae Yan area. Approximately 160 meters of drilled core from two drilled holes of Tha Takiap area were logged. Thirteen core samples were collected for further laboratory works.

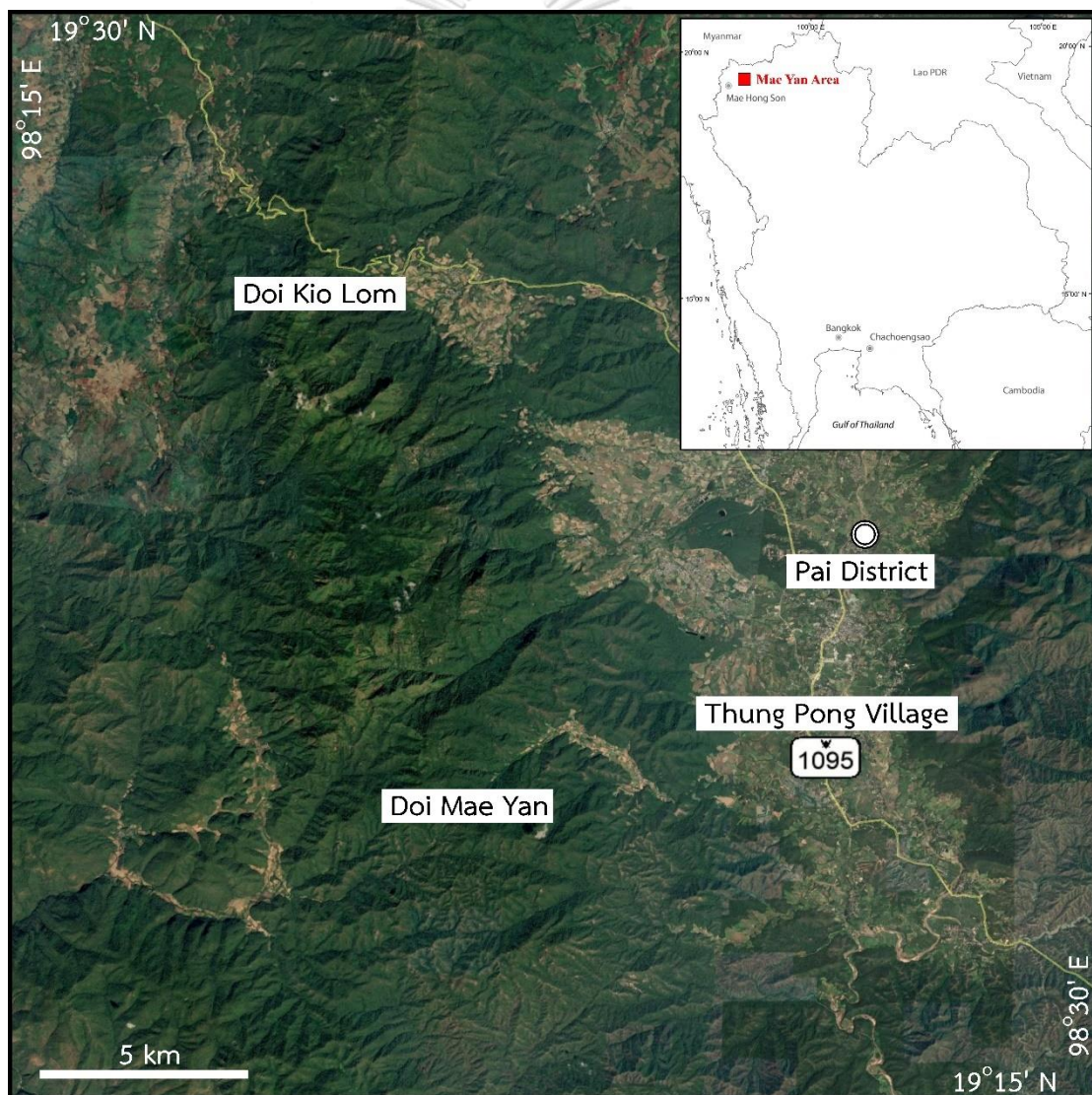


**Fig. 1.2** Satellite image of Mae Yan area (modified from Google satellite, 2020).

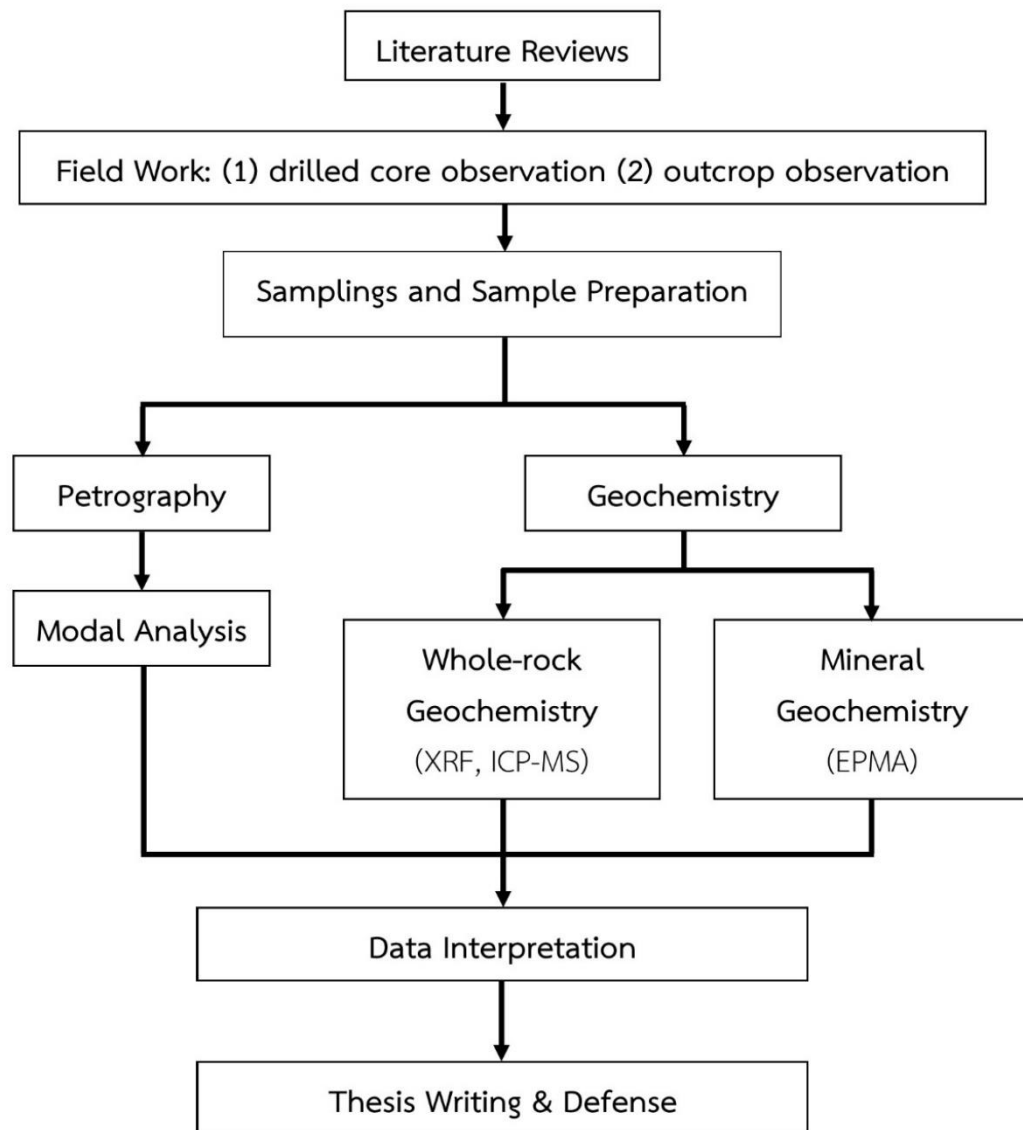


**Fig. 1.3** Diagram of research methodology.

### **Petrography**

The petrographic investigation provides detailed descriptions of essential minerals and accessory minerals, and identified rock type to improved field data. Twenty thin sections (twelve thin sections from Tha Takiap area and eight thin sections from Mae Yan area) were described under a polarized light microscope.

## **Geochemistry**

Whole-rock geochemistry analysis for major oxides was carried out by using X-ray fluorescence (XRF) at Mineral Resources Analysis and Identification Division, DMR. Trace element and REE were carried out by using Inductively coupled plasma mass spectrometry (ICP-MS) at SGS Thailand Limited. Moreover, mineral geochemistry of feldspar and hornblende was analyzed using electron probe microanalyzer (EPMA) at the Department of Geology, Chulalongkorn University to find out the condition of crystallization.

### **1.5 Thesis structure**

The thesis is divided into 5 chapters as following;

**Chapter 1 (Introduction)** provides the general background of this study, location and access of study area, scope of study and thesis structure.

**Chapter 2 (Geological Setting)** explains the regional tectonic setting that related to study area, including geology of granitic rock of Thailand and overview the geology of the Tha Takiap and Mae Yan area.

**Chapter 3 (Geology and Petrography)** give basic data of field investigation in the study areas, diamond-drilled core logging, sample collection, and detail describes characteristic of plutonic rocks under microscope and modal analysis.

**Chapter 4 (Geochemistry)** describes characteristic of plutonic rocks using whole-rock geochemistry and mineral geochemistry.

**Chapter 5 (Discussion and Conclusion)** discuss the petrographic and geochemical data in this study to explain the petrogenesis and tectonic implication, and summarizes the results of this study.

## CHAPTER 2

# GEOLOGICAL SETTING

### 2.1 Regional Tectonic Setting

Thailand consists of two continental blocks that used to be part of Gondwana in the southern hemisphere: 1) Indochina Terrane in the east and 2) Shan-Thai Terrane (also called SIBUMASU (Metcalf, 1984) which is the combination of SI for Sino (China) and Siam (Thailand); BU for Burma; MA for Malaysia; and SU for Sumatra) in the west. These two continental blocks are adjacent to each other with Nan–Sra Kaeo Suture situated in the middle (Bunopas, 1981; Bunopas and Vella, 1978; Charusiri et al., 1993; Gatinsky and Hutchison, 1986; Mitchell, 1981). Based on stratigraphic, palaeomagnetic and paleontological data, the Indochina Terrane was separated from Gondwana during Devonian, while the Shan-Thai Terrane was departed from Gondwana during Permian (Bunopas, 1981; Metcalfe, 1993, 2002, 2017). The earlier works indicated that Nan–Sra Kaeo Suture represents the Palaeo-Tethys which were closed during Late Paleozoic to Early Mesozoic, moreover, the closure of the Palaeo-Tethys also generated a pair of subduction zones and magmatic arcs along the east margin of the Shan-Thai Terrane, as Sukhothai Fold Belt, and the west margin of the Indochina Terrane as Loei Fold Belt (Bunopas, 1981; Bunopas and Vella, 1983; Charusiri et al., 1993). Subduction arc magmatism is important source of Permo-Triassic volcanic and Eastern Granitic Belt of Thailand (Beckinsale et al., 1979; Charusiri et al., 1993; Nakapadungrat and Putthapiban, 1992).

However, the later studies suggested that the Sukhothai Arc (including Sukhothai terrane and Chanthaburi terrane that equivalent to Sukhothai Fold Belt) is not part of Shan-Thai Terrane, but the Sukhothai Arc is a Permo-Triassic arc system that related to eastward dipping subduction of oceanic lithosphere beneath the western margin of the Indochina Terrane (Metcalf, 2017; Sone and Metcalfe, 2008; Sone, Metcalfe, and Chaodumrong, 2012). The geological process of subduction developed an extensive accretionary complex on the east flank of the Shan-Thai Terrane as Inthanon Zone (Barr and Macdonald, 1991; Metcalfe, 2002; Metcalfe, Henderson, and Wakita, 2017; Ridd, 2015; Sone and Metcalfe, 2008). The Nan–Sra Kaeo Suture represents back-arc basin suture which developed behind the Sukhothai Arc, and the Palaeo-Tethys was

represented by Chiang Mai-Chiang Rai Tectonic Line (Cryptic Suture), Klaeng Tectonic Line and Bentong-Raub Suture Zone (Hara et al., 2018; Metcalfe, 2017; Metcalfe et al., 2017; Sone and Metcalfe, 2008; Sone et al., 2012) as same as the approximate boundary between Eastern Granitic Belt and Central Granitic Belt (Charusiri et al., 1993; Cobbing et al., 1992; Mitchell, 1977). Recent works tend to use “Sibumasu Terrane” instead of Shan-Thai Terrane. After the closure of the Palaeo-Tethys, the Central Granitic Belt was generated by the collision of Sibumasu Terrane and the Sukhothai Arc during Late Triassic (Gardiner et al., 2016; Qian et al., 2017; Sone and Metcalfe, 2008; Khin Zaw et al., 2014).

The closure of Meso-Tethys during Jurassic-Early Cretaceous (Beckinsale et al., 1979; Charusiri et al., 1993; Zhang et al., 2017), caused by the eastward subduction of oceanic lithosphere of West Myanmar Terrance beneath the western margin of Sibumasu Terrance, triggers the emplacement of I-type granite in the Western Granitic Belt. Subsequently, during Late Cretaceous to Early Eocene, the collision between the West Myanmar Terrance and Sibumasu Terrance trigger the emplacement of S-type granite in the Western Granitic Belt (Beckinsale et al., 1979; Charusiri et al., 1993; Zhang et al., 2017).

## 2.2 Granitic rock of Thailand

Granitic belts of Thailand are part of Southeast Asia granitic belts or their continuation. At least three main granitic belts have been defined based on geochemistry, tectonic setting, associated mineralization including tin (Mitchell, 1977). Beckinsale (1979) and Beckinsale et al. (1979) has been classified the granitic rocks in Southeast Asia into three provinces based on characteristic features of granitic rocks into I- and S-type granite using the classification of Chappell and White (1974) especially the initial  $^{87}\text{Sr}/^{86}\text{Sr}$  ratio. Cobbing et al. (1986) established classical model of Southeast Asia granitic belt that strongly influence granitic research until recent. On the other hand, Nakapadungrat and Putthapiban (1992) compiled geochronological data (Rb-Sr whole-rock isochron ages,  $^{40}\text{Ar}/^{39}\text{Ar}$  mineral ages and U-Pb mineral ages (zircon and monazite) with the distribution of granitic rock in Thailand to produce the master granitic map of Thailand.

Presently, the granitic rocks of Thailand were divided into three belts along N-S trend (Fig. 2.1) from their specific characteristics namely Eastern Granitic Belt,

Central Granitic Belt and Western Granitic Belt (Charusiri et al., 1993; Cobbing, 2011; Cobbing et al., 1986; Nakapadungrat and Putthapiban, 1992; Department of Mineral Resources, 2014). These granitic belts are connected or equivalent to granite in neighboring countries such as Malaysia, Myanmar, Indonesia and Lao PDR, which have the following characteristics.

**Eastern Granitic Belt** occurs as small plutons in northern Thailand (Chiang Rai, Nan, Phrae, Lampang, Uttaradit, Sukhothai and Tak province), along the rim of the Khorat Plateau (Loei, Phetchabun, Nakhon Sawan, Saraburi, Nakhon Nayok, Prachin Buri, Chachoengsao, Chon Buri, Rayong and Chanthaburi province), southern Thailand (Narathiwat province) and extend southwards to Malaysia. The granitic rock mainly comprises equal-sized crystals of medium-coarse grained and various rocks ranging from syenogranite to gabbro. It is usually found hornblende as an accessory mineral, mafic intrusive rock and volcanic rock as xenolith (Department of Mineral Resources, 2014). Most granitic rocks in the Eastern Granitic Belt were classified as I-type granite and Magnetite series, associated with copper-gold, base-metal and molybdenum deposits (Charusiri et al., 1993; Nakapadungrat and Putthapiban, 1992; Khin Zaw et al., 2014). However, S-type and A-type are also found with rare outcrops (Cobbing, 2011). The age of this granitic belt was reported as 213-256 Ma (Department of Mineral Resources, 2014). Nevertheless, some publications showed that the age of this granitic belt is between Late Carboniferous (Pennsylvanian) to Late Triassic (Fanka et al., 2018; Gardiner et al., 2018; Gardiner et al., 2016; Ng, Whitehouse, et al., 2015; Qian et al., 2017).

Based on Salam et al. (2014), is demonstrated distinction of mineralization in the Sukhothai Arc and the Loei Fold Belt. The Eastern Granitic Belt tends to be accompanied by antimony-gold mineralization whereas in Loei Fold Belt tends to be copper-gold-iron mineralization. Charusiri et al. (1993) reported there are widespread I-type, metaluminous Triassic (220-235 Ma) granitic rocks in Sukhothai Arc including Tak, Lampang, Phrae and Nan provinces. Similar I-type, metaluminous Triassic-Early Jurassic (195-243 Ma) granitic rocks are widespread along the western edge of the

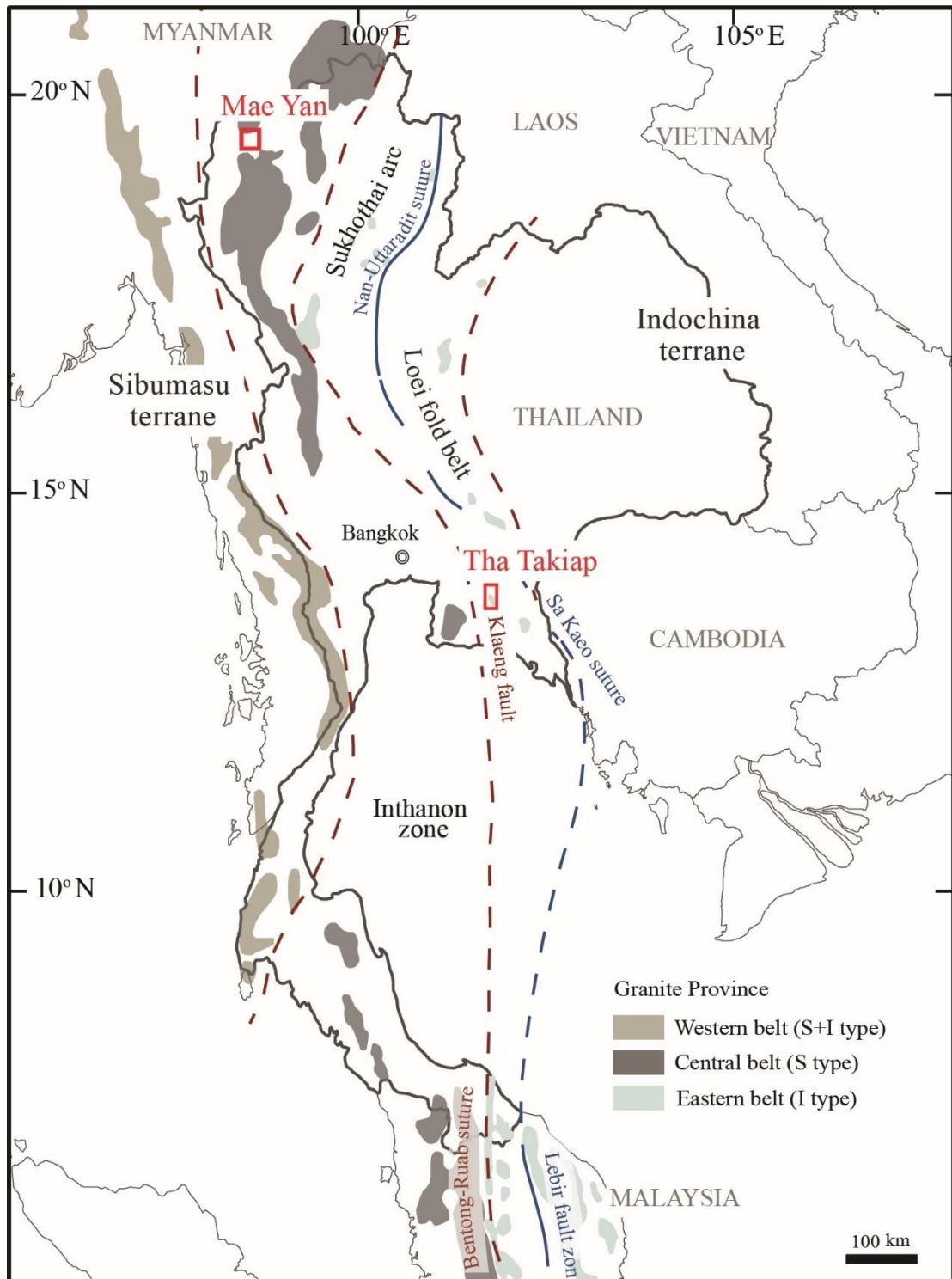


**Fig. 2.1** Simplify granite belts of Thailand and neighboring Southeast Asia countries (Study area are showed in red square; granitic belt boundary are showed in red dashed line; and Nan-Uttaradit-Sa Kaeo suture are showed in blue line) (modified from Cobbing et al. (1992); Metcalfe (2011); Sone and Metcalfe (2008); Khin Zaw et al. (2014)).



Khorat Plateau from Loei province, Phetchabun to Saraburi province in Loei Fold Belt. Therefore, the Eastern Granitic Belt should be divided into two separate subbelts; (1) Eastern Province of Eastern Granitic Belt (the distribution area equivalent to Loei Fold Belt), and (2) Western Province of Eastern Granitic Belt (the distribution area equivalent to Sukhothai Arc (Salam, personal communication), Both are separated with Nan–Sa Kaeo Suture (Khin Zaw et al., 2014) that were a result of the closure of back-arc basin. Recent geochronological data revealed the granitic rocks in the Loei Fold Belt formed during Early Permian to Late Triassic (Gardiner et al., 2016; Qian et al., 2017), with some older age of Late Carboniferous (Fanka et al., 2018) and younger age as Middle Jurassic (Nualkhao et al., 2018) also have been reported. In Sukhothai Arc, granitic rocks of Late Triassic are also present (Qian et al., 2017; Wang et al., 2016).

**Central Granitic Belt** occurs as large batholiths from the North to the South, this range covers Northern Thailand (Chiang Rai, Chiang Mai, Mae Hong Son, Lampang, Lamphun and Tak Province), Central Thailand (Uthai Thani, Kanchanaburi, Ratburi and Phetchaburi province), Eastern Thailand (Chon Buri and Rayong province), Southern Thailand (Nakhon Si Thammarat, Songkhla, Yala and Pattani province) and extends southward to Malaysia and Indonesia. Most granitic rock in this belt is medium-coarse grained with large K-feldspar megacryst, ranging in composition from syenogranite to monzogranite and to quartz monzonite (Department of Mineral Resources, 2014). However, some granite in this belt especially in the Northern area was metamorphosed to gneissic granite and some become migmatite. Moreover, there are some pluton of the younger age (Cretaceous) of alkaline complex and pluton (including Mae Yan Alkaline Complex) intruded through the main phase which is medium-coarse grained with large K-feldspar megacryst (Cobbing et al., 1986; Nakapadungrat and Putthapiban, 1992). Most granitic rocks in the Central Granitic Belt has high initial  $^{87}\text{Sr}/^{86}\text{Sr}$  ratio and low magnetic susceptibility (Cobbing, 2011), and it was classified as S-type granite and Ilmenite series commonly associated with tin-tungsten mineralization. The age of granitic rocks in this belt ranging from 210-241 Ma (Department of Mineral Resources, 2014).

**Western Granitic Belt** used to be one of major world producer of tin-tungsten during Middle to Late 20<sup>th</sup> Century. This belt is located along the border between Thailand and Myanmar extending from northern Thailand and Myanmar to peninsular

Thailand-Myanmar to Sumatra. In Thailand, it covers area of Mae Hong Son (northern Thailand), Kanchanaburi, Ratchaburi, Phetchaburi and Prachuap Khiri Khan (western Thailand), including Ranong, Phang Nga and Phuket Province in the south. The composition of granitic rocks in this belt ranges from granodiorite to syenogranite with high variation texture. There are S-type granite which is coarse K-feldspar megacrystic to medium-grained, slightly small K-feldspar megacrystic (some area granite are moderately deformed) and I-type equigranular medium-grained (Cobbing et al., 1986). The age of this granitic belt was reported as 78-130 Ma (Department of Mineral Resources, 2014).

### **2.3 Regional Geology**

#### **Tha Takiap Area**

Tha Takiap area located on the west of Nan-Sa Kaeo Suture that recent research works confirmed as Permian-Triassic arc system namely Sukhothai Arc (Fig. 2.1) (Barr and Macdonald, 1991; Sone and Metcalfe, 2008; Sone et al., 2012). Base on geological map of Tiypiract (1996), Tha Takiap area consists of Carboniferous marine sedimentary rocks (Fig. 2.2) as the oldest rock unit consisting of limestone, mudstone and sandstone which covered by Permian-Triassic volcanic rocks unit consisting of rhyolitic tuff. Both units were cut through by Triassic granite and syenite along the NNW-SSE lineament (Fig. 2.2). Uppermost of stratigraphy is Quaternary alluvial and terrace deposits. Moreover, diamond drill cores of DMR also found limestone and basaltic dykes (Paipana, 2014; Department of Mineral Resources, 2003). Paipana (2014) described the Tha Takiap syenite as coarse-grained hornblende syenite, mainly consists of alkaline feldspar (dominated by microcline), a few of quartz (less than 5%) and plagioclase (less than 3%). The zircon U-Pb geochronology yielded as  $260.8 \pm 2.6$  Ma. Because of construction of new reservoir in the area, the Tha Takiap syenite still can be observed in several hills at Ban Sam Tha Han, Ban Krok Sakae, and across Khlong Si Yat Dam to Khao Bararun (Fig. 2.2).

#### **Mae Yan Area**

In northern Thailand, the alkaline rocks (syenite) has been reported at the “Mae Yan Alkaline Complex” in Mae Yan area. Chauviroj and Chaturongkawanich (1985)

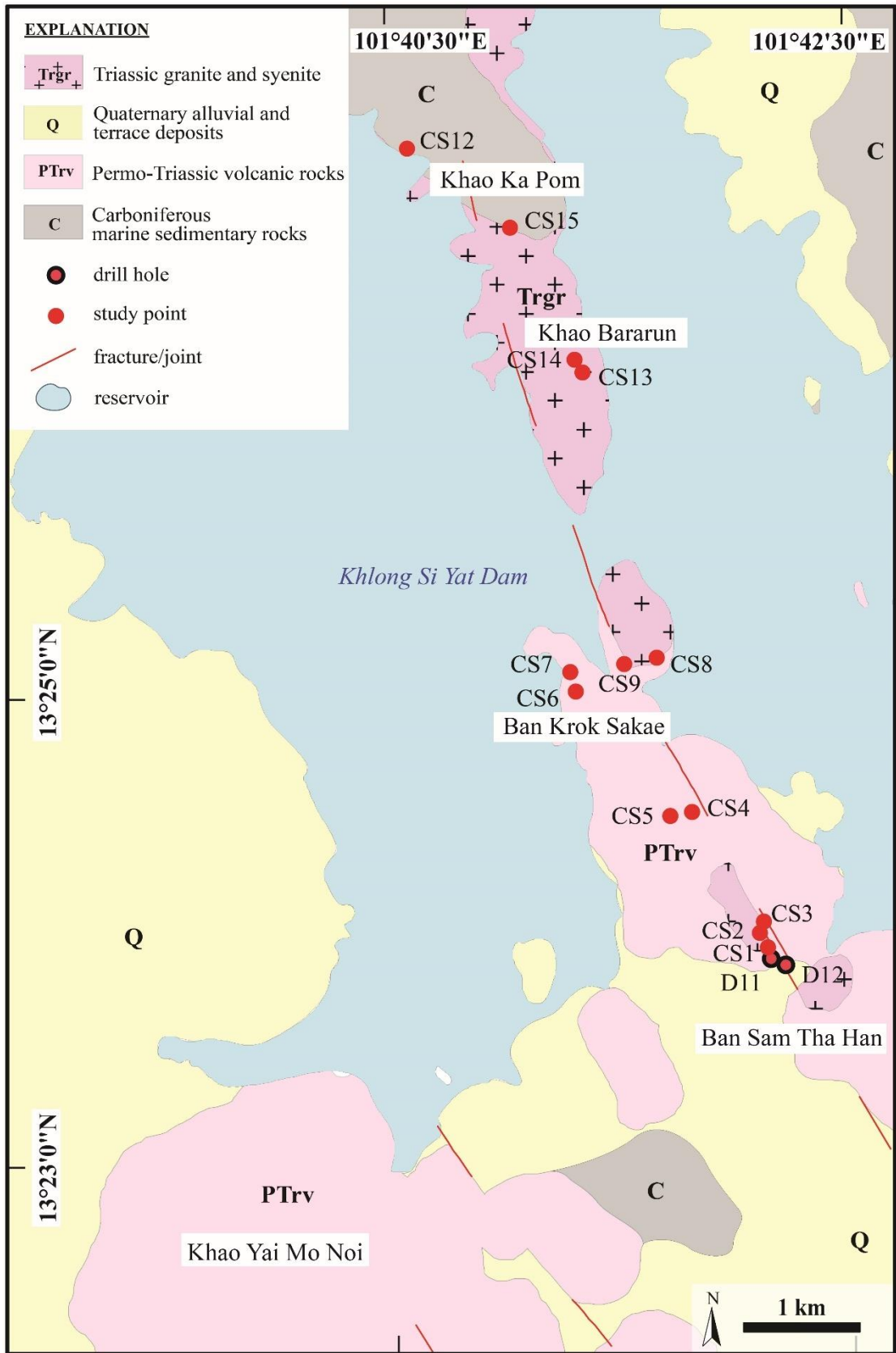


**Fig. 2.2** Geological map of Tha Takiap area (modified from Department of Mineral Resources (2003); Tiyaipiract (1996)).

reported the exposure of coarse-grained biotite granite and hornblende granite in the area. Granitic rock is locally uncovered near Doi Mae Yan continuing northwardly to Doi Kiew Lom (Fig. 2.3), where it is known as “Mae Yan Alkaline Complex” (Nakapadungrat and Putthapiban, 1992; Pitfield, 1988) and has been interpreted as Cretaceous pluton (Cobbing, 2011). The Complex comprises the central complex of pyroxene ± amphibole-bearing monzodiorite, syenite and quartz syenite, surrounded by biotite ± hornblende granite-granodiorite (Pitfield, 1988). Darbyshire (1988) dated the rock using method of Rb-Sr whole rock isochron age dating obtained age of  $100 \pm 12$  Ma (Cretaceous). In additional, zircon grains in granitic rocks from the Doi Kio Lom on the north of Mae Yan area yield age of  $72.06 \pm 0.79$  Ma and  $73.36 \pm 0.86$  Ma obtained by using LA-ICP-MS technique (Duangkhamawat, 2015). The dated samples are mainly consist of K-feldspar that were classified in QAPF diagram as quartz syenite to alkali feldspar syenite. The country rocks surrounded Mae Yan area are Paleozoic strata (Fig. 2.3) consisting of Cambrian quartzite as the oldest rock unit overlain by Ordovician argillaceous limestone, Silurian to Carboniferous clastic sedimentary rock and low grade metamorphic rock, and Permian fusulinids limestone interbedded with shale. Upper most strata are either semi-consolidated Tertiary sediments or Quaternary sediments (Chauviroj and Chaturongkawanich, 1985).

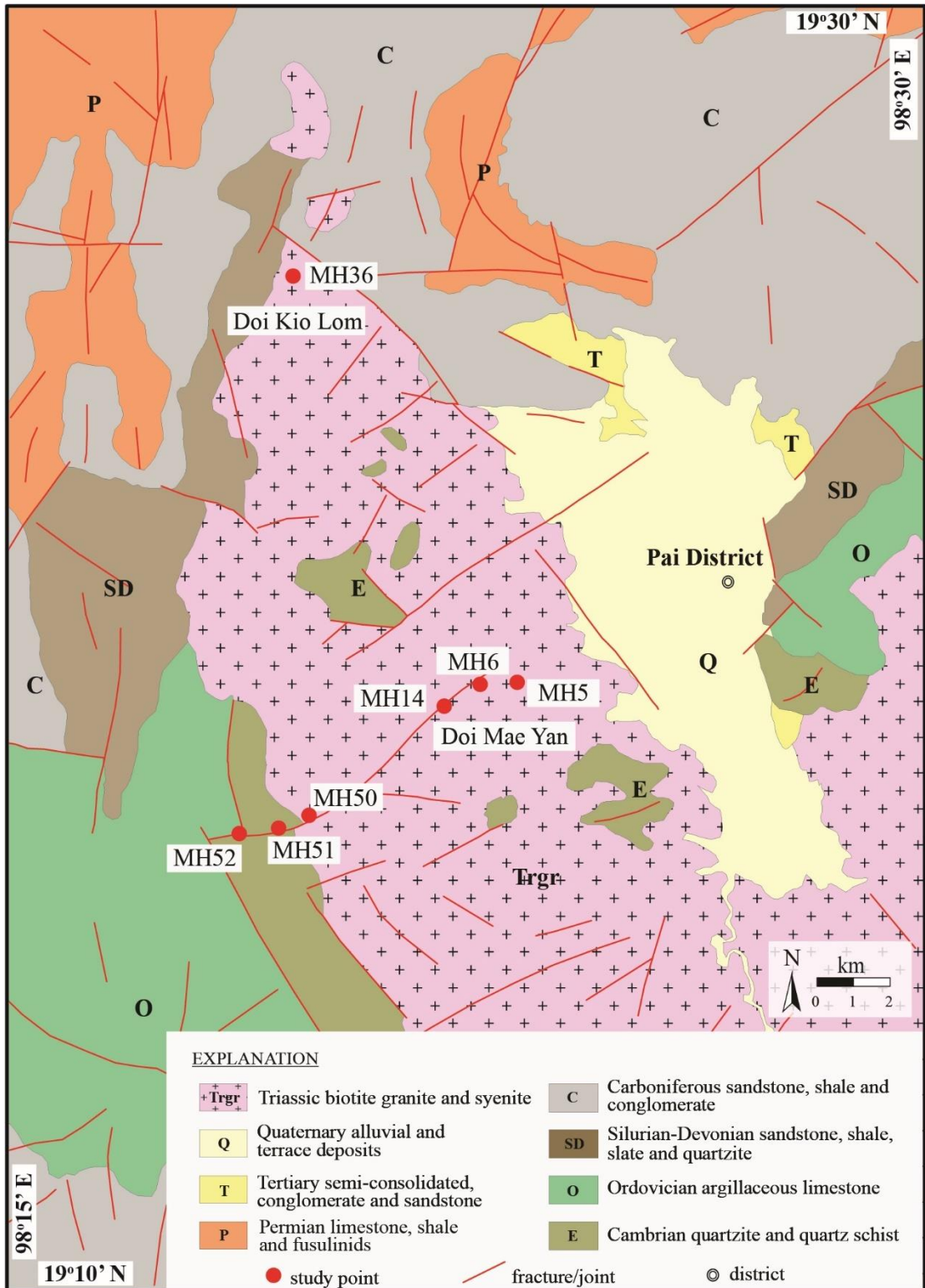


Fig. 2.3 Geological map of Tha Takiap area (modified from Chauviroj and Chaturongkawanich (1985)).

## CHAPTER 3

### GEOLOGY AND PETROGRAPHY

This chapter describes base on field observations and diamond-drilled core logging, geology and petrography of syenite from two areas; 1) Tha Takiap area and 2) Mae Yan area. In the Tha Takiap area, field observations and diamond-drilled core logging were conducted, while the Mae Yan area focused on outcrop observation. Representative samples of both areas were collected for laboratory work, petrographic study and modal analysis, and geochemical analysis.

#### 3.1 Tha Takiap area

##### Field investigation

Plutonic rocks in Tha Takiap area are exposed on small hills (Fig. 3.1a). Their outcrops (Fig. 3.1b) are commonly found at the foothill, often found not far from the outcrop of low-grade metamorphic rock (slate to phyllite) (Fig. 3.1c). The outcrops investigation in this study are shown in Fig. 2.3 and their description is shown in Table 3.1. Outcrops of plutonic rock in Tha Takiap area are strong weathered, yellowish gray to brownish gray colored, medium- to coarse-grained, equigranular texture, composed mainly of K-feldspar and hornblende with minor amounts of quartz, and some Fe-oxide tarnishes on weathering surface. Their characteristics are quite distinction from the surrounding Triassic granites (Fig. 3.1d) which composed mainly of quartz, K-feldspar and plagioclase with minor amounts of biotite and/or hornblende. However, samples from field investigation are strongly weathered, unsuitable for petrographic study and geochemistry. All samples for petrographic study and geochemical analysis were selected from diamond-drilled cores (drill hole No. D11 and D12) which are located nearby Ban Sam Tha Han (Fig. 2.3).

Two drill holes; 1) D11 (total depth of 97 meters) is located at latitudes  $13^{\circ} 23' 48''$  N and longitudes  $101^{\circ} 42' 14''$  E and 2) D12 (total depth of 60 meters) is located at latitudes  $13^{\circ} 23' 49''$  N and longitudes  $101^{\circ} 42' 11''$  E. Both of them mostly intersected medium- to coarse-grained hornblende syenite (Fig. 3.1e) whereas the rest of diamond-drilled holes have intersected volcanic rock (Fig. 3.1f) and limestone. Thus, the main phase of medium- to coarse-grained hornblende syenite was used in

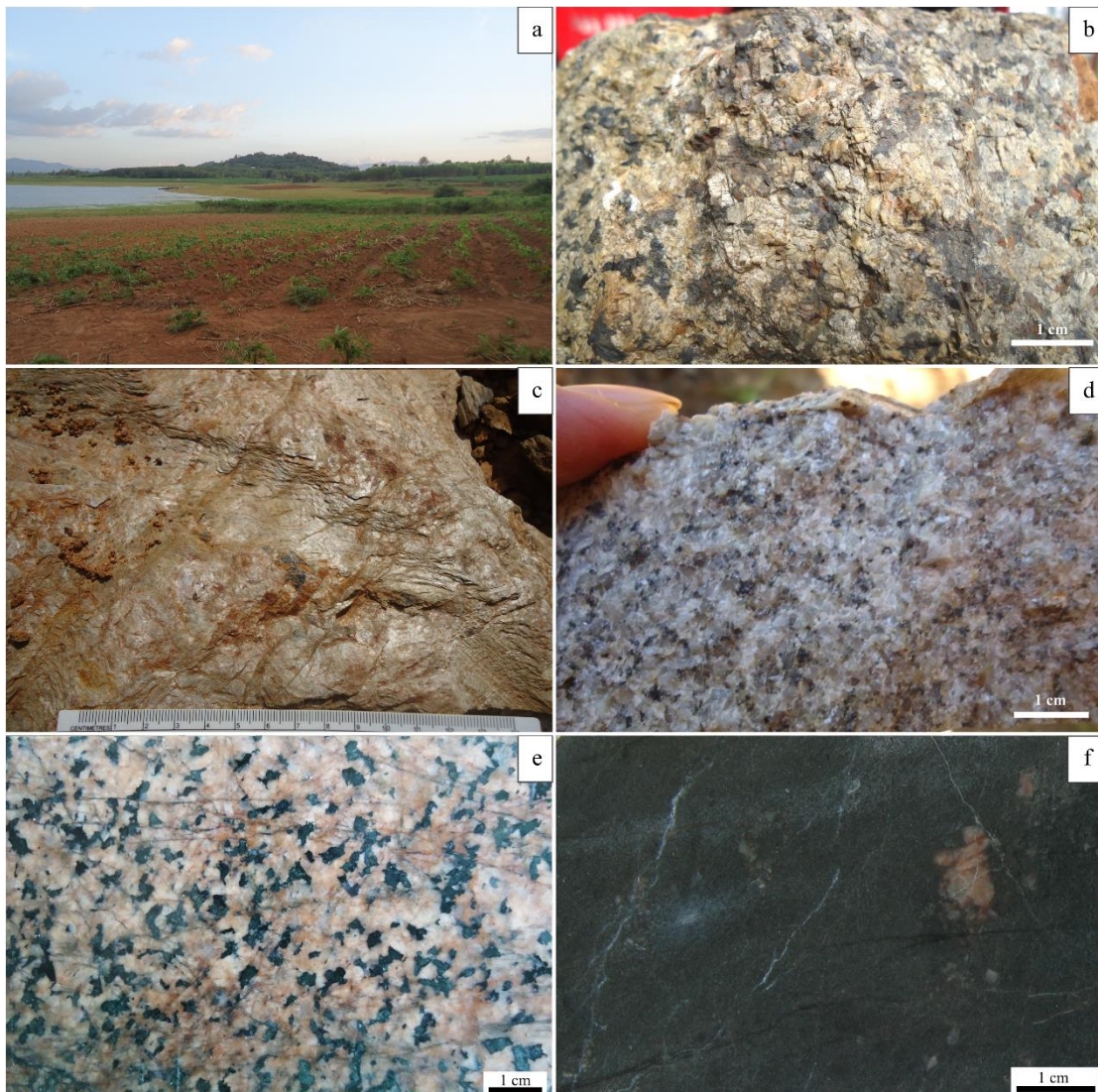


**Fig. 3.1** Field investigation of Tha Takiap area. **a)** Undulating plain landform with small hill at Ban Sam Ta Han. **b)** Photograph of plutonic rock from study point CS14. **c)** Photograph of low grade metamorphic rock from study point CS2. **d)** Photograph of Triassic granites nearby Tha Takiap area from study point CS11. **e)** Photograph of diamond-drilled core of medium- to coarse-grained syenite (D12 at depth 23.6-23.8 m). **f)** Photograph of diamond-drilled core of volcanic rock (D11 at depth 44.8-45.0 m).

this study. The medium- to coarse-grained hornblende syenite from both drill holes are similar in mineral assemblage, color and texture. They are gray to yellowish gray colored, mainly composed of feldspar, and hornblende with a minor amount of quartz. The diamond-drilled cores are shown in Fig. 3.2 and 3.3. The list of diamond-drilled core samples used for petrographic study, modal analysis, and geochemistry are shown in Table 3.2.

**Table 3.1** List of outcrops description of Tha Takiap area.

Study point	Coordinate		Description	Magnetic susceptibility value ( $\times 10^{-3}$ SI)
	Easting	Northing		
CS1	792706	1482747	Medium-grained plutonic rock, equigranular texture, mainly consist of feldspar and hornblende	0.2725
CS2	792659	1482881	Phyllite, foliation= $48^{\circ}/060^{\circ}$ (dip angle/dip direction)	-
CS3	792705	1482895	Strongly weathered plutonic rock contact with phyllite	-
CS4	792090	1483773	Medium-grained plutonic rock, equigranular texture, mainly consist of feldspar and hornblende, with mafic enclave	0.386
CS5	791910	1483776	Medium-grained plutonic rock, equigranular texture, mainly consist of feldspar and hornblende	-
CS6	791151	1484757	Medium-grained plutonic rock, equigranular texture, mainly consist of feldspar and hornblende, abundant mafic mineral	-
CS7	791099	1484911	Medium-grained plutonic rock, equigranular texture, mainly consist of feldspar and hornblende, abundant mafic mineral	0.240
CS8	791789	1485040	Phyllite	0.173
CS9	791562	1485027	Phyllite, foliation= $70^{\circ}/085^{\circ}$ (dip angle/dip direction)	-
CS10	789223	1474416	Fine- to medium-grained plutonic rock, equigranular texture, mainly consist of feldspar, hornblende, and quartz.	0.0772
CS11	787956	1473805	Biotite granite, medium-grained, equigranular texture, mainly consist of quartz and feldspar	0.0767
CS12	789842	1489082	Limestone and dolomitic limestone (maybe alteration)	0.307
CS13	791235	1487355	Medium-grained plutonic rock, equigranular texture, mainly consist of feldspar and hornblende	0.405
CS14	791178	1487461	Medium-grained plutonic rock, equigranular texture, mainly consist of feldspar and hornblende	2.24
CS15	790624	1488482	Medium-grained plutonic rock, equigranular texture, mainly consist of feldspar and hornblende, small amount of quartz	1.349



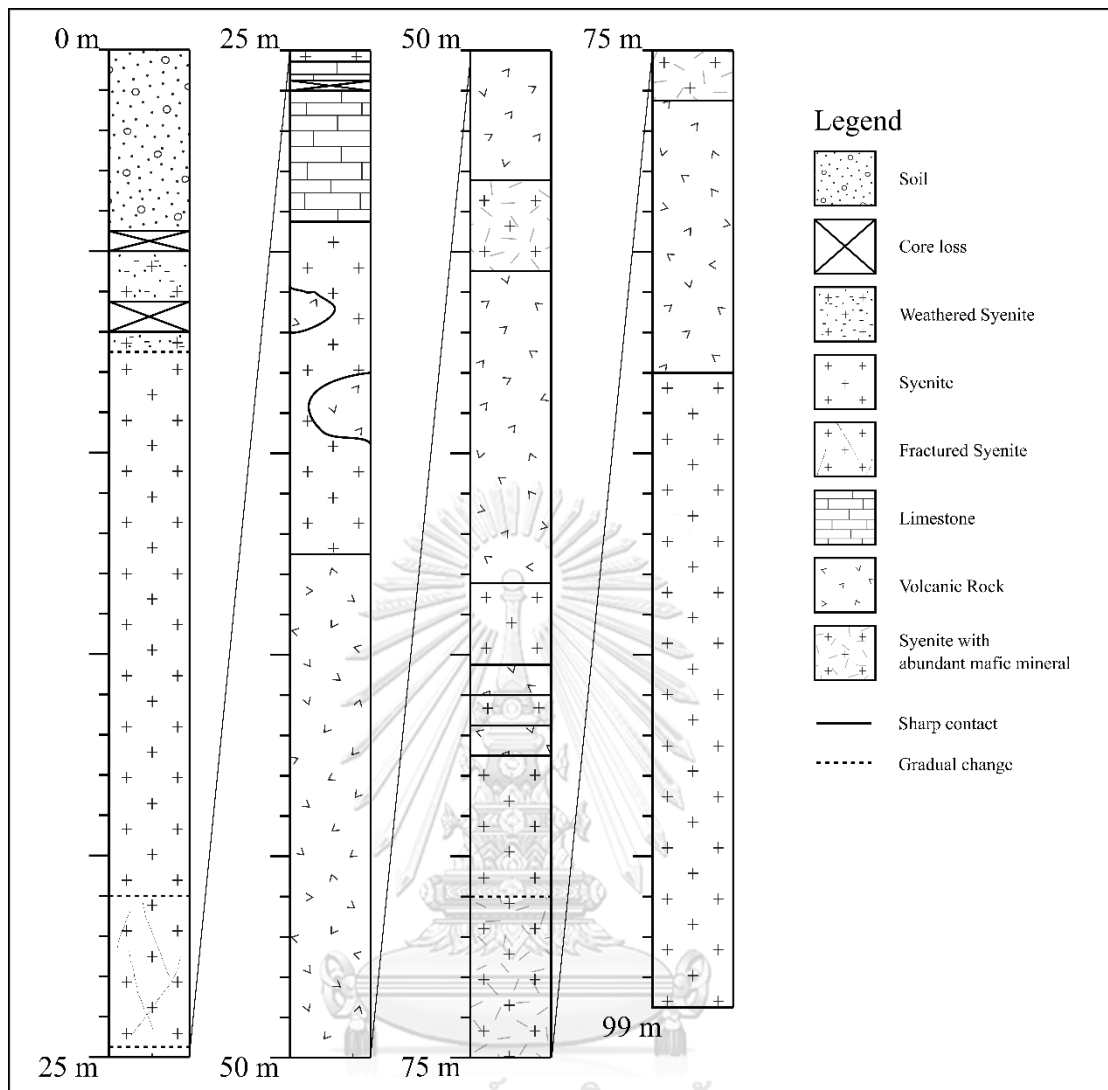


**Fig. 3.2** Simplified graphic log of diamond-drilled hole No. D11.

Medium- to coarse-grained (2.0 to 6.0 cm in diameter) plutonic rock of equigranular texture are cropped out on small hill found around Ban Sam Tha Han village, Ban Krok Sakae village, and at Khao Bararun hill. This rock also intersected in the diamond-drilled hole No. D11 and D12. It has gray to brownish gray colored, mainly consists of feldspar, hornblende, and a small amount of quartz (Fig. 3.1e). In outcrop samples, hornblende is slight to highly weathered and change to chlorite. Magnetic susceptibility values vary from  $0.246 \times 10^{-3}$  SI to  $0.542 \times 10^{-3}$  SI (Table 3.2). cores and surface of the outcrops which expose as small hill

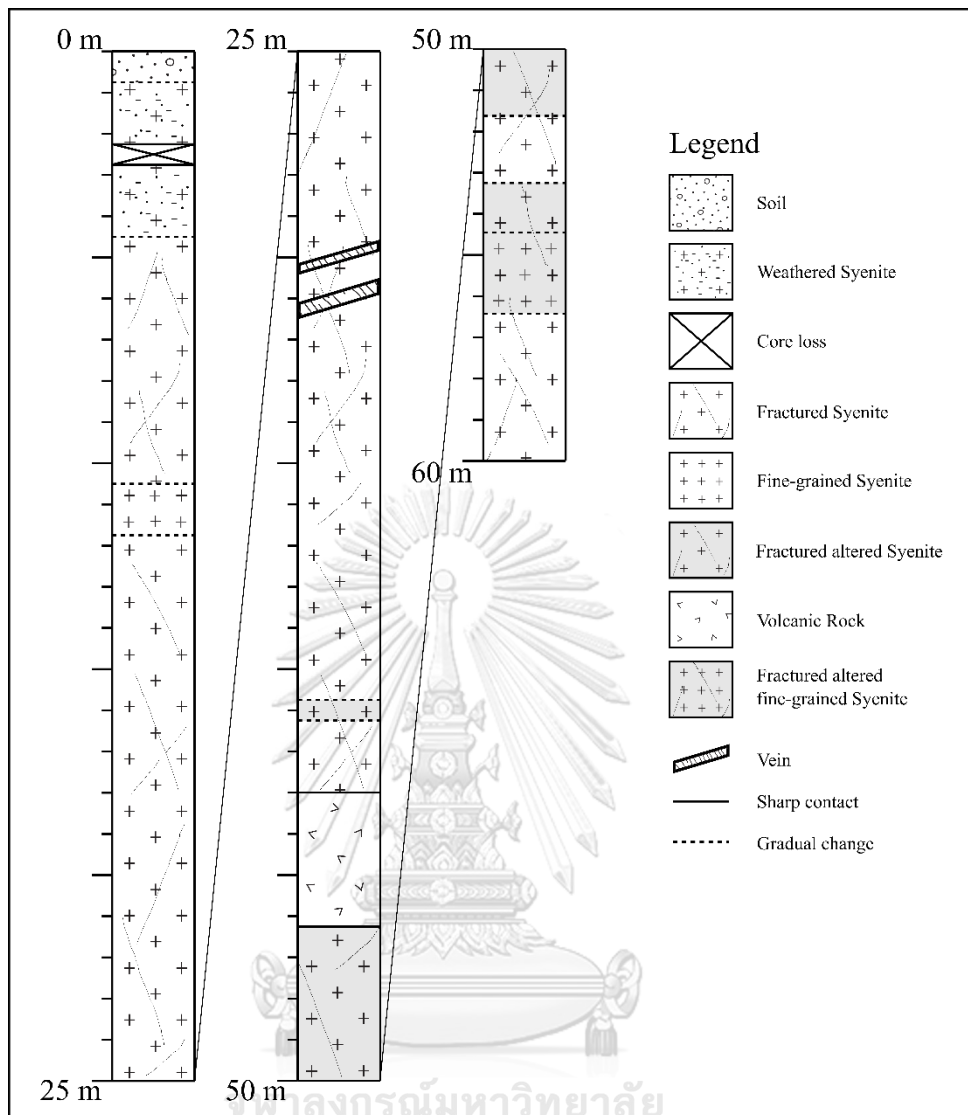


**Fig. 3.3** Simplified graphic log of diamond-drilled hole No. D12.

### **Petrographic study**

Medium- to coarse-grained plutonic rock shows equigranular texture (Fig. 3.4a), grain sizes ranging in 1.0 to 6.0 mm (average 1.0-3.5 mm in diameter), mainly consists of K-feldspars (65-85%) and mafic mineral (hornblende and pyroxene) (10-25%). Quartz and plagioclase constitute 0-15% and less than 3%, respectively (Fig. 3.4b). Pyroxene exhibits overgrowth of hornblende at the rim (Fig. 3.4c). Apatite is also found as inclusions in hornblende (Fig. 3.4d) and K-feldspar. Other accessory minerals are rarely found in these rocks.

**Table 3.2** List of diamond-drilled cores samples from Tha Takiap area used for petrographic study, modal analysis, and geochemistry analysis.

Sample No.	Drill Hole	Depth (m)		Magnetic susceptibility value ( $\times 10^{-3}$ SI)			
		Start	End	1 <sup>st</sup> Measurement	2 <sup>nd</sup> Measurement	3 <sup>rd</sup> Measurement	Average
D11-4	D11	20.40	20.60	0.520	0.535	0.571	0.542
D11-6	D11	36.30	36.40	0.280	0.266	0.267	0.271
D11-7	D11	55.00	55.10	0.282	0.178	0.176	0.212
D11-11	D11	69.20	69.30	0.451	0.474	0.428	0.451
D11-19	D11	86.60	86.80	0.387	0.366	0.381	0.378
D11-20	D11	91.50	91.60	0.418	0.390	0.387	0.398
D11-22	D11	96.20	96.35	0.372	0.381	0.414	0.389
D12-1	D12	7.20	7.40	0.239	0.244	0.237	0.240
D12-6	D12	14.75	14.95	0.245	0.272	0.341	0.305
D12-8	D12	19.30	19.40	0.339	0.323	0.347	0.336
D12-9	D12	23.60	23.80	0.295	0.256	0.246	0.266
D12-11	D12	26.70	26.85	0.282	0.279	0.245	0.269
D12-25	D12	51.80	52.00	0.267	0.264	0.206	0.246

K-feldspars are subhedral to anhedral crystal (grain sizes varying from 0.80 to 5.00 mm in diameter), commonly shows perthitic texture and grid twins of microcline. Quartz is anhedral crystal (grain sizes varying from 0.20 to 1.50 mm in diameter). Plagioclase is subhedral crystal (grain sizes varying from 0.15 to 0.50 mm in diameter), commonly shows multiple/albite twins.

Hornblende exhibits subhedral to anhedral outlines (grain sizes varying from 0.50 to 3.00 mm in diameter). Apatite is euhedral to subhedral crystal (grain sizes varying from 0.05 to 0.20 mm in diameter). These rocks commonly contained chlorite veinlet fill-in fracture (Fig. 3.4b).

### 3.2 Mae Yan Area

#### Field investigation

In Mae Yan Area, plutonic rocks cropped out at Doi Kio Lom and Doi Mae Yan where they were mapped as Triassic granite (Chauviroj and Chaturongkawanich, 1985) (Fig. 2.3). In Doi Kio Lom area, the outcrops of plutonic rock have limited exposures, mainly along road cut on the mountain ridge northwest of Pai district, covering an area of about 1-3 km<sup>2</sup>. They are gray to dark gray colored, fine- to medium-grained, equigranular texture, compose mainly of feldspar and hornblende (Fig. 3.5a). Whereas, in Doi Mae Yan area, outcrops of plutonic rock are exposed along hill's slope which lies

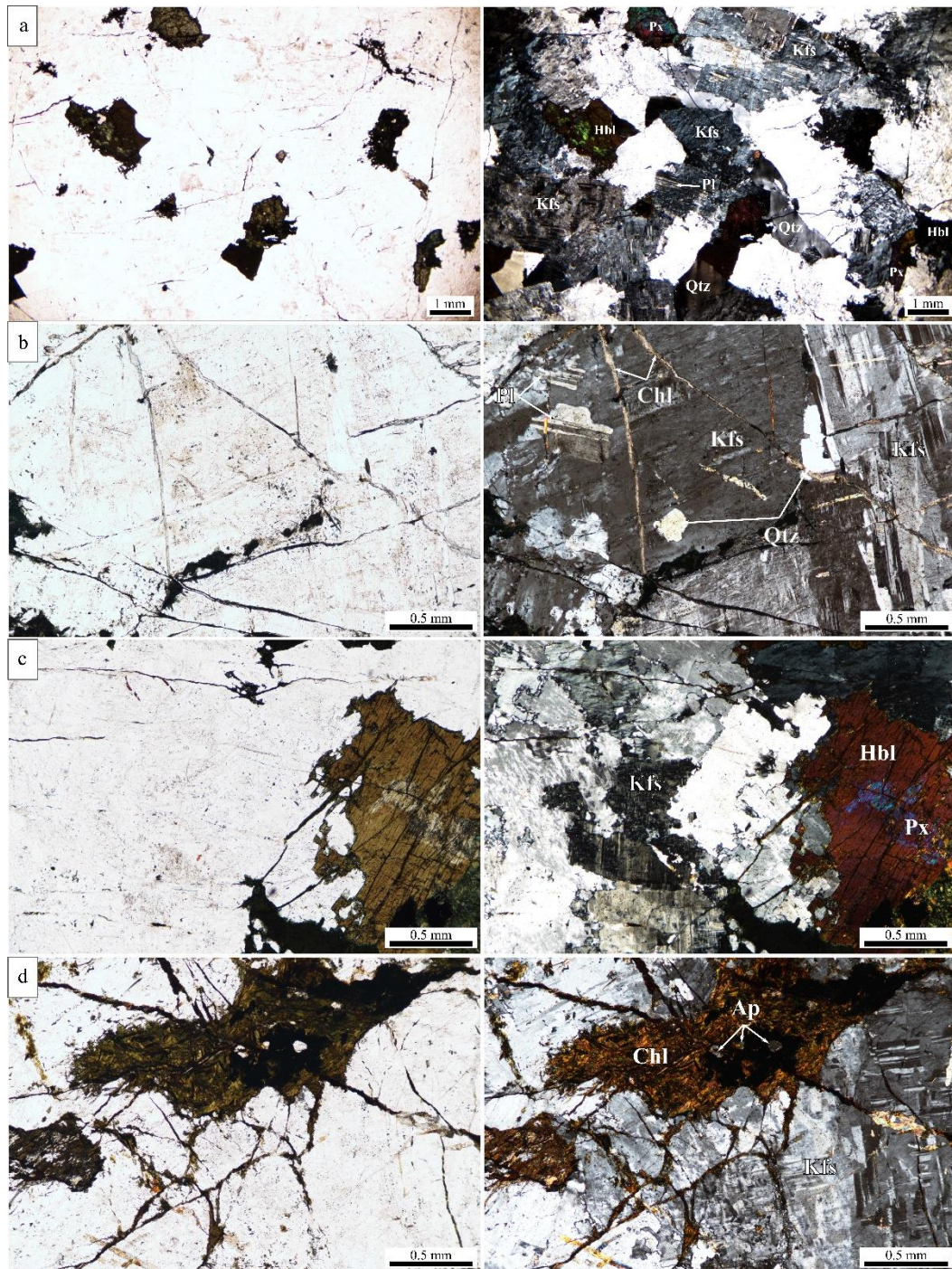


**Fig. 3.4** Petrographic characteristics of syenitic rocks from Tha Takiap area. **a)** Photomicrograph of syenite showing equigranular texture with K-feldspar showing perthitic texture and grid twin, hornblende, quartz and plagioclase. **b)** Photomicrograph of syenite, showing K-feldspar with perthitic texture and grid twin, quartz, plagioclase, and veinlet of chlorite. **c)** Photomicrograph of syenite, showing hornblende which is partly replaced by chlorite and K-feldspar. **d)** Photomicrograph of syenite, showing inclusion of apatite in hornblende which is replaced by chlorite, and K-feldspar which shows grid twin. Mineral abbreviations: Kfs (K-feldspar); Hbl (hornblende); Qtz (quartz); Pl (plagioclase); Px (pyroxene); Chl (chlorite); Ap (apatite). (left: plane polarized light, right: cross polarized light).

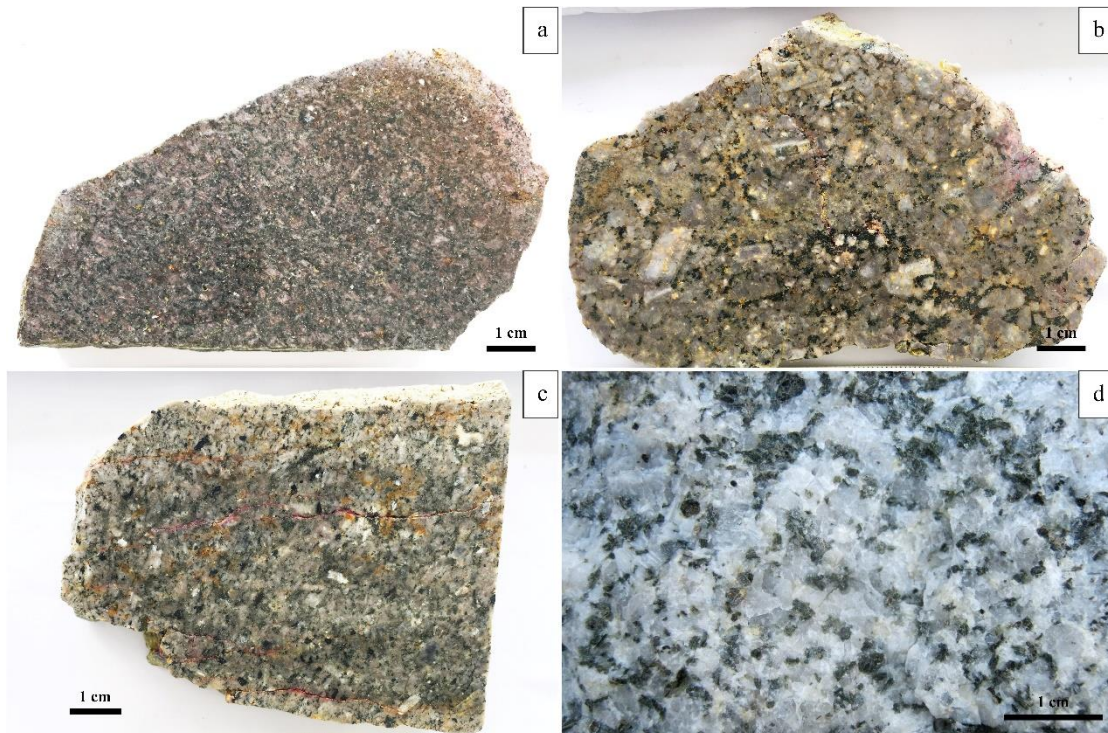


**Fig. 3.5** Photograph of hand specimen sample of Mae Yan area. **a)** Photograph of fine- to medium-grained plutonic rock at Doi Kio Lom mountain (sample No. MH36-1). **b)** Photograph of medium- to coarse-grained plutonic rock of Doi Mae Yan (sample No. MH5-3). **c)** Photograph of fine- to medium-grained plutonic rock of Doi Mae Yan (sample No. MHPP5-1). **d)** Photograph of Triassic medium-grained porphyritic biotite granite in adjacent area of Mae Yan area.

along NE-SW lineament, and sometimes overlain by roof pendant of Paleozoic metasedimentary rocks (Chauviroj and Chaturongkawanich, 1985).

Base on field investigation, the plutonic rocks are equigranular texture which can be distinguished into two phase; 1) medium- to coarse-grained (3.0-8.0 mm in diameter) were exposed in Doi Mae Yan. It has gray to light gray colored, mainly composed of feldspar and hornblende with some magnetite and strongly active to magnetic pen. Magnetic susceptibility values vary from  $0.267 \times 10^{-3}$  SI to  $12.767 \times 10^{-3}$  SI (Table 3.3). 2) fine- to medium-grained (0.5-4.0 mm in diameter) were exposed in Doi Kio Lom and Doi Mae Yan. It has gray to dark gray colored, mainly composed of feldspar and hornblende with some Fe-oxides tarnish on the weathering surface. Magnetic susceptibility values vary from  $0.278 \times 10^{-3}$  SI to  $24.933 \times 10^{-3}$  SI (Table 3.3). List of outcrops and values of magnetic susceptibility are shown in Table 3.3. Both phases of plutonic rock are rarely composed of quartz, different from surrounding Triassic porphyritic biotite granites (Fig. 3.5d) of the Central Granitic belt which comprises

mainly quartz, K-feldspar and plagioclase with a minor amount of biotite. Most of samples were collected from the least weathered outcrops, for laboratory works (petrographic study, modal analysis, and geochemistry).

### Petrographic study

#### 1. Medium- to coarse-grained hornblende syenite

Medium- to coarse-grained hornblende syenite showing inequigranular texture (Fig. 3.6a), that can be distinguished into two-phase variants of coarser-grained (70-80%) and finer-grained (20-30%) texture.

Coarser-grained texture (1.5 to 7.5 mm, average 2.5-5.5 mm in diameter) mainly consists of subhedral to euhedral K-feldspars (> 95%) that commonly shows perthitic texture with a small amount of microcline crystals. Subhedral to anhedral quartz less than 5%.

Finer-grained texture (average 0.15-1.20 mm and up to 1.50 mm in diameter) consisting of K-feldspar (70-80%), quartz (10-20%), plagioclase (< 3%), hornblende (5-10%) and other mineral (< 5%); clinopyroxene (aegirine-augite), sphene, apatite, zircon and opaque minerals) (Fig. 3.6b-c).

**Table 3.3** List of rock sample from Mae Yan Area that were collected for petrographic study, modal analysis, and geochemistry analysis.

Sample No.	Location	Coordinate (Zone 47Q)		Phase	Magnetic susceptibility ( $\times 10^{-3}$ SI) value			
		Easting	Northing		1 <sup>st</sup> Measurement	2 <sup>nd</sup> Measurement	3 <sup>rd</sup> Measurement	Average
MH 5-1	Doi Mae Yan	435328	2137570	F-M	11.0	7.5	8.2	8.903
MH 5-2	Doi Mae Yan	435328	2137570	F-M	20.9	22.5	31.4	24.933
MH 5-3	Doi Mae Yan	435328	2137570	M-C	5.79	5.51	5.29	5.530
MH 6	Doi Mae Yan	434026	2137676	M-C	0.796	0.718	0.776	0.763
MH 14	Doi Mae Yan	432823	2136859	F-M	43.0	28.5	27.4	32.967
MH 36-1	Doi Kio Lom	428412	2149341	F-M	6.63	5.40	4.60	5.543
MH 36-2	Doi Kio Lom	428412	2149341	F-M	3.11	2.09	4.59	3.263
MH 50	Doi Mae Yan	429712	2134189	F-M	0.22	0.25	0.37	0.278
MH 51	Doi Mae Yan	429198	2133718	M-C	0.29	0.22	0.30	0.267
MH 52-1	Doi Mae Yan	427429	2133772	F-M	3.63	1.93	3.84	3.133
MH 52-2	Doi Mae Yan	427429	2133772	M-C	12.7	15.4	10.2	12.767

\*Note; F-M = fine- to medium-grained plutonic rock, M-C = medium- to coarse-grained plutonic rock

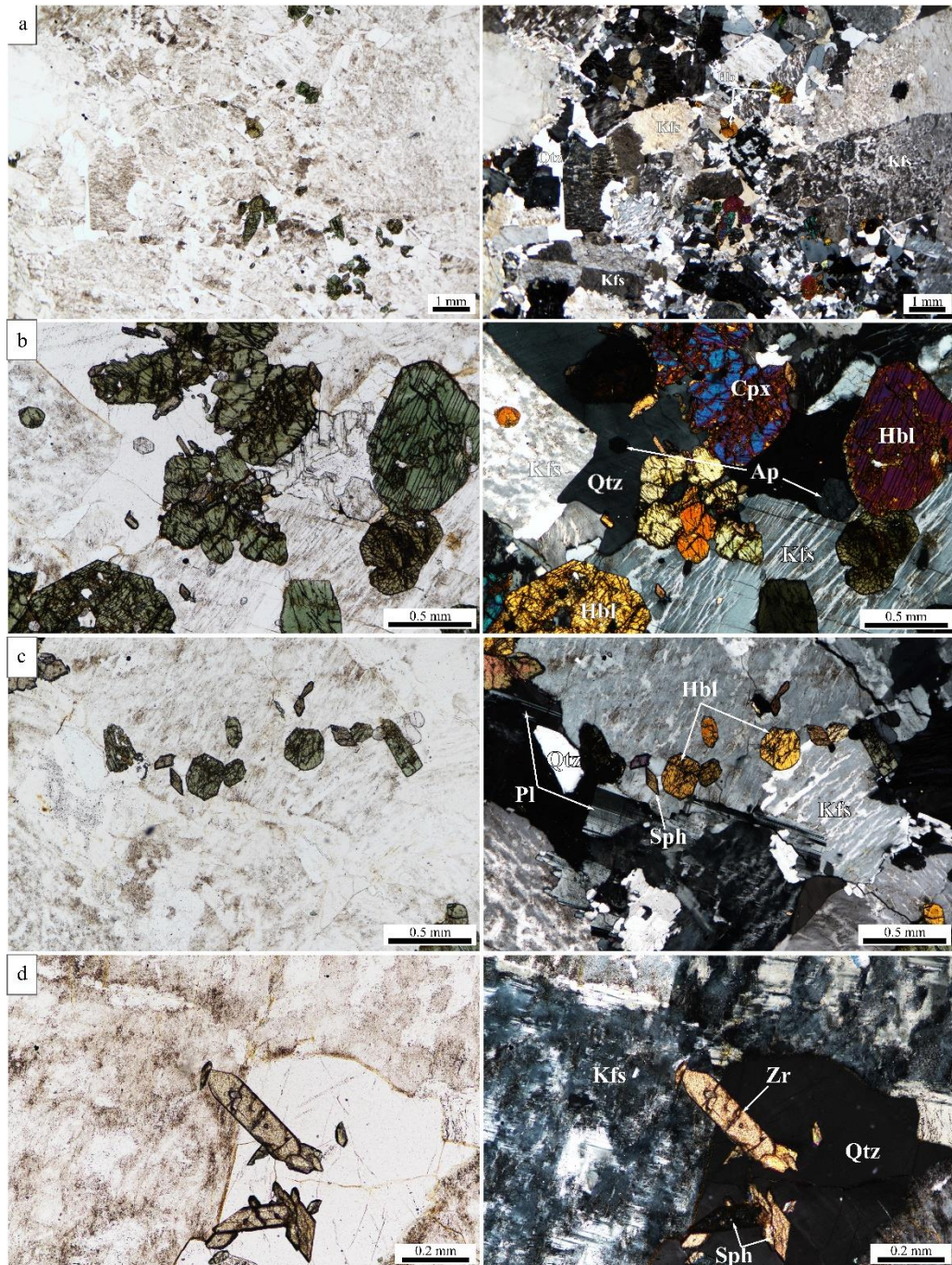


**Fig. 3.6** Petrographic characteristics of medium- to coarse-grained syenitic rocks from Mae Yan area. **a)** Photomicrograph of medium- to coarse-grained syenitic rock showing inequigranular with K-feldspar which shows perthitic texture. **b)** Photomicrograph of syenitic rock, showing K-feldspar which shows perthitic texture, hornblende, quartz, clinopyroxene, and apatite. **c)** Photomicrograph of medium- to coarse-grained syenitic rock, showing K-feldspar which shows perthitic texture, hornblende, quartz, sphene, and plagioclase. **d)** Photomicrograph of medium- to coarse-grained syenitic rock, showing zircon, sphene, K-feldspar which shows grid twin, and quartz. Mineral abbreviations: Kfs (K-feldspar); Hbl (hornblende); Qtz (quartz); Cpx (Clinopyroxene); Pl (plagioclase); Chl (chlorite); Ap (apatite); Sph (sphene); Zr (Zircon). (left: plane polarized light, right: cross polarized light).

K-feldspars are subhedral to anhedral crystal (0.75 to 1.25 mm in diameter), often shows perthitic texture and Carlsbad twin with a small amount of microcline crystals which shows grid twin. Quartz is subhedral to anhedral crystal (0.20 to 0.60 mm across in diameter). Plagioclase is subhedral to anhedral crystal (0.20 to 0.50 mm in diameter), shows albite twin. Hornblende is euhedral to subhedral crystal (0.30 to 1.10 mm in diameter) are green to greenish brown colored. Inclusions of euhedral to subhedral apatite, zircon, and opaque minerals have been found in hornblende. Hornblende crystals are partly replaced by chlorite.

Most of accessory minerals are found in finer-grained texture. Clinopyroxene is euhedral to subhedral in shape (0.2 to 0.5 mm in diameter), partly replaced by chlorite. Sphene/titanite is euhedral to subhedral crystal with elongate prismatic shape (0.80 to 0.18 mm in diameter). Zircon is subhedral, elongate prismatic shape.

## **2. Fine- to medium-grained hornblende syenite**

Fine- to medium-grained plutonic rock showing porphyritic texture (Fig. 3.7a) to equigranular texture (Fig. 3.7b). Porphyritic texture can be distinguished into coarser-grained (30-35%) and finer-grained groundmass (65-70%) texture.

Coarser-grained (from 0.7 to 2.5 mm across, average 0.9-2.0 mm) mainly consists of euhedral to subhedral K-feldspars (more than 95%) that shows perthitic texture and Carlsbad twin in common. A few of anhedral quartz (less than 5%) are also founded.

Finer-grained groundmass (grain sizes up to 0.6 mm across, (average 0.10-0.30 mm)) consists of K-feldspar (40-50%), quartz (20-30%), plagioclase (10-15%), amphibole/hornblende (15-20%) and other minerals (1-5%; clinopyroxene, sphene, apatite, zircon, monazite and opaque minerals (Fig. 3.7b-d).

K-feldspar is subhedral to anhedral in shape (grain sizes varying from 0.15 to 0.30 mm across), often shows perthitic texture and Carlsbad twin with a small amount of microcline crystals which shows grid twin. Quartz is anhedral crystal (grain sizes varying from 0.10 to 0.25 mm across), shows undulatory extinction in common. Plagioclase is subhedral to anhedral crystal (grain sizes varying from 0.10 to 0.20 mm across), shows multiple/albite twins in common.



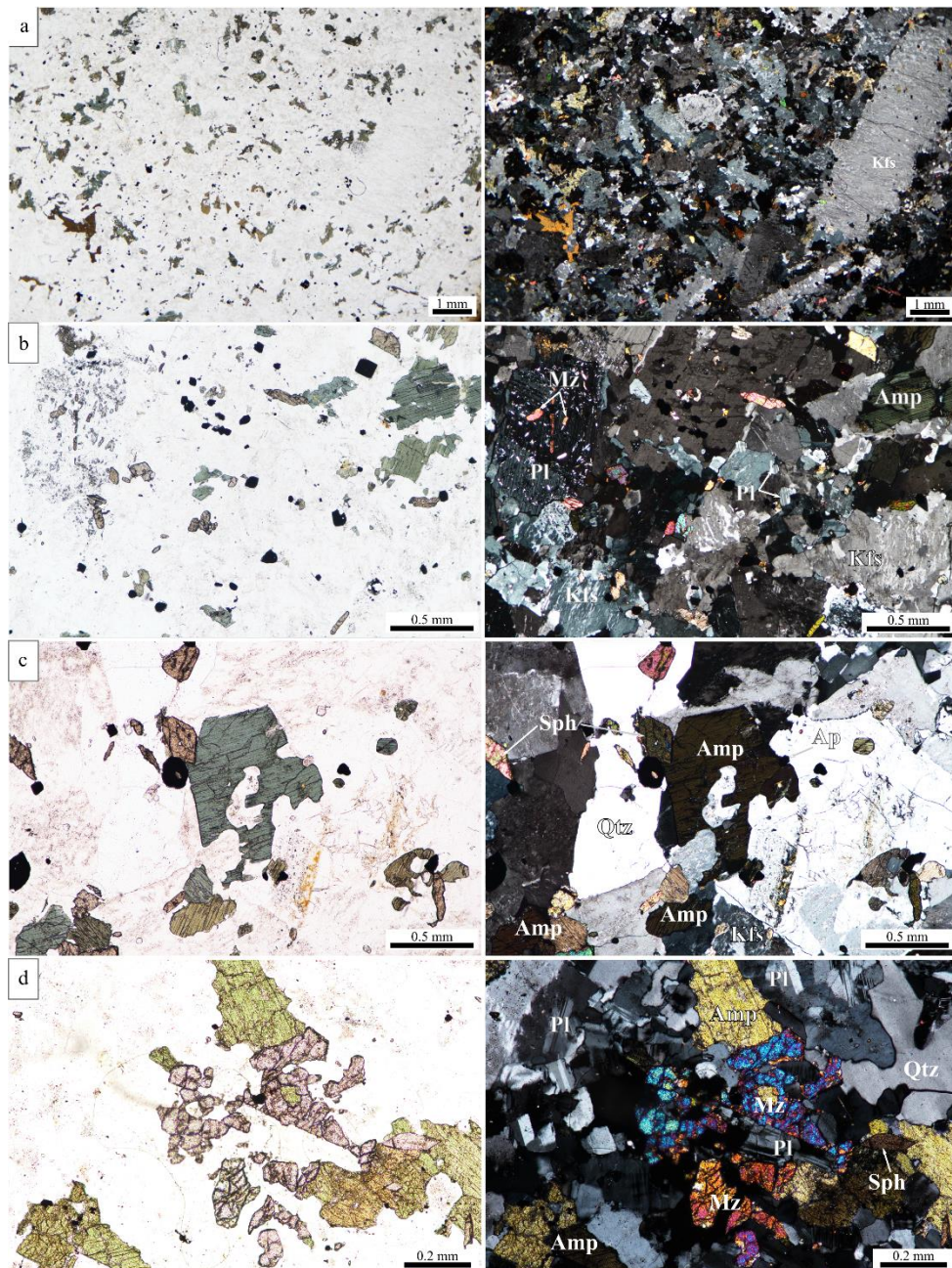


**Fig. 3.7** Petrographic characteristics of fine- to medium-grained syenitic rock from Mae Yan area. **a)** Photomicrograph of fine- to medium-grained syenitic rock with porphyritic texture, showing K-feldspar phenocrysts in perthitic texture and Carlsbad twin with finer-grained K-feldspar rich groundmass. **b)** Photomicrograph of fine- to medium-grained syenitic rock with equigranular texture, showing plagioclase with poikilitic texture, amphibole, K-feldspar, and quartz with monazite inclusion in plagioclase. **c)** Photomicrograph of fine- to medium-grained syenitic rock, showing amphibole with blue to greenish blue pleochroism that indicate riebeckite (Na-amphibole), K-feldspar, quartz, sphene, and apatite. **d)** Photomicrograph of fine- to medium-grained syenitic rock, showing monazite, amphibole and sphene assemblage. Mineral abbreviations: Kfs (K-feldspar); Hbl (hornblende); Qtz (quartz); Pl (plagioclase); Mz (monazite); Sph (sphene); Ap (apatite). (left: plane polarized light, right: cross polarized light).

Amphibole is euhedral to subhedral crystal (grain sizes varying from 0.25 to 0.6 mm across) with irregular outlines, green to greenish brown colored, shows undulatory extinction that might be related to deformation. However, some samples show blue to greenish blue pleochroism that indicate riebeckite (Na-amphibole) (Fig. 3.7b-c). Spene/titanite is euhedral to subhedral crystal with elongate prismatic shape (average grain size 0.1-0.3 mm across). Monazite is anhedral to subhedral with grain sizes 0.02 to 0.10 mm across.

### 3.3 Modal analysis

Eight rock slabs from Tha Takiap area and six rock slabs from Mae Yan area were studied using modal analysis. Rock slabs were stained using Sodium Cobaltinitrite ( $\text{Na}_3\text{Co}(\text{NO}_2)_6$ ) and Amaranth ( $\text{C}_{20}\text{H}_{11}\text{N}_2\text{Na}_3\text{O}_{10}\text{S}_3$ ). After the staining process, K-feldspar was stained by Sodium Cobaltinitrite and turned into yellow while plagioclase was stained by Amaranth and turned into red (Fig. 3.8). Images of stained rock slab were analyzed using Image Pro software to classify color into four classes which are 1) yellow color represents K-feldspar, 2) black color represents mafic minerals (hornblende and pyroxene), 3) white color represents quartz and 4) red color represents plagioclase (Fig. 3.9). Then, percentages of quartz, K-feldspar, plagioclase and mafic mineral were computerized (Table 3.4), and plotted on QAPF diagram for plutonic rock following the recommendation of (Streckeisen, 1976) (Fig. 3.10). However, some samples compose of small crystal of plagioclase that cannot be observed by hand specimens. The petrographic data are combined for estimating the percentage of plagioclase in the samples. QAPF diagram indicates that the plutonic rocks of the Tha Takiap area are composed of various types from alkaline feldspar syenite which absent of quartz to alkaline feldspar quartz syenite with a sample of alkaline feldspar granite. The plutonic rocks of the Mae Yan area are plotted to narrow range compositions from alkaline feldspar syenite to alkaline feldspar quartz syenite.

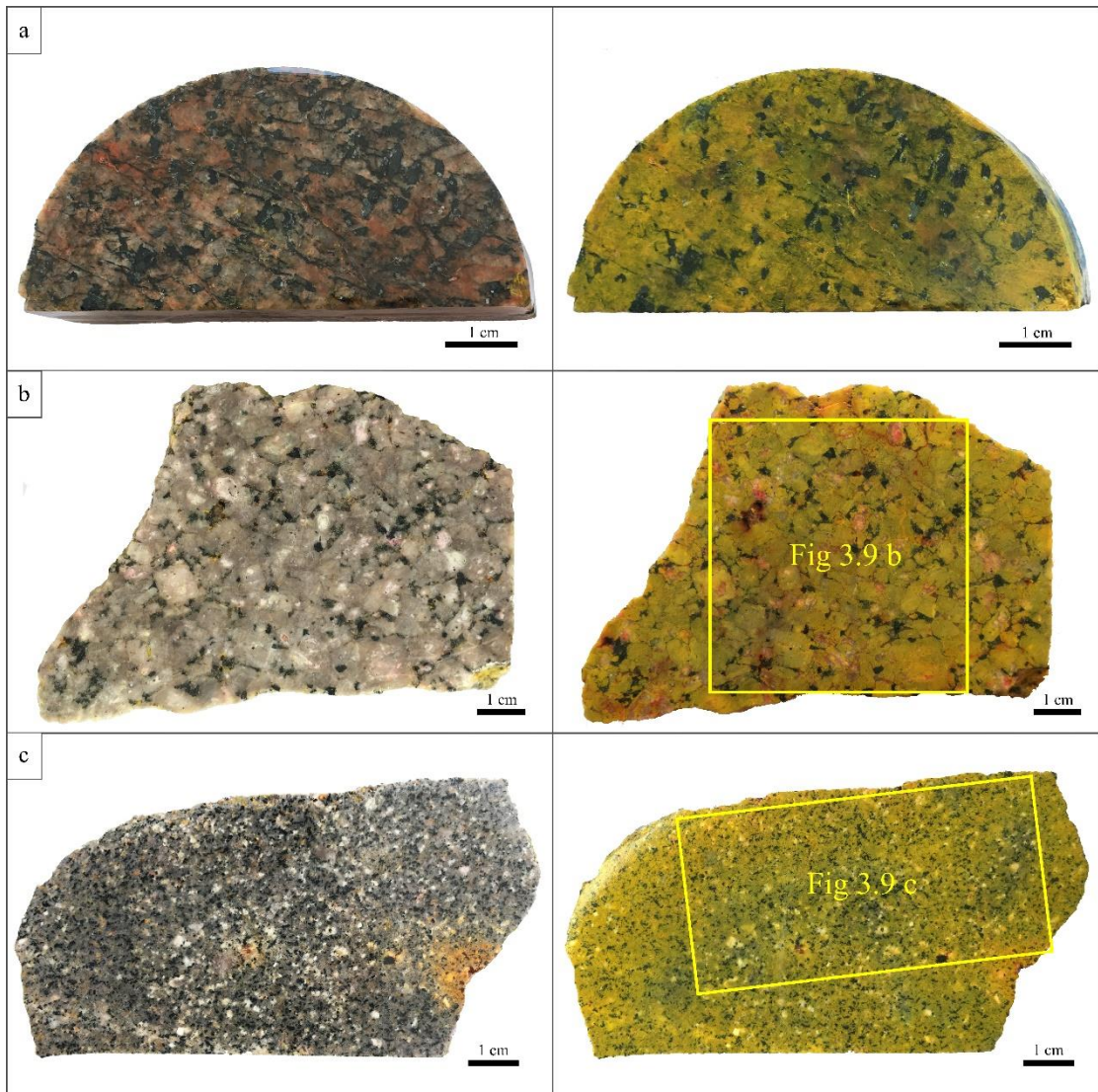


**Fig. 3.8** Photograph of unstained and stained hand specimen sample. **a)** Photograph medium-grained syenitic rock of Tha Takiap area. **b)** Photograph of medium- to coarse-grained syenitic rock of Mae Yan area. **c)** Photograph of fine- to medium-grained syenitic rock of Mae Yan area. (left: unstained sample, right: stained sample).

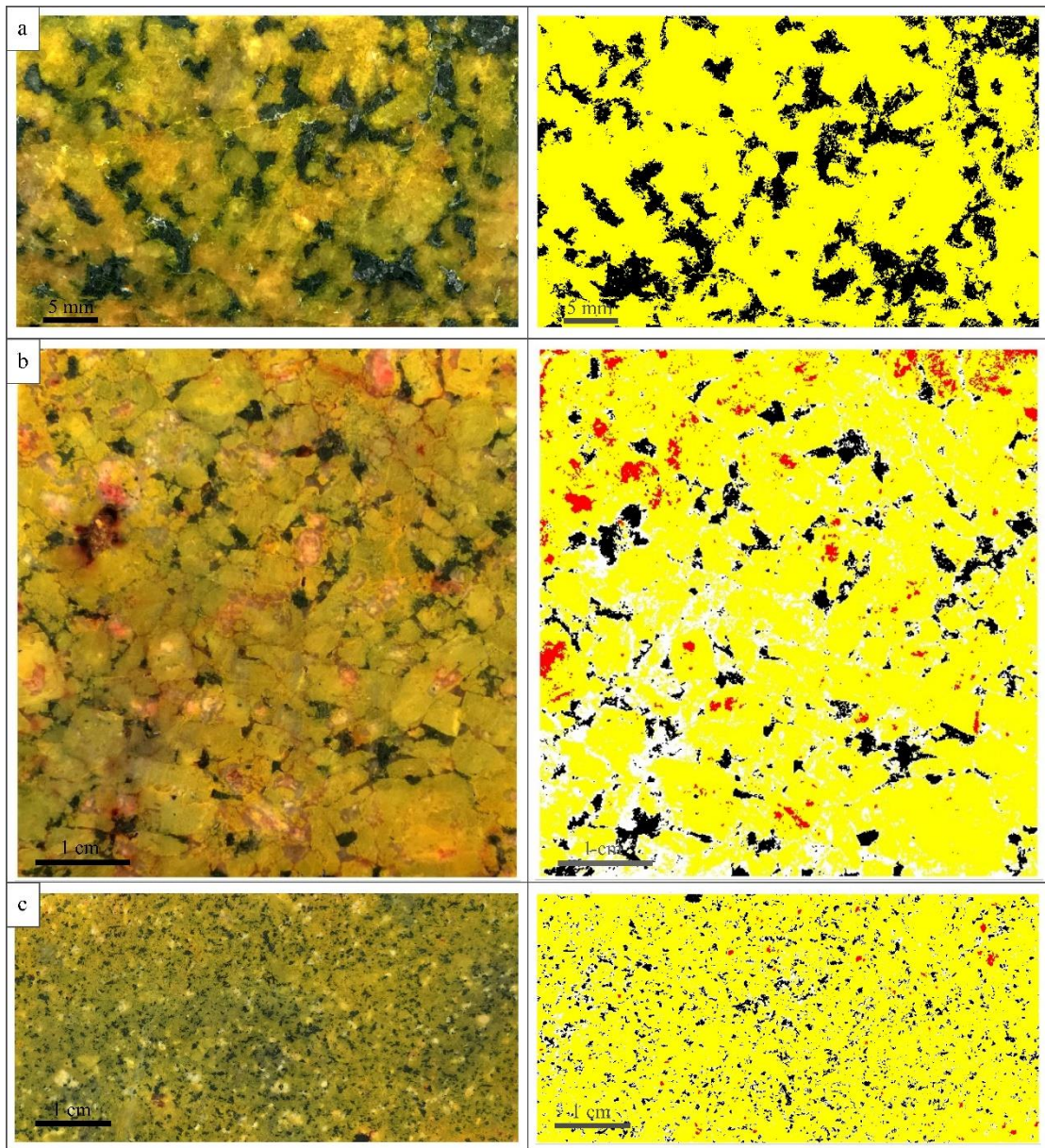


**Fig. 3.9** Image of stained surface which were analyzed using Image Pro software. **a)** Photograph medium-grained syenitic rock of Tha Takiap area. **b)** Photograph of medium- to coarse-grained syenitic rock of Mae Yan area. **c)** Photograph of fine- to medium-grained syenitic rock of Mae Yan area. (left: unclassified by Image Pro software, right: classed by Image Pro software).

**Table 3.4** Summary of petrography (modal analysis, texture and mineral).

Sample no.	Mineral assemblage (%) (Modal analysis)				Texture and grained size	Mineral					
	Quartz	K-feldspar	Plagioclase	Mafic mineral		Hornblende	Pyroxene	Apatite	Sphene	Zircon	Monazite
D11-4	7	70	1	22	Equi, 1.0-3.5 mm	Gr-Br	++	+			
D11-6	0	79	0	21	Equi, 1.0-4.5 mm	Gr-Br		+			
D11-7	No analysis				Equi, 1.0-5.0 mm	Gr-Br	+	+			
D11-11	0	86	0	14	Equi, 1.5-6.0 mm	Gr-Br	++	+			
D11-19	10	77	0	13	Equi, 1.5-6.0 mm	Gr-Br	++	+		+	
D11-20	18	65	0	17	Equi, 1.0-5.0 mm	Gr-Br	++	+			
D11-22	No analysis				Equi, 1.0-3.0 mm	Gr-Br	+++	+		+	
D12-1	9	77	0	14	Equi, 1.0-5.0 mm	Gr-Br	++	++			
D12-6	12	68	0	20	Equi, 1.5-6.0 mm	Gr-Br	++	++			
D12-8	No analysis				Equi, 1.5-6.0 mm	Gr-Br	+++	+		+	
D12-9	16	66	0	18	Equi, 1.0-4.5 mm	Gr-Br	++	+			
D12-11	No analysis				Equi, 1.0-5.0 mm	Gr-Br	++	+			
MH5-1	5	85	1	9	Inequi, 0.5-3.0 mm	Gr-BI	+++	+	+	+	++
MH5-2	8	80	4	8	Por, 0.5-1.5 mm	Gr-BI	+++	++	+	+	++
MH5-3	10	82	2	6	Inequi, 2.0-5.5 mm	Gr	+++	++	++	+	++
MH6	6	88	1	6	Inequi, 3.0-7.0 mm	Gr	++	+	+	+	+
MH14	No analysis				Equi, 0.2-1.0 mm	Gr-BI	+	++	+	+	++
MH36-1	No analysis				Por, 0.5-2.0 mm	Gr	+	++	++	+	++
MH52-1	2	62	1	35	Por, 0.2-1.0 mm	Gr-BI	+++	++	+	+	++
MH52-2	14	76	2	8	Inequi, 1.0-7.0 mm	Gr-BI	++	+	+	+	+

Abbreviations: Equi (equigranular); Inequi (inequigranular); Por (porphyritic); Gr (green); Br (brown); BI (blue); +++ (dominant (>2%)); ++ (common (2-0.5%)), + (minor (<0.5%)).

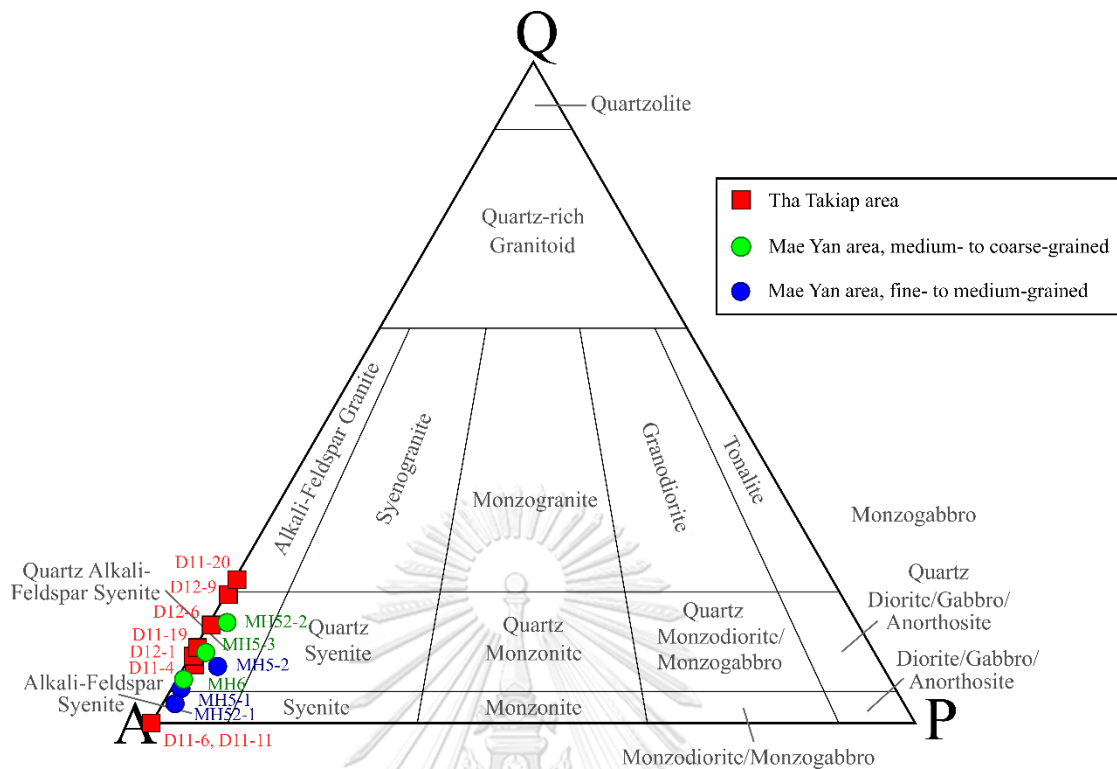


**Fig. 3.10** Modal QAPF diagram (Streckeisen, 1976) of the syenitic rocks in the Tha Takiap and Mae Yan areas (Q=quartz; A=K-feldspar; P=plagioclase). (Red square is syenitic rocks from Tha Takiap area, green circle is medium- to coarse-grained syenitic rocks from Mae Yan area, blue circle is fine- to medium-grained syenitic rocks from Mae Yan area).

## CHAPTER 4

### GEOCHEMISTRY

This chapter describes the geochemistry of syenitic rocks in Tha Takiap and Mae Yan areas. Geochemical data of whole-rock analysis consisting of major oxides, trace elements and rare earth elements were used to classify plutonic rocks, constrain the tectonic setting, and compare the petrogenesis of syenitic rocks from both areas. Moreover, mineral chemistry of amphibole, K-feldspar and plagioclase were carried out using EPMA for geobarometer and geothermometer calculation.

#### 4.1 Sampling and analytical methods

Base on the petrographic study in Chapter 3 the same samples were selected for whole-rock geochemical analysis. In addition, samples were prepared for polished thin sections for mineral chemical analysis. Eleven samples of diamond drill core of syenitic rock from the Tha Takiap area and ten samples of syenitic rock from the Mae Yan area were prepared for the whole-rock geochemistry. Weathered surface on look and small fractures of samples were removed, subsequently crushed to smaller fragment using jaw crusher and pulverized by tungsten carbide ring mill. Moreover, five samples of diamond drill core of syenitic rock from the Tha Takiap area and three samples of syenitic rock from the Mae Yan area were prepared for polished thin sections for the mineral chemical analysis. All sample preparation was conducted at Department of Geology, Chulalongkorn University.

#### **XRF major and minor element analysis**

All samples for XRF analysis were prepared as fused bead. Fused bead was prepared using 1 g of fine powder sample with 5 g of a flux agent (di-lithium tetraborate: lithium metaborate, 66:34) in Platinum crucibles fused at temperature ranging from 1,000-1,200 °C. Major oxides were performed by using a PANalytical (Zetium) wavelength dispersive X-ray fluorescence (WDXRF) spectrometer at DMR. A summary of the instrumental operating conditions is given in Table 4.1. International reference materials namely SY-2 (Syenite), NIM-S (Syenite), G-2 (granite), JG-1a (Granodiorite), and JB-1a (Basalt) were used for calibration. Loss on ignition was determined by heating 1 g of fine powder sample at 1,100 °C for 1 hour and

reweighting. Moreover, ferrous oxide (Iron (II) oxide: FeO) was determined by Gravimetric Titrations Technique described by Rice (1982).

**Table 4.1** Operating conditions for a PANalytical (Zetium) WDXRF spectrometer.

<b>X-ray tube</b>	4 kW, 60 kV, 160 mA, Rh tube
<b>Elemental range</b>	Na to U
<b>Sample loader</b>	64 positions with automatic sample changer
<b>Optic</b>	10 primary beam filter, 4 positions collimator, 6 Analyzer crystals, Vacuum seal
<b>Detectors</b>	Scintillation counter (for heavy elements) Flow proportional counter (for light elements)
<b>Software</b>	Super Q version 6.1
<b>Measurement time</b>	5 mins

#### **Trace elements and REE analysis**

Powder samples were sent to SGS Thailand Limited for further method of sample preparation and ICP-MS analysis. Powder samples were fused with a flux agent (sodium peroxide), totally digested with acid, and prepared sample in form of solutions. REE and Trace elements were determined using Perkin Elmer Elan 6100 Inductivity Coupled Plasma Mass Spectrometer (ICP-MS) by SGS Canada Inc. International reference materials namely SY-4 (Diorite Gneiss) and RTS-3a (Sulphide Ore Mill Tailings), and internal standard solution of 50 ppb Re and 10 ppb Rh were used for calibration. Results of the whole-rock geochemistry were summarized in Table 4.2 and 4.3.

#### **Mineral chemical analysis**

The polished thin sections of all samples were prepared for mineral chemical analysis. The experiment was performed by using a JXA 8100 EPMA at Department of Geology, Chulalongkorn University.

#### **4.2 Major and minor element geochemistry**

The syenitic rocks from the Tha Takiap area have a narrow range of SiO<sub>2</sub> contents from 59.89-64.01 wt.% while those from the Mae Yan area show wider range of SiO<sub>2</sub> from 55.99-71.09 wt.%. Bivariate plots of SiO<sub>2</sub> versus other key major and minor elements are shown in Fig. 4.1a-i. Negative correlations are found between SiO<sub>2</sub> versus TiO<sub>2</sub>, Al<sub>2</sub>O<sub>3</sub>, Fe<sub>2</sub>O<sub>3</sub><sup>(total)</sup>, MgO, CaO, P<sub>2</sub>O<sub>5</sub> and MnO (Fig. 4.1 a-g),



**Table 4.2** Whole-rock major and trace elements data of syenitic rock in Tha Takiap area.

Sample No.	D11-4	D11-7	D11-11	D11-19	D11-20	D11-22	D12-6	D12-8	D12-9	D12-11	D12-25
TAS classification	Syenite	Syenite	Syenite	Syenite	Syenite	Syenite	Syenite	Syenite	Syenite	Syenite	Syenite
<i>Major element (wt%)</i>											
SiO <sub>2</sub>	60.82	60.86	60.65	59.89	64.01	61.42	60.23	60.78	62.28	61.73	60.59
TiO <sub>2</sub>	0.56	0.60	0.79	0.67	0.48	0.70	0.63	0.67	0.56	0.59	0.63
Al <sub>2</sub> O <sub>3</sub>	15.88	17.91	16.38	16.14	15.04	16.97	16.25	16.43	16.00	15.75	16.42
Fe <sub>2</sub> O <sub>3</sub> <sup>(total)</sup>	6.87	4.83	7.05	7.75	7.12	6.35	6.51	7.39	6.94	6.69	7.09
FeO	5.10	2.78	5.36	5.45	5.64	4.84	4.11	5.21	5.02	4.84	5.29
MnO	0.18	0.10	0.18	0.22	0.17	0.16	0.20	0.18	0.18	0.16	0.17
MgO	0.17	0.67	0.25	0.31	0.25	0.15	0.25	0.28	0.19	0.22	0.31
CaO	2.84	1.75	2.71	2.98	2.52	2.46	2.62	2.94	2.51	2.40	2.61
Na <sub>2</sub> O	4.95	5.58	4.98	5.12	4.41	5.06	4.85	5.10	4.84	5.93	5.06
K <sub>2</sub> O	5.52	5.64	5.91	5.32	5.22	5.87	5.83	5.14	5.68	5.53	5.56
P <sub>2</sub> O <sub>5</sub>	0.12	0.14	0.14	0.16	0.11	0.11	0.11	0.13	0.11	0.11	0.13
LOI	1.57	1.40	0.60	1.05	0.28	0.41	1.97	0.57	0.37	0.53	1.10
Sum	99.49	99.49	99.63	99.61	99.63	99.67	99.44	99.60	99.67	99.65	99.66
CIA	45.16	49.23	45.63	45.17	46.25	46.98	46.04	45.98	46.14	43.91	46.26
K <sub>2</sub> O/Na <sub>2</sub> O	1.12	1.01	1.19	1.04	1.18	1.16	1.20	1.01	1.17	0.93	1.10
A/CNK	0.82	0.97	0.84	0.82	0.86	0.89	0.85	0.85	0.86	0.78	0.86
A/NK	1.12	1.17	1.12	1.14	1.17	1.16	1.14	1.18	1.13	1.00	1.15
<i>Trace element (ppm)</i>											
Sc	<5.00	<5.00	6.00	9.00	5.00	6.00	<5.00	11.0	<5.00	<5.00	6.00
V	<5.00	5.00	<5.00	25.0	21.0	10.00	<5.00	68.0	<5.00	<5.00	<5.00
Cr	<10.0	<10.0	<10.0	20.0	10.0	<10.00	<10.0	80.0	<10.0	<10.0	<10.0
Co	1.20	0.60	1.60	1.60	1.40	1.00	<0.50	28.5	<0.50	1.30	2.90
Ni	5.00	<5.00	6.00	11.0	10.0	8.00	6.00	32.0	<5.00	6.00	8.00
Cu	42.0	14.0	20.0	17.0	12.0	13.0	13.0	21.0	230	11.0	34.0
Zn	33.0	46.0	73.0	53.0	33.0	30.0	10.0	77.0	21.0	50.0	26.0
Ga	67.0	37.0	60.0	62.0	37.0	43.0	63.0	18.0	18.0	50.0	48.0
Rb	522	1220	1270	574	413	398	472	50.5	90.9	851	1250
Sr	9.40	10.9	11.0	8.10	8.70	4.50	8.60	9.40	10.0	7.30	7.40
Y	82.4	144	303	87.5	35.0	56.6	56.9	69.3	395	123	273.0
Zr	60.2	380	318	646	403	496	192	637	22.1	478	379
Nb	40.0	52.0	139	75.0	47.0	60.0	164	13.0	5.00	97.0	46.0
Cs	101	121	218	153	101	99.2	64.5	9.4.0	16.5	136	89.9
Ba	5.80	5.50	20.3	25.2	21.9	4.70	3.80	167	3.80	2.60	22.5
Hf	4.00	15.0	17.0	23.0	13.0	17.0	11.0	18.0	<1.00	17.0	16.0
Ta	17.6	39.7	56.9	20.4	15.0	16.9	123	1.10	3.20	39.6	60.8
Tl	2.70	7.90	8.30	3.00	2.10	2.10	2.80	<0.5	0.70	4.90	8.90
Pb	68.0	91.0	148	60.0	22.0	15.0	113	33.0	77.0	78.0	174
Bi	6.7	2.80	10.0	7.70	5.50	5.90	1.90	0.50	8.20	9.30	4.40
Th	42.5	39.3	80.1	144	86.6	97.6	36.6	21.1	9.8	56.7	24.9
U	7.50	30.5	22.1	32.1	6.22	5.98	9.11	3.99	12.6	15.3	17.6
<i>Rare earth element (ppm)</i>											
La	15.7	27.0	66.9	46.5	16.7	20.9	30.4	104	59.3	46.6	43.9
Ce	35.8	67.4	167	107	35.9	45.6	59.1	70.3	17.8	110	74.3
Pr	4.30	9.36	20.4	11.8	3.96	5.26	7.48	23.2	16.6	13.3	14.2
Nd	17.3	37.2	74.9	42.2	13.8	18.5	24.4	83.4	70.0	47.6	58.4
Sm	7.10	15.2	26.9	10.7	3.00	4.00	8.40	15.3	24.3	15.2	21.7
Eu	0.15	0.09	0.17	0.15	0.11	0.06	0.15	2.91	1.38	0.07	0.75
Gd	8.52	17.5	32.5	9.44	3.07	4.37	7.61	15.0	29.9	15.4	27.1
Tb	1.80	3.62	6.94	1.90	0.67	1.01	1.44	2.21	5.81	3.18	5.53
Dy	11.9	23.3	46.7	12.9	5.03	7.60	8.97	13.1	37.0	19.6	35.9
Ho	2.45	4.77	9.44	2.85	1.10	1.81	1.55	2.54	7.17	3.85	7.12
Er	7.39	14.1	29.4	8.56	3.68	5.67	4.69	6.91	21.8	11.3	22.2
Tm	1.25	2.43	4.89	1.48	0.62	0.96	0.88	0.95	3.87	1.97	4.01
Yb	8.60	17.0	35.4	10.0	4.30	6.60	7.50	6.20	30.0	15.2	30.3
Lu	1.31	2.68	5.55	1.61	0.64	1.05	1.23	0.92	4.65	2.37	4.63
ΣREE	124	242	527	267	92.6	123	164	347	330	306	350
ΣREE+Y	206	386	830	355	128	180	221	416	725	429	623
LREE/HREE	2.06	2.03	2.28	4.67	4.01	3.39	4.06	6.57	1.56	3.41	1.76
Ce/Ce*	1.07	1.04	1.11	1.12	1.08	1.07	0.96	0.35	0.14	1.08	0.73
Eu/Eu*	0.06	0.02	0.02	0.05	0.11	0.04	0.06	0.59	0.16	0.01	0.09
(La/Yb) <sub>N</sub>	1.31	1.14	1.36	3.34	2.79	2.27	2.91	12.0	1.42	2.20	1.04

Note: TAS=Total-alkali versus silica. Fe<sub>2</sub>O<sub>3</sub><sup>(total)</sup> is total iron which were determined by XRF. FeO is ferrous oxide that were determined by gravimetric titrations technique. LOI, loss on ignition. A/CNK = molar ratio Al<sub>2</sub>O<sub>3</sub>/(CaO+Na<sub>2</sub>O+K<sub>2</sub>O), A/NK = molar ratio Al<sub>2</sub>O<sub>3</sub>/(Na<sub>2</sub>O+K<sub>2</sub>O), CIA (chemical index of alteration) = molar ratio Al<sub>2</sub>O<sub>3</sub>/(Al<sub>2</sub>O<sub>3</sub>+CaO+Na<sub>2</sub>O+K<sub>2</sub>O)×100 (Nesbitt and Young, 1982), ΣREE= total REE content, LREE= La, Ce, Pr, Nd, Sm and Eu, HREE=Gd, Tb, Dy, Ho, Er, Tm, Yb and Lu, Ce/Ce\*=Ce<sub>N</sub>/(La<sub>N</sub>×Pr<sub>N</sub>)<sup>0.5</sup>, Eu/Eu\*=Eu<sub>N</sub>/(Sm<sub>N</sub>×Gd<sub>N</sub>)<sup>0.5</sup>

**Table 4.3** Whole-rock major and trace elements data of syenitic rock in Mae Yan area.

Sample No.	MH5-1	MH5-2	MH5-3	MH6	MH36-1	MH36-2	MH50	MH51	MH52-1	MH52-2
TAS classification	Syenite	Syenite	Syenite	Syenite	Syenite	Syenite	Granite	Granite	Syenite	Syenite
<i>Major element (wt%)</i>										
SiO <sub>2</sub>	61.70	59.40	64.87	63.47	65.27	65.15	71.09	70.62	55.99	64.33
TiO <sub>2</sub>	0.77	0.67	0.37	0.33	0.59	0.49	0.24	0.31	0.85	0.41
Al <sub>2</sub> O <sub>3</sub>	15.47	17.19	16.14	16.70	13.87	16.71	13.53	13.86	15.99	16.82
Fe <sub>2</sub> O <sub>3</sub> <sup>(total)</sup>	4.78	5.45	2.69	2.25	4.25	3.36	1.99	2.35	6.44	3.23
FeO	1.70	2.24	1.16	0.90	1.08	0.36	0.72	0.36	3.13	1.25
MnO	0.08	0.11	0.07	0.06	0.18	0.14	0.06	0.04	0.12	0.07
MgO	0.90	1.00	0.69	0.62	0.81	0.27	0.36	0.26	3.07	0.57
CaO	3.59	2.84	2.60	2.01	2.73	0.34	1.41	1.27	5.72	2.32
Na <sub>2</sub> O	3.64	3.71	4.74	4.19	3.05	3.37	3.63	4.78	3.01	4.90
K <sub>2</sub> O	7.65	8.47	7.06	9.23	8.23	8.78	6.83	5.57	7.38	6.68
P <sub>2</sub> O <sub>5</sub>	0.33	0.26	0.24	0.10	0.41	0.06	0.13	0.12	0.80	0.20
LOI	0.46	0.38	0.28	0.56	0.27	0.94	0.29	0.32	0.28	0.17
Sum	99.37	99.48	99.74	99.52	99.63	99.61	99.55	99.51	99.65	99.72
CIA	42.63	45.69	44.48	44.86	42.35	51.61	45.93	46.10	40.66	46.28
K <sub>2</sub> O/Na <sub>2</sub> O	2.10	2.28	2.70	2.60	1.88	2.45	1.49	2.20	1.17	1.36
A/CNK	0.74	0.84	0.80	0.81	0.73	1.07	0.85	0.86	0.69	0.86
A/NK	1.08	1.13	1.05	0.99	1.00	1.11	1.01	1.00	1.24	1.10
<i>Trace element (ppm)</i>										
Sc	<5.00	<5.00	<5.00	<5.00	<5.00	<5.00	<5.00	<5.00	9.00	<5.00
V	95.0	90.0	38.0	43.0	106	50.0	21.0	27.0	129	40.0
Cr	19.0	<10.0	14.0	<10.0	15.0	<10.0	11.0	<10.0	32.0	<10.0
Co	5.90	7.30	3.00	2.70	4.40	2.30	2.10	1.10	17.5	3.80
Ni	11.0	10.0	13.0	9.00	9.00	<5.00	<5.00	5.00	25.0	7.00
Cu	11.0	<10.0	<10.0	<10.0	<10.0	<10.0	<10.0	<10.0	17.0	<10.0
Zn	103	91.0	55.0	42.0	172	114	98.0	34.0	104	73.0
Ga	24.0	23.0	24.0	24.0	23.0	28.0	27.0	26.0	21.0	26.0
Rb	289	310	317	329	455	487	457	464	265	292
Sr	3700	3553	2606	2444	681	557	843	614	3533	2090
Y	62.7	43.3	31.5	25.1	134	89.3	28.6	78.2	50.5	36.9
Zr	573	603	254	199	758	745	595	786	611	1000
Nb	47.0	35.0	23.0	27.0	47.0	77.0	29.0	39.0	29.0	28.0
Cs	4.20	2.90	5.50	7.50	10.6	14.8	7.40	7.40	9.00	10.4
Ba	5143	2959	1907	3907	2384	842	1489	5084	3781	1720
Hf	12.0	13.0	6.00	5.00	17.0	17.0	16.0	21.0	15.0	21.0
Ta	3.70	1.90	1.70	1.50	1.90	3.70	1.70	2.50	1.80	2.10
Tl	1.90	1.80	1.90	2.40	2.80	3.30	2.40	2.00	1.60	1.80
Pb	121	162	131	146	110	643	46.0	65.0	155	164
Bi	0.20	0.30	0.40	0.90	0.60	2.50	0.30	0.30	0.50	0.20
Th	70.1	107	37.2	35.6	126	288	108	143	72.5	49.3
U	11.5	13.1	7.45	6.43	11.2	27.6	15.0	21.9	13.8	12.0
<i>Rare earth element (ppm)</i>										
La	361	375	189	203	387	564	246	685	335	235
Ce	628	663	329	312	378	469	323	380	611	361
Pr	68.4	68.2	34.2	32.0	61.8	149	39.7	91.2	73.2	38.1
Nd	219	211	108	98.9	207	464	121	269	252	117
Sm	34.0	29.5	16.2	14.2	27.6	66.1	15.6	34.8	36.4	17.5
Eu	6.70	6.61	3.28	3.14	5.89	12.4	3.04	6.37	9.12	3.78
Gd	19.5	14.8	9.11	7.45	22.2	33.3	8.43	21.1	21.5	10.5
Tb	2.46	1.87	1.15	0.94	2.52	3.95	1.04	2.55	2.4	1.33
Dy	12.3	8.47	5.54	4.30	12.9	18.4	4.88	12.7	10.8	6.38
Ho	2.14	1.46	0.95	0.71	2.80	3.07	0.84	2.25	1.81	1.10
Er	5.23	3.65	2.39	1.70	7.78	7.85	2.23	6.16	4.31	2.94
Tm	0.72	0.51	0.32	0.22	1.05	1.15	0.34	0.94	0.61	0.45
Yb	3.90	3.10	1.80	1.20	5.90	7.20	2.10	6.30	3.50	2.70
Lu	0.58	0.47	0.28	0.19	1.09	1.07	0.36	0.98	0.52	0.44
ΣREE	1364	1388	701	680	1124	1800	769	1519	1362	798
ΣREE+Y	1427	1431	733	705	1258	1890	797	1598	1413	835
LREE/HREE	28.5	39.9	32.0	40.1	19.4	23.1	37.4	28.1	29.4	30.3
Ce/Ce*	0.98	1.02	1.00	0.95	0.60	0.40	0.80	0.96	0.37	0.94
Eu/Eu*	0.80	0.97	0.83	0.93	0.73	0.81	0.81	1.00	0.72	0.85
(La/Yb) <sub>N</sub>	66.4	86.8	75.3	121.3	47.1	56.2	84.0	68.7	78.0	62.4

Note: TAS=Total-alkali versus silica. Fe<sub>2</sub>O<sub>3</sub><sup>(total)</sup> is total iron which were determined by XRF. FeO is ferrous oxide that were determined by gravimetric titrations technique. LOI, loss on ignition. A/CNK = molar ratio Al<sub>2</sub>O<sub>3</sub>/(CaO+Na<sub>2</sub>O+K<sub>2</sub>O), A/NK = molar ratio Al<sub>2</sub>O<sub>3</sub>/(Na<sub>2</sub>O+K<sub>2</sub>O), CIA (chemical index of alteration) = molar ratio Al<sub>2</sub>O<sub>3</sub>/(Al<sub>2</sub>O<sub>3</sub>+CaO+Na<sub>2</sub>O+K<sub>2</sub>O)×100 (Nesbitt and Young, 1982), ΣREE= total REE content, LREE= La, Ce, Pr, Nd, Sm and Eu, HREE=Gd, Tb, Dy, Ho, Er, Tm, Yb and Lu, Ce/Ce\*=Ce<sub>N</sub>/(La<sub>N</sub>×Pr<sub>N</sub>)<sup>0.5</sup>, Eu/Eu\*=Eu<sub>N</sub>/(Sm<sub>N</sub>×Gd<sub>N</sub>)<sup>0.5</sup>

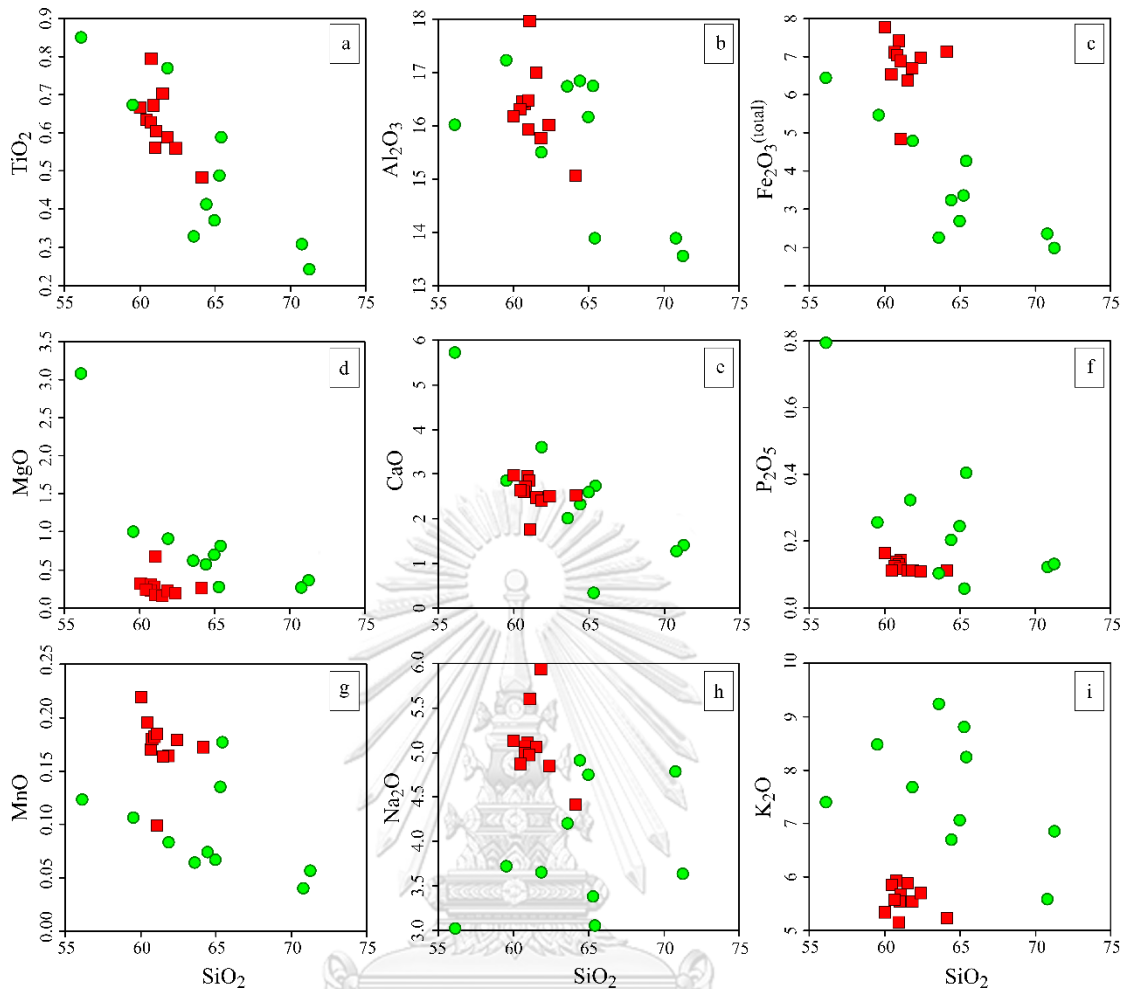


**Fig. 4.1** Major and minor element bivariate diagrams plot against  $\text{SiO}_2$  for syenitic rocks from the Tha Takiap and the Mae Yan areas; (a)  $\text{SiO}_2$  versus  $\text{TiO}_2$  (wt%); (b)  $\text{SiO}_2$  versus  $\text{Al}_2\text{O}_3$  (wt%); (c)  $\text{SiO}_2$  versus  $\text{Fe}_2\text{O}_3^{\text{(total)}}$  (wt%); (d)  $\text{SiO}_2$  versus  $\text{MgO}$  (wt%); (e)  $\text{SiO}_2$  versus  $\text{CaO}$  (wt%); (f)  $\text{SiO}_2$  versus  $\text{P}_2\text{O}_5$  (wt%); (g)  $\text{SiO}_2$  versus  $\text{MnO}$  (wt%); (h)  $\text{SiO}_2$  versus  $\text{Na}_2\text{O}$  (wt%); (i)  $\text{SiO}_2$  versus  $\text{K}_2\text{O}$  (wt%) (Red square is syenitic rocks from the Tha Takiap area, green circle is syenitic rocks from the Mae Yan area).

whereas  $\text{Na}_2\text{O}$  and  $\text{K}_2\text{O}$  are unclear correlation with  $\text{SiO}_2$  (Fig. 4.1h-i). However, the bivariate plots show distinct concentration of  $\text{Fe}_2\text{O}_3^{\text{(total)}}$ ,  $\text{MgO}$ ,  $\text{MnO}$ ,  $\text{Na}_2\text{O}$  and  $\text{K}_2\text{O}$  in the rocks from the two study areas including higher concentration of  $\text{Fe}_2\text{O}_3^{\text{(total)}}$ ,  $\text{MnO}$  and  $\text{Na}_2\text{O}$  in the rocks from the Tha Takiap area, and higher concentration of  $\text{MgO}$  and  $\text{K}_2\text{O}$  in the rocks from the Mae Yan area.

Base on their total-alkali ( $\text{Na}_2\text{O}+\text{K}_2\text{O}$ ) versus silica (TAS) diagram by (Cox, Bell, and Pankhurst, 1979) (Fig. 4.2), all of the rocks are classified as alkaline and all of their plots are fallen within syenite field excepted two samples from the Tha Takiap area which are showing plots on granite fields. Based on the total molar alkali versus

alumina content ( $A/NK$  ( $Al_2O_3/(Na_2O+K_2O)$ ) versus  $A/CNK$  ( $Al_2O_3/(CaO + Na_2O + K_2O)$ ) diagram suggested by (Shand, 1943) (Fig. 4.3), most of the syenitic rocks are classified as metaluminous and are classified as I-type granite based on Alumina Saturation Index (ASI) (Chappell and White, 1974).  $K_2O$  versus  $Na_2O$  (wt%) diagram for alkali magma series (Middlemost, 1975) (Fig. 4.4) subdivided syenitic rocks from the Mae Yan area into K-series to High-K-series, whereas those from the Tha Takiap area were subdivided into K-series. Moreover, geochemical classification diagrams for granitic rocks of Frost et al. (2001) can subdivide syenitic rocks from the study areas as alkalic ferroan granitoid (Fig. 4.5a-b).

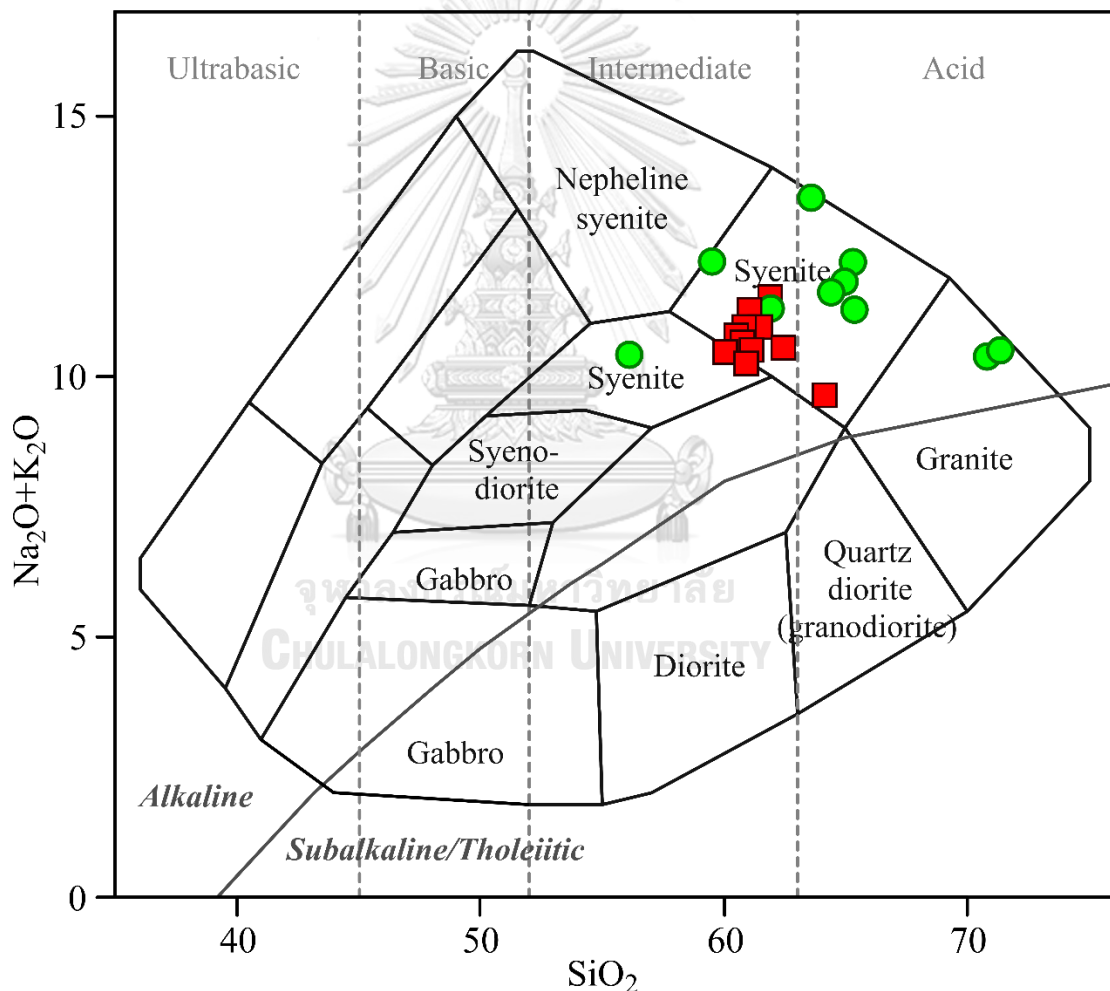


**Fig. 4.2** Total-alkali versus silica (TAS) diagram of plutonic rock after (Cox et al., 1979) and adapted by (Wilson, 1989) for plutonic rocks showing rocks ranged in composition from syenite to granite within the field of alkaline, and differentiation trends. (Rock type symbols are same as Fig. 4.1).

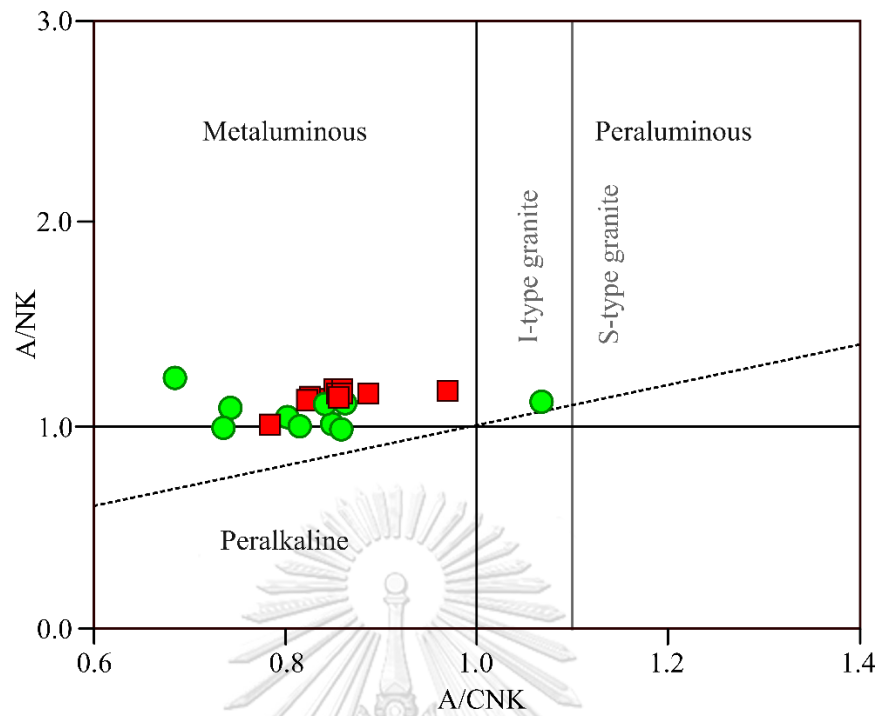


**Fig. 4.3** A/NK versus A/CNK diagram (after Shand (1943)) and I- and S-type granite classification boundary based on alumina saturation index (ASI) (gray line) (after Chappell and White (1974)). (Rock type symbols are same as Fig. 4.1).

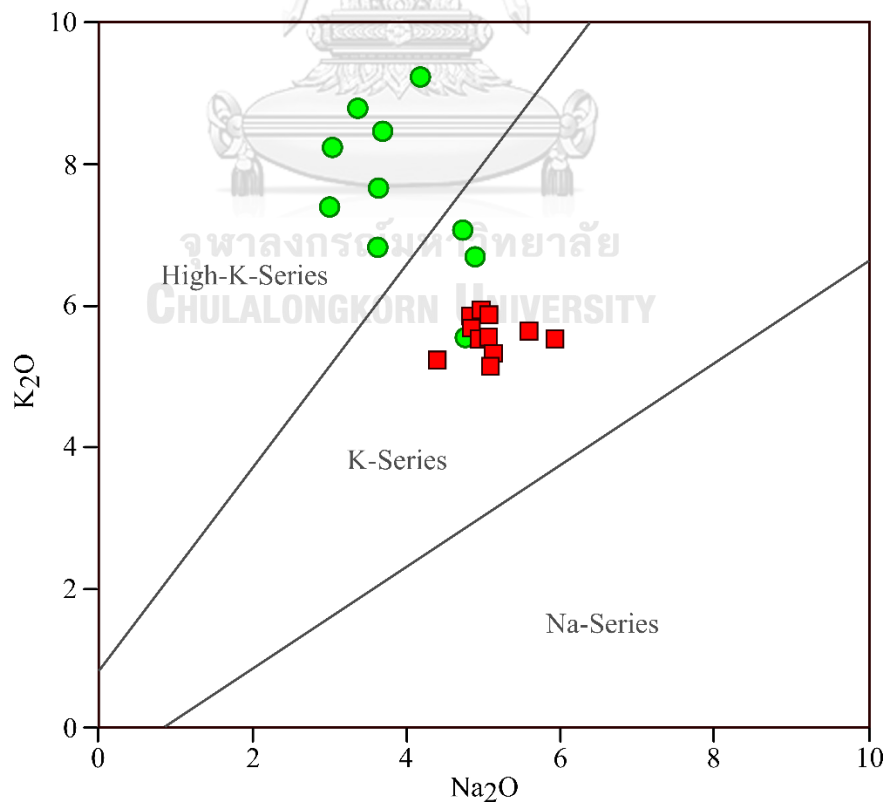


**Fig. 4.4** K<sub>2</sub>O versus Na<sub>2</sub>O (wt%) diagram subdividing the alkaline magma series (after Middlemost (1975)). (Rock type symbols are same as Fig. 4.1).

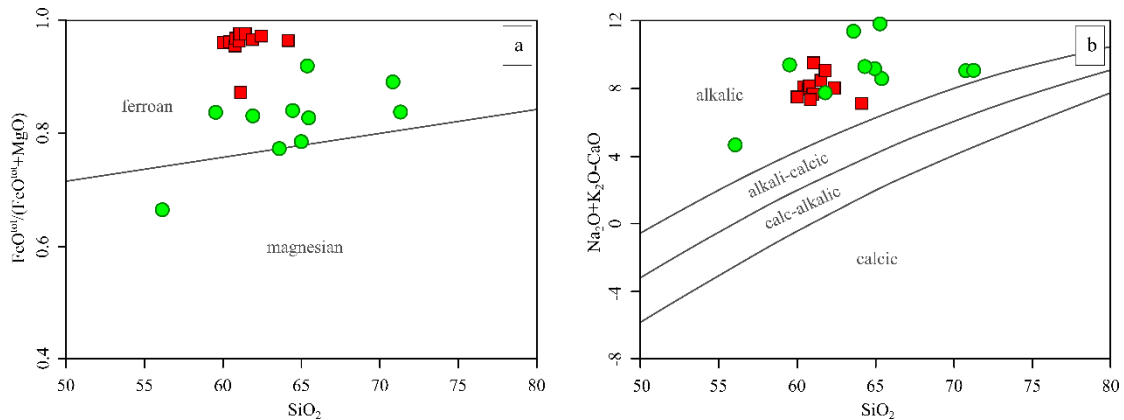


**Fig. 4.5** Geochemical classification diagrams for syenitic rocks (after Frost et al. (2001)); (a)  $\text{FeO}^{\text{tot}}/(\text{FeO}^{\text{tot}}+\text{MgO})$  versus  $\text{SiO}_2$  (wt%) diagram classifies the studied syenitic rocks into ferroan granitoids; (b)  $\text{Na}_2\text{O}+\text{K}_2\text{O}-\text{CaO}$  versus  $\text{SiO}_2$  (wt%) diagram classifies the studied syenitic rocks into alkalic affinity. (Rock type symbols are same as Fig. 4.1).

### 4.3 Trace element and REE geochemistry

Plots of high field strength elements (HFSE), such as Ga, Zr, Nb, Ce, and Y (Whalen, Currie, and Chappell, 1987) (Fig. 4.6 a-d) indicate that syenitic rocks of the Tha Takiap and Mae Yan areas are A-type granite affinities. The primitive mantle normalized and chondrite-normalized (Sun and McDonough, 1989) trace and rare earth elements (REE) spider diagrams of the syenitic rocks from both areas were presented in Fig. 4.7a-d. Samples from the Tha Takiap area show the depletion of some large ion lithophile elements LILE (Ba, Sr and Eu) and Ti, and the enrichment of Cs, Th, U, Ta, and Pb (Fig. 4.7a). Three samples of the Tha Takiap area have slightly different patterns showing more distinct negative anomalies of Nb and Ce and less distinct anomaly of Eu (Fig. 4.7a). The syenitic rock samples of the Tha Takiap area exhibit nearly flat REE patterns with  $(\text{La}/\text{Yb})_{\text{N}}$  ratios ranging from 1.04-3.34 (one exception having  $(\text{La}/\text{Yb})_{\text{N}}$  ratio of 12.03) ( $(\text{La}/\text{Sm})_{\text{N}}$  ratio range from 1.15-4.39 and  $(\text{Sm}/\text{Tb})_{\text{N}}$  ratio range from 0.67-2.74.), and prominent negative Eu anomalies ( $\text{Eu}/\text{Eu}^*=0.01-0.59$  (average=0.11)) in all of the patterns and weak negative Ce anomalies ( $\text{Ce}/\text{Ce}^*=0.14-1.12$  (average=0.89)) in few patterns were found (Fig. 4.7b). In contrast, the samples from the Mae Yan area show the depletion of Nb, Ta, P, and Ti (Fig. 4.7c), and the enrichment of Th, U, La, Pb and Nd. The syenitic rocks of the Mae Yan area exhibit high light rare earth elements (LREE) chondrite-normalized patterns and moderately steep slope of depletion in heavy rare earth element (HREE) ( $(\text{La}/\text{Yb})_{\text{N}}$  ratio range from 47.1-121.3 ( $(\text{La}/\text{Sm})_{\text{N}}$  ratio range from 5.51-12.71 and  $(\text{Sm}/\text{Tb})_{\text{N}}$  ratio range from 5.20-

13.15) with weak negative Ce anomalies ( $Ce/Ce^*=0.37-1.02$  (average=0.80)) in few patterns and very weak negative Eu anomalies ( $Eu/Eu^*=0.72-1.00$  (average=0.84)) (Fig. 4.7d)

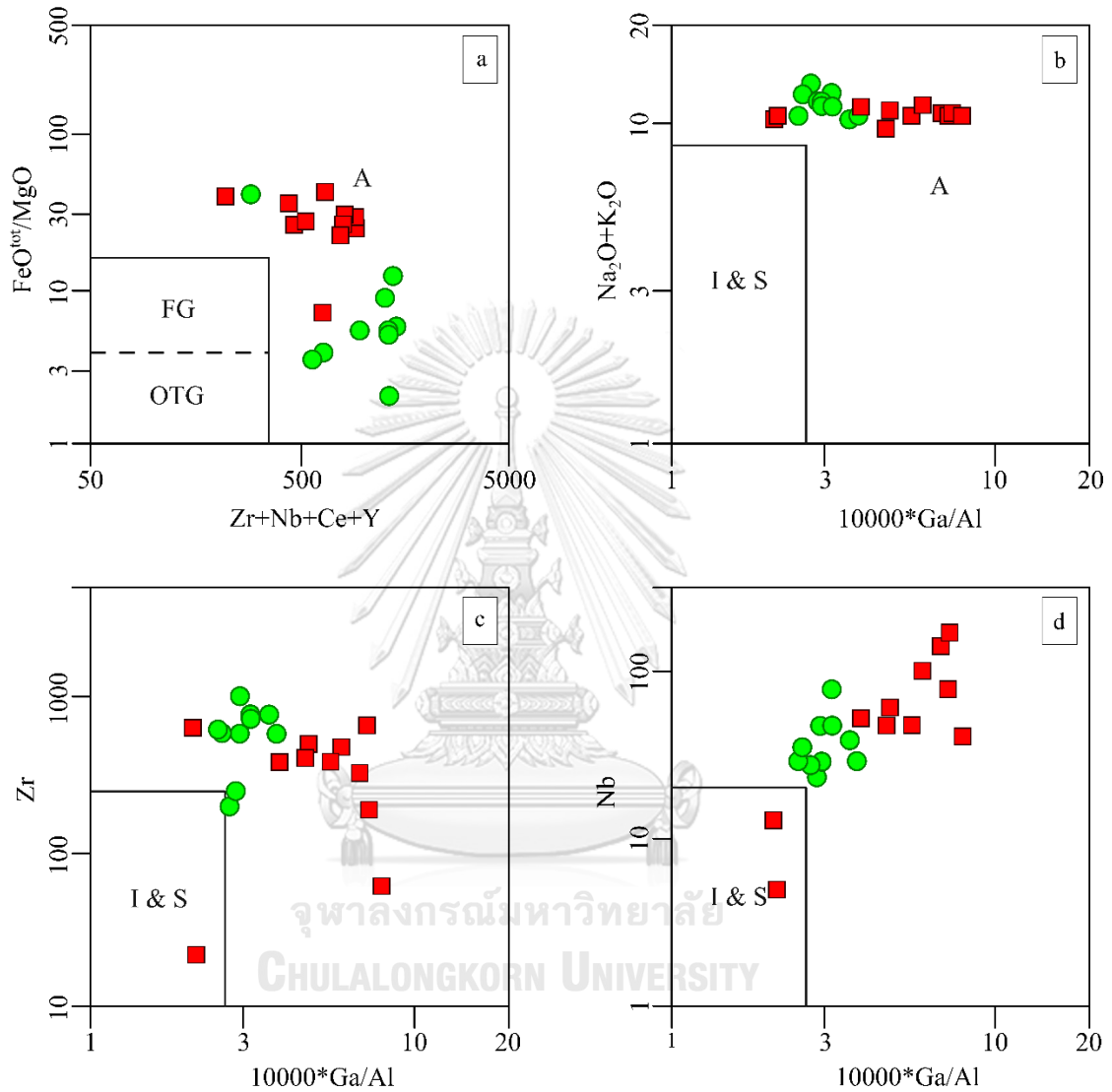


**Fig. 4.6** Bivariate plots after Whalen et al. (1987) of syenitic rocks from the Tha Takiap and Mae Yan areas showing the enrichment of HFSEs indicate that syenitic rocks of the both areas are A-type granite affinities; **(a)**  $FeO^{tot}/MgO$  versus  $Zr+Nb+Ce+Y$ ; **(b)**  $Na_2O+K_2O$  versus  $10000*Ga/Al$ ; **(c)**  $Zr$  versus  $10000*Ga/Al$ ; **(d)**  $Nb$  versus  $10000*Ga/Al$  (FG = field for fractionated felsic granites; OTG = field for unfractionated A-, I- and S-type granites; I=I-type; S=S-type; A=A-type) (Rock type symbols are same as Fig. 4.1).

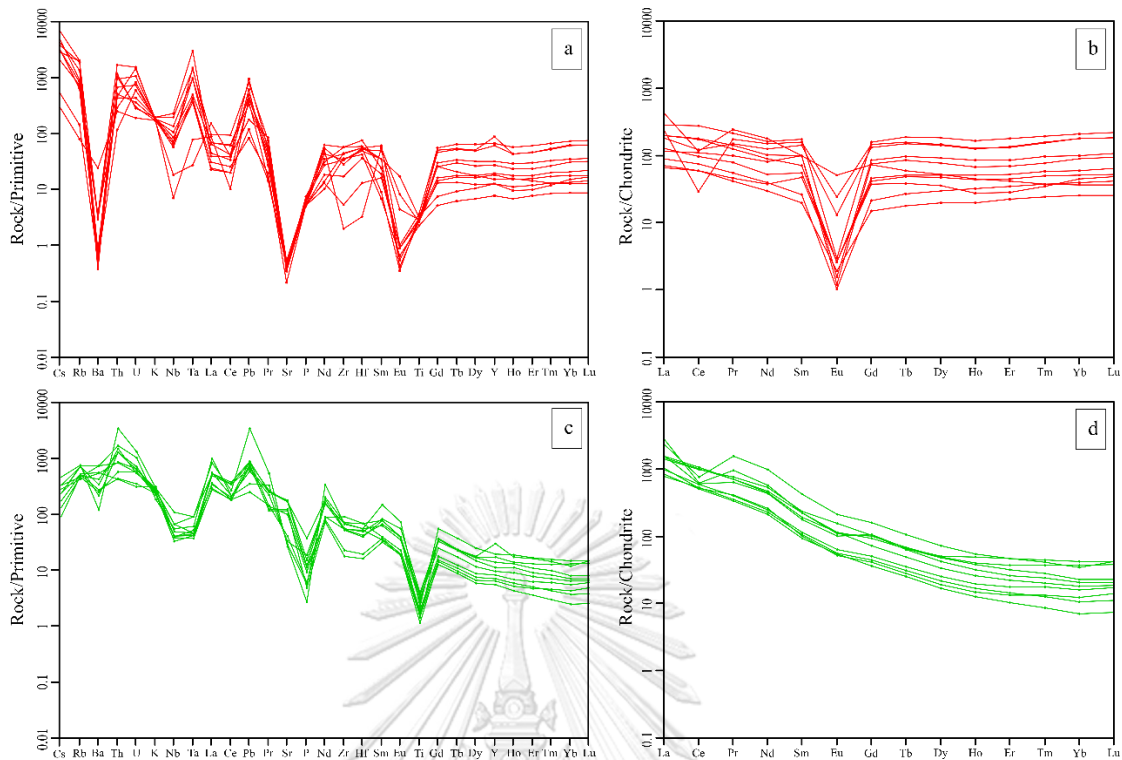


**Fig. 4.7** Spider diagrams of syenitic rocks in the study areas plotted using normalized values of (Sun and McDonough, 1989). **(a, b)** Primitive mantle-normalized spider diagrams and chondrite-normalized REE patterns of the Tha Takiap syenitic rocks, respectively. **(c, d)** Primitive mantle-normalized spider diagrams and chondrite-normalized REE patterns of the Mae Yan syenitic rocks, respectively.

#### 4.4 Interpretation of whole-rock geochemistry

Based on petrographic study, the syenitic rocks from both areas are mainly composed of K-feldspar with a few of quartz and plagioclase. Riebeckite (sodic amphibole) is usually found as an accessory mineral in syenitic rock from the Mae Yan area. Together with geochemical data of major oxides in TAS diagram (Cox et al., 1979) (Fig. 4.2) and  $\text{Na}_2\text{O}+\text{K}_2\text{O}-\text{CaO}$  versus  $\text{SiO}_2$  (wt%) diagram (Frost et al., 2001) (Fig. 4.5b) indicate that these syenitic rocks from both areas relate with alkaline magmatism. However,  $\text{K}_2\text{O}$  (wt%) versus  $\text{Na}_2\text{O}$  (wt%) diagram (Middlemost, 1975) (Fig. 4.4) indicates all the Tha Takiap syenitic rocks are potassic series, while the Mae Yan syenitic rocks are potassic to high potassic series that reflect the distinct of magmatic source. Negative correlations between  $\text{SiO}_2$  versus  $\text{TiO}_2$ ,  $\text{Al}_2\text{O}_3$ ,  $\text{Fe}_2\text{O}_3^{\text{(total)}}$ ,  $\text{MgO}$ ,  $\text{CaO}$ ,  $\text{P}_2\text{O}_5$ , and  $\text{MnO}$  (Fig. 4.1a-g) possibly depend on fractional crystallization and removal of ferromagnesian mineral, clinopyroxene ( $\text{MgO}$  – and  $\text{CaO}$ - rich), plagioclase ( $\text{Al}_2\text{O}_3$ -rich), titanomagnetite/ilmenite ( $\text{TiO}_2$ - and  $\text{FeO}$ -rich) and apatite



(CaO- and P<sub>2</sub>O<sub>5</sub>-rich). Moreover, Fe and Mg content in whole-rock analysis conform to Fe and Mg content in hornblende and plagioclase from mineral chemistry analysis. There is higher Fe content in syenitic rocks from the Tha Takiap area, whereas higher Mg content in syenitic rocks from the Mae Yan area.

#### **Tha Takiap area**

According to composition of continental crust of Rudnick and Gao (2003), flat chondrite-normalized REE patterns of the Tha Takiap syenitic rocks (Fig. 4.7b) indicate that source of magmatism could not be mainly originated by crust. Also, it cannot be directly originated by partial melting of mantle-derived magma due to high concentration of SiO<sub>2</sub> and low concentration of MgO (Jiang et al., 2017). The primitive mantle normalized (Sun and McDonough, 1989) spider diagrams of the Tha Takiap syenitic rocks (Fig. 4.7a) show the positive anomalies of U and Pb that reflect continental crust or island arc basalt derived material (Niu and O'Hara, 2009). On the other hand, the positive anomalies of Ta that reflect upper oceanic crust (Guo et al., 2015; Hofmann, 1988; Niu and O'Hara, 2009) are also found. Therefore, both crust-derived and mantle-derived material/magma are source of syenitic rocks from Tha Takiap area. In combination with ternary plots of A-type granite discrimination after Eby (1992) (Fig. 4.8a-b), most of the Tha Takiap syenitic rocks are classified as A<sub>2</sub> subtype that could be generated by continental crust or underplate crust derived magmas after continental-continental collision or island arc magmatism (Eby, 1992). Negative anomalies of Ba, Sr and Eu possibly indicate plagioclase and/or feldspar involvement, and negative anomalies of Ti might be related to titanomagnetite fractionation process (Gill, 2010; Niu and O'Hara, 2009; Wilson, 1989).

#### **Mae Yan area**

The primitive mantle normalized (Sun and McDonough, 1989) spider diagrams of the Mae Yan syenitic rocks show the depletion of Nb, Ta, and Ti and positive anomalies of Th, U, and Pb (Fig. 4.7c) that related to continental crust source and indicate subduction-related magmatism (Guo et al., 2015; Hofmann, 1988; Rudnick and Gao, 2003). The enrichment of LREE and the depletion of HREE in chondrite-normalized REE patterns of the Mae Yan syenitic rocks (Fig. 4.7d) indicate that the dominant source of partial melting could be continental crust (Rudnick and Gao, 2003). Significantly, negative anomalies of P and Ti in the spider diagrams might be related to

the depletion of P and Ti in the source rock or apatite and titanomagnetite fractionation process, and weak negative anomalies of Ba, Sr and Eu might be related to the depletion of them in the source rock or possibly indicate plagioclase and/or feldspar involvement (Gill, 2010; Wilson, 1989). Ternary plots of A-type granite discrimination after Eby (1992) (Fig. 4.8a-b) suggest that the Mae Yan syenitic rocks also were classified as A<sub>2</sub> subtype (post-orogenic A-type).

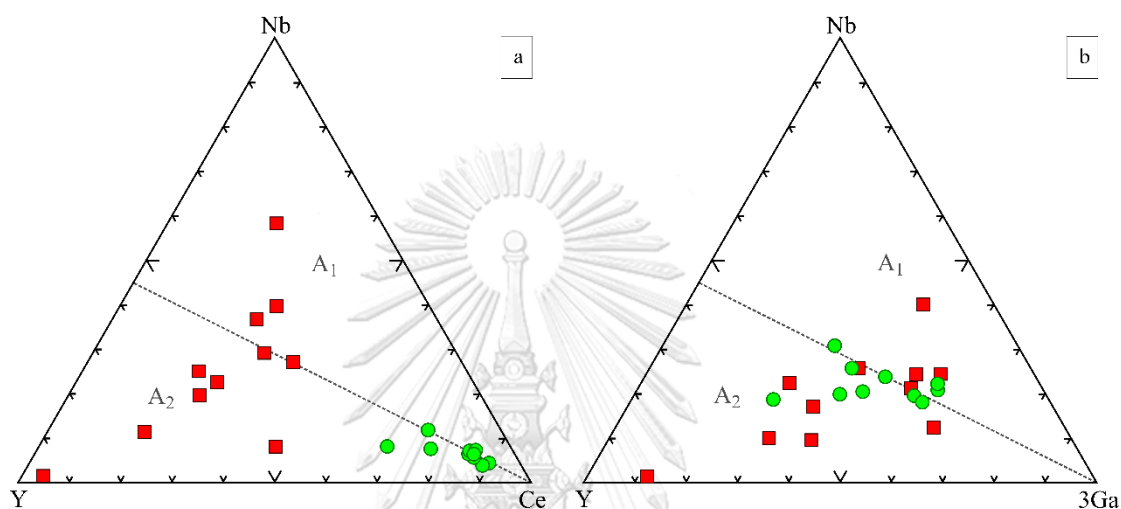


**Fig. 4.8** Ternary plots of A-type granite discrimination after Eby (1992) of Tha Takiap syenitic rocks and Mae Yan syenitic rocks showing the most of sample were fall within A<sub>2</sub> field (a) Y-Nb-Ce plot and (b) Y-Nb-3\*Ga plot (Rock type symbols are same as Fig. 4.1).

#### 4.5 Mineral chemistry

Mineral chemistry of this study focuses on amphibole and feldspar which are solid-solution minerals and can be observed in these syenitic rocks. By using the equation of Schmidt (1992) and Holland and Blundy (1994), the amphibole and plagioclase composition are calculated to estimate the equilibration pressures and temperature of crystallization (geothermobarometry). Moreover, the composition of feldspar pairs in perthite is calculated to estimate the pre-exsolution temperatures.

##### Amphibole

Amphibole is a major component of syenitic rock from the Tha Takiap and the Mae Yan areas. The mineral chemistry of amphibole is summarized in Table 4.4 and 4.5. Nomenclature and calculation of amphiboles in this study were based on Leake et al. (1997). H<sub>2</sub>O and halogen content are uncertain, so cations of amphibole

**Table 4.4** Mineral chemistry of amphibole (hornblende) in syenitic rocks from the Tha Takiap area.

Sample No.	D11-19-1	D11-19-2	D11-19-4	D11-19-5	D11-20-9	D11-20-10	D12-6-1	D12-6-2	D12-6-3	D12-6-4	D12-6-9	D12-6-12
Remark	Rim	Rim	Core	Core	Rim	Core	Rim	Rim	Core	Core	Rim	Core
SiO <sub>2</sub>	41.94	41.87	40.77	41.30	41.82	42.52	42.46	42.73	42.24	41.63	42.07	42.44
Al <sub>2</sub> O <sub>3</sub>	6.85	6.97	6.69	6.77	7.59	7.06	7.61	7.00	7.34	7.85	7.08	6.95
TiO <sub>2</sub>	1.78	1.22	1.63	1.69	0.66	1.48	1.90	1.65	1.19	2.21	1.43	1.34
Cr <sub>2</sub> O <sub>3</sub>	0.00	0.00	0.00	0.01	0.03	0.00	0.00	0.00	0.02	0.00	0.04	0.00
FeO	32.85	33.46	33.47	33.15	33.37	30.35	34.04	33.52	33.43	32.55	33.11	33.78
MnO	0.93	0.87	1.07	1.03	1.25	1.19	1.18	1.32	1.19	1.18	1.32	1.32
MgO	1.33	1.77	1.18	1.21	1.54	3.69	0.95	0.94	1.20	1.24	1.32	1.00
CaO	10.36	10.46	10.95	10.41	10.77	10.68	9.55	10.64	10.90	10.65	10.10	10.60
Na <sub>2</sub> O	1.60	1.06	1.65	1.54	0.77	1.01	0.97	0.91	0.78	1.00	1.01	0.84
K <sub>2</sub> O	1.21	1.17	1.22	1.83	0.98	0.46	1.09	1.09	1.16	1.26	1.06	1.17
F	0.22	0.00	0.00	0.00	0.00	0.00	0.00	0.00	0.00	0.00	0.00	0.00
Cl	0.03	0.02	0.02	0.02	0.01	0.01	0.02	0.02	0.02	0.02	0.02	0.03
Total	99.09	98.86	98.64	98.97	98.79	98.44	99.78	99.81	99.47	99.58	98.55	99.46
Calculated cation proportions (on the basis of 23 oxygen)												
Si	6.742	6.735	6.634	6.665	6.732	6.761	6.750	6.800	6.749	6.626	6.778	6.793
Al	1.297	1.322	1.283	1.288	1.440	1.323	1.426	1.312	1.383	1.473	1.344	1.311
Ti	0.215	0.148	0.199	0.205	0.080	0.177	0.227	0.197	0.143	0.265	0.173	0.161
Cr	0.000	0.000	0.000	0.001	0.004	0.000	0.000	0.000	0.002	0.000	0.004	0.000
Fe	4.416	4.502	4.554	4.474	4.491	4.036	4.525	4.461	4.467	4.332	4.460	4.522
Mn	0.126	0.118	0.147	0.141	0.171	0.160	0.159	0.178	0.161	0.158	0.180	0.179
Mg	0.318	0.424	0.287	0.292	0.370	0.875	0.226	0.223	0.286	0.295	0.316	0.238
Ca	1.784	1.803	1.909	1.801	1.858	1.820	1.626	1.814	1.866	1.815	1.743	1.818
Na	0.498	0.329	0.520	0.482	0.239	0.312	0.298	0.280	0.242	0.308	0.315	0.259
K	0.248	0.241	0.253	0.376	0.201	0.092	0.220	0.221	0.236	0.255	0.218	0.238
Total	15.644	15.621	15.785	15.725	15.586	15.557	15.459	15.487	15.536	15.527	15.532	15.520
Ideal site assignment of cation (minimum formula)												
Si	6.742	6.735	6.634	6.665	6.732	6.761	6.750	6.800	6.749	6.626	6.778	6.793
Al <sup>IV</sup>	1.258	1.265	1.283	1.288	1.268	1.230	1.250	1.200	1.251	1.374	1.222	1.207
Ti	0.000	0.000	0.083	0.046	0.000	0.009	0.000	0.000	0.000	0.000	0.000	0.000
sum T	<b>8.000</b>	<b>8.000</b>	<b>8.000</b>	<b>8.000</b>	<b>8.000</b>	<b>8.000</b>	<b>8.000</b>	<b>8.000</b>	<b>8.000</b>	<b>8.000</b>	<b>8.000</b>	<b>8.000</b>
Al <sup>VI</sup>	0.038	0.057	0.000	0.000	0.172	0.093	0.176	0.112	0.132	0.098	0.122	0.104
Ti	0.215	0.148	0.116	0.159	0.080	0.168	0.227	0.197	0.143	0.265	0.173	0.161
Fe <sup>3+</sup>	0.000	0.000	0.000	0.000	0.000	0.000	0.000	0.000	0.000	0.000	0.000	0.000
Cr	0.000	0.000	0.000	0.001	0.004	0.000	0.000	0.000	0.002	0.000	0.004	0.000
Mg	0.318	0.424	0.287	0.292	0.370	0.875	0.226	0.223	0.286	0.295	0.316	0.238
Fe <sup>2+</sup>	0.416	4.372	4.554	4.474	4.375	3.864	4.370	4.461	4.437	4.332	4.385	4.497
Mn	0.012	0.000	0.043	0.074	0.000	0.000	0.000	0.007	0.000	0.009	0.000	0.000
sum C	<b>5.000</b>	<b>5.000</b>	<b>5.000</b>	<b>5.000</b>	<b>5.000</b>	<b>5.000</b>	<b>5.000</b>	<b>5.000</b>	<b>5.000</b>	<b>5.000</b>	<b>5.000</b>	<b>5.000</b>
Mg	0.000	0.000	0.000	0.000	0.000	0.000	0.000	0.000	0.000	0.000	0.000	0.000
Fe <sup>2+</sup>	0.000	0.130	0.000	0.000	0.117	0.172	0.155	0.000	0.030	0.000	0.076	0.025
Mn	0.114	0.118	0.104	0.067	0.171	0.160	0.159	0.171	0.161	0.149	0.180	0.179
Ca	1.784	1.803	1.909	1.801	1.858	1.820	1.626	1.814	1.866	1.815	1.743	1.818
Na	0.102	0.000	0.000	0.132	0.000	0.000	0.059	0.015	0.000	0.036	0.001	0.000
sum B	<b>2.000</b>	<b>2.051</b>	<b>2.013</b>	<b>2.000</b>	<b>2.146</b>	<b>2.152</b>	<b>2.000</b>	<b>2.000</b>	<b>2.058</b>	<b>2.000</b>	<b>2.000</b>	<b>2.022</b>
Na	0.396	0.329	0.520	0.349	0.239	0.312	0.239	0.265	0.242	0.272	0.314	0.259
K	0.248	0.241	0.253	0.376	0.201	0.092	0.220	0.221	0.236	0.255	0.218	0.238
sum A	<b>0.644</b>	<b>0.570</b>	<b>0.773</b>	<b>0.725</b>	<b>0.440</b>	<b>0.405</b>	<b>0.459</b>	<b>0.487</b>	<b>0.479</b>	<b>0.527</b>	<b>0.532</b>	<b>0.498</b>
Mg/(Fe+Mg)	0.067	0.086	0.059	0.061	0.076	0.178	0.048	0.048	0.060	0.064	0.066	0.050
(Ca+Na) <sub>B</sub>	1.886	1.803	1.909	1.933	1.858	1.820	1.686	1.829	1.866	1.851	1.744	1.818
(Na+K) <sub>A</sub>	0.644	0.570	0.773	0.725	0.440	0.405	0.459	0.487	0.479	0.527	0.532	0.498
<i>P</i> (kbar)	3.16	3.28	3.10	3.12	3.85	3.29	3.78	3.24	3.57	4.00	3.39	3.23
<i>T</i> (°C)	750	753	-	-	714	-	679	701	-	-	713	-

Note: Ideal site assignment of cation were based on the calculation method of Leake et al. (1997), *P* were calculated by Al<sup>IV</sup> content in hornblende as suggest by Schmidt (1992), *T* were calculated by equilibrium relation of hornblende-plagioclase as suggest by Holland and Blundy (1994).

**Table 4.5** Mineral chemistry of amphibole (hornblende) in syenitic rocks from the Mae Yan area.

Sample No.	MH 14-6	MH 14-7	MH 14-8	MH 14-9	MH 14-14	MH 14-15	MH 5-2-1	MH 5-2-2	MH 5-2-3	MH 5-2-4	MH 5-2-6
Remark	Rim	Rim	Core	Core	Core	Rim	Rim	Core	Core	Core	Rim
SiO <sub>2</sub>	44.39	44.32	44.51	44.11	41.95	41.95	42.69	41.47	40.76	41.17	41.94
Al <sub>2</sub> O <sub>3</sub>	7.12	8.13	8.57	8.49	9.25	9.47	9.73	10.68	11.07	10.15	9.48
TiO <sub>2</sub>	0.36	0.50	0.70	0.63	0.70	0.89	0.61	0.85	0.94	0.79	0.56
Cr <sub>2</sub> O <sub>3</sub>	0.00	0.00	0.03	0.01	0.00	0.00	0.01	0.00	0.00	0.01	0.00
FeO	18.97	20.64	20.54	20.35	21.23	21.55	19.41	20.50	20.24	20.78	20.20
MnO	1.6	1.46	1.60	1.54	1.65	1.57	1.19	1.18	1.19	1.30	1.27
MgO	10.19	9.41	8.94	8.95	8.57	8.33	9.87	9.29	8.94	9.54	9.96
CaO	11.54	11.48	11.42	11.44	11.41	11.50	11.22	11.33	11.32	11.37	11.23
Na <sub>2</sub> O	2.11	2.14	2.19	2.11	2.04	1.84	1.98	2.04	2.01	1.87	1.88
K <sub>2</sub> O	1.40	1.64	1.79	1.83	2.17	2.44	1.73	1.89	2.02	1.85	1.64
F	0.00	0.00	0.00	0.00	0.00	0.00	0.00	0.00	0.00	0.00	0.00
Cl	0.01	0.01	0.00	0.00	0.02	0.02	0.02	0.00	0.00	0.00	0.00
Total	97.67	99.73	100.29	99.45	98.97	99.56	98.46	99.22	98.48	98.81	98.16
Calculated cation proportions (on the basis of 23 oxygen)											
Si	6.784	6.673	6.659	6.653	6.424	6.392	6.476	6.291	6.232	6.291	6.420
Al	1.282	1.443	1.511	1.509	1.669	1.701	1.739	1.909	1.995	1.829	1.711
Ti	0.041	0.057	0.079	0.072	0.080	0.102	0.070	0.097	0.108	0.090	0.064
Cr	0.000	0.000	0.003	0.001	0.000	0.000	0.001	0.000	0.000	0.001	0.000
Fe	2.425	2.599	2.570	2.567	2.718	2.745	2.463	2.601	2.589	2.656	2.585
Mn	0.206	0.186	0.202	0.197	0.214	0.203	0.153	0.152	0.154	0.168	0.165
Mg	2.321	2.112	1.992	2.012	1.956	1.891	2.233	2.101	2.037	2.173	2.274
Ca	1.889	1.851	1.830	1.848	1.873	1.877	1.823	1.841	1.855	1.861	1.841
Na	0.625	0.624	0.635	0.617	0.605	0.543	0.584	0.600	0.595	0.553	0.559
K	0.273	0.315	0.342	0.352	0.423	0.474	0.334	0.366	0.395	0.360	0.321
Total	15.846	15.860	15.823	15.829	15.963	15.928	15.876	15.957	15.960	15.981	15.939
Ideal site assignment of cation (minimum formula)											
Si	6.784	6.673	6.659	6.653	6.424	6.392	6.476	6.291	6.232	6.291	6.420
Al <sup>IV</sup>	1.216	1.327	1.341	1.347	1.576	1.608	1.524	1.709	1.768	1.709	1.580
Ti	0.000	0.000	0.000	0.000	0.000	0.000	0.000	0.000	0.000	0.000	0.000
sum T	<b>8.000</b>	<b>8.000</b>	<b>8.000</b>	<b>8.000</b>	<b>8.000</b>	<b>8.000</b>	<b>8.000</b>	<b>8.000</b>	<b>8.000</b>	<b>8.000</b>	<b>8.000</b>
Al <sup>VI</sup>	0.066	0.116	0.169	0.162	0.093	0.093	0.215	0.200	0.228	0.119	0.131
Ti	0.041	0.057	0.079	0.072	0.080	0.102	0.070	0.097	0.108	0.090	0.064
Fe <sup>3+</sup>	0.000	0.000	0.000	0.000	0.000	0.000	0.000	0.000	0.000	0.000	0.000
Cr	0.000	0.000	0.003	0.001	0.000	0.000	0.001	0.000	0.000	0.001	0.000
Mg	2.321	2.112	1.992	2.012	1.956	1.891	2.233	2.101	2.037	2.173	2.274
Fe <sup>2+</sup>	2.425	2.599	2.570	2.567	2.718	2.745	2.463	2.601	2.589	2.617	2.531
Mn	0.147	0.116	0.186	0.186	0.152	0.169	0.018	0.001	0.039	0.000	0.000
sum C	<b>5.000</b>	<b>5.000</b>	<b>5.000</b>	<b>5.000</b>	<b>5.000</b>	<b>5.000</b>	<b>5.000</b>	<b>5.000</b>	<b>5.000</b>	<b>5.000</b>	<b>5.000</b>
Mg	0.000	0.000	0.000	0.000	0.000	0.000	0.000	0.000	0.000	0.000	0.000
Fe <sup>2+</sup>	0.000	0.000	0.000	0.000	0.000	0.000	0.000	0.000	0.000	0.039	0.054
Mn	0.060	0.070	0.016	0.011	0.062	0.034	0.135	0.151	0.115	0.168	0.165
Ca	1.889	1.851	1.830	1.848	1.873	1.877	1.823	1.841	1.855	1.861	1.841
Na	0.052	0.079	0.154	0.140	0.065	0.089	0.042	0.008	0.030	0.000	0.000
sum B	<b>2.000</b>	<b>2.000</b>	<b>2.000</b>	<b>2.000</b>	<b>2.000</b>	<b>2.000</b>	<b>2.000</b>	<b>2.000</b>	<b>2.000</b>	<b>2.068</b>	<b>2.060</b>
Na	0.573	0.545	0.481	0.477	0.540	0.454	0.542	0.591	0.565	0.553	0.559
K	0.273	0.315	0.342	0.352	0.423	0.474	0.334	0.366	0.395	0.360	0.321
sum A	<b>0.846</b>	<b>0.860</b>	<b>0.823</b>	<b>0.829</b>	<b>0.963</b>	<b>0.928</b>	<b>0.876</b>	<b>0.957</b>	<b>0.960</b>	<b>0.913</b>	<b>0.879</b>
Mg/(Fe+Mg)	0.489	0.448	0.437	0.439	0.419	0.408	0.476	0.447	0.440	0.450	0.468
(Ca+Na) <sub>B</sub>	1.940	1.930	1.984	1.989	1.938	1.966	1.865	1.849	1.885	1.861	1.841
(Na+K) <sub>A</sub>	0.846	0.860	0.823	0.829	0.963	0.928	0.876	0.957	0.960	0.913	0.879
<i>P</i> (kbar)	3.09	3.86	4.18	4.17	4.93	5.09	5.27	6.08	6.49	5.69	5.13
<i>T</i> (°C)	819	816	-	-	-	934	853	-	-	-	833

Note: Ideal site assignment of cation were based on the calculation method of Leake et al. (1997), *P* were calculated by Al<sup>IV</sup> content in hornblende as suggest by Schmidt (1992), *T* were calculated by equilibrium relation of hornblende-plagioclase as suggest by Holland and Blundy (1994).

are calculated on the basis of 23 oxygens. Based on the nomenclature of Leake et al. (1997), all amphiboles from both areas were classified as calcic amphiboles according to their cation of  $(Ca+Na)_B$  more than 1.00,  $Na_B$  less than 0.50 and  $Ca_B$  more than 1.50 (Table 4.4 and 4.5). XMg ( $Mg/Fe+Mg$ ) of calcic amphibole in syenitic rock from the Tha Takiap area range from 0.048 to 0.178, while Si range from 6.626 to 6.800 that indicate to be ferro-edenite (Fig. 4.9). On the other hand, calcic amphibole in syenitic rock from the Mae Yan area are more enriched in Mg content ( $(Mg/Fe+Mg)=0.408$  to 0.489) than the Tha Takiap area, while Si range from 6.291 to 6.784 that indicate to be ferro-pargasite and ferro-edenite (Fig. 4.9).

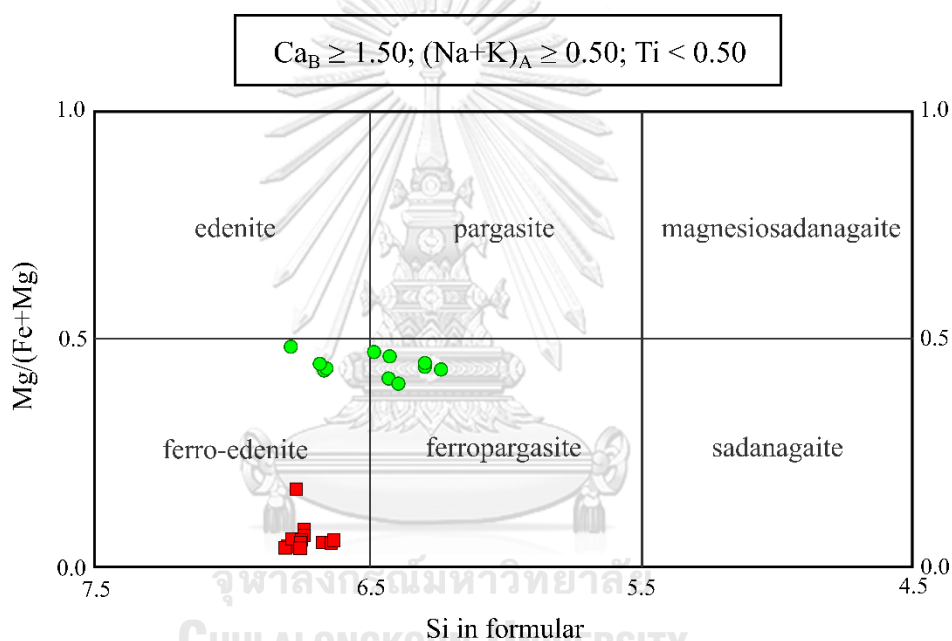


**Fig. 4.9** Classification diagram for calcic amphibole (after Leake et al. (1997)) of syenitic rocks from the Tha Takiap and Mae Yan areas (Rock type symbols are same as Fig. 4.1).

### Feldspar

K-feldspar is a major component of syenitic rocks from Tha Takiap and Mae Yan areas. The mineral chemistry of plagioclase was summarized in Table 4.6 and 4.7. K-feldspar is calculated on the basis of 8 oxygens. Atomic Ca-Na-K proportion of plagioclase from the Tha Takiap syenitic rocks range in 0.00-0.79% An, 3.04-20.23% Ab and 79.68-96.91% Or, while the Mae Yan syenitic rocks range in 0.00-0.40% An, 3.19-24.31% Ab and 75.41-93.92% Or. Most of K-feldspar from both areas were classified as orthoclase according to Ab-An-Or ternary classification diagram for feldspar (Smith and Brown, 1988) (Fig. 4.10).

**Table 4.6** Mineral chemistry of feldspar in syenitic rocks from the Tha Takiap area.

Analysis No.	D11-4-1	D11-4-2	D11-4-3	D11-4-4	D11-19-6	D11-19-11	D11-19-13	D11-19-14	D11-20-12	D11-20-13	D11-20-14
Remark	Kfs	Kfs	Kfs	Kfs	Pl	Pl	Pl	Pl	Pl	Pl	Pl
	Rim	Rim	Core	Core	Rim	Rim	Core	Core	Rim	Rim	Core
SiO <sub>2</sub>	66.77	66.21	66.87	66.86	69.64	68.25	69.23	69.40	67.88	67.38	66.93
Al <sub>2</sub> O <sub>3</sub>	14.82	15.30	14.72	16.16	18.19	17.88	17.47	17.63	18.73	19.18	20.57
TiO <sub>2</sub>	0.02	0.02	0.03	0.00	0.00	0.01	0.00	0.02	0.00	0.00	0.02
Cr <sub>2</sub> O <sub>3</sub>	0.00	0.00	0.02	0.04	0.05	0.04	0.00	0.04	0.04	0.00	0.00
FeO	0.18	0.16	0.04	0.01	0.15	0.00	0.00	0.00	0.00	0.00	0.05
MnO	0.01	0.00	0.04	0.06	0.03	0.02	0.01	0.01	0.00	0.01	0.00
MgO	0.00	0.00	0.00	0.00	0.00	0.00	0.01	0.00	0.00	0.00	0.00
CaO	0.03	0.02	0.01	0.17	0.19	0.81	0.85	0.95	0.21	0.60	2.22
Na <sub>2</sub> O	0.05	2.31	1.16	1.07	11.33	11.67	11.36	11.46	11.58	11.98	11.20
K <sub>2</sub> O	16.14	13.83	15.42	15.98	1.01	0.10	0.51	0.06	0.08	0.10	0.10
F	0.00	0.00	0.00	0.00	0.00	0.00	0.00	0.00	0.00	0.00	0.00
Cl	0.00	0.00	0.01	0.00	0.00	0.01	0.00	0.00	0.00	0.00	0.01
Total	98.47	97.85	98.32	100.34	100.57	98.78	99.43	99.56	98.52	99.25	101.09
Calculated cation proportions (on the basis of 8 oxygen)											
Si	3.128	3.103	3.131	3.078	3.026	3.025	3.044	3.046	3.009	2.977	2.915
Al	0.818	0.845	0.812	0.877	0.931	0.934	0.906	0.912	0.979	0.999	1.056
Ti	0.001	0.001	0.001	0.000	0.000	0.000	0.000	0.001	0.000	0.000	0.001
Cr	0.000	0.000	0.001	0.001	0.002	0.002	0.000	0.001	0.002	0.000	0.000
Fe	0.007	0.006	0.001	0.001	0.005	0.000	0.000	0.000	0.000	0.000	0.002
Mn	0.000	0.000	0.002	0.002	0.001	0.001	0.000	0.000	0.000	0.000	0.000
Mg	0.001	0.000	0.000	0.000	0.000	0.000	0.000	0.000	0.000	0.000	0.000
Ca	0.002	0.001	0.001	0.008	0.009	0.038	0.040	0.045	0.010	0.029	0.104
Na	0.046	0.210	0.106	0.095	0.955	1.003	0.969	0.975	0.996	1.026	0.946
K	0.964	0.827	0.921	0.938	0.056	0.005	0.028	0.003	0.004	0.006	0.006
Total	4.967	4.992	4.975	5.000	4.985	5.008	4.988	4.984	4.999	5.037	5.029
An	0.16	0.09	0.05	0.79	0.85	3.67	3.84	4.37	0.96	2.70	9.82
Ab	4.52	20.23	10.29	9.17	93.68	95.82	93.41	95.31	98.59	96.78	89.65
Or	95.32	79.68	89.66	90.05	5.47	0.51	2.74	0.32	0.44	0.52	0.53

Plagioclase is a minor component of syenitic rocks from the Mae Yan areas. However, it is rarely found in syenitic rock from the Tha Takiap area. The mineral chemistry of plagioclase was summarized in Table 4.6 and 4.7. Plagioclase is calculated on the basis of 8 oxygens. Atomic Ca-Na-K proportion of plagioclase from the Tha Takiap syenitic rocks range in 0.58-9.82% An, 89.65-98.86% Ab and 0.28-5.47% Or, while the Mae Yan syenitic rocks range in 2.02-19.52% An, 75.08-97.01% Ab and 0.45-13.33% Or. Plagioclase from Tha Takiap area was classified as Na-albite, while Plagioclase from Mae Yan area was classified as Na-albite to oligoclase according to Ab-An-Or ternary classification diagram for feldspar (Smith and Brown, 1988) (Fig. 4.10).

**Table 4.6** (continued)

Analysis No.	D11-20-15	D11-20-16	D11-20-17	D11-20-18	D12-6-13	D12-6-16	D12-6-17	D12-6-19	D12-6-21	D12-6-22	D12-6-23
Remark	Pl	Kfs	Kfs	Kfs	Pl	Pl	Pl	Pl	Kfs	Kfs	Kfs
	Core	Rim	Rim	Core	Rim	Core	Core	Rim	Rim	Core	Core
SiO <sub>2</sub>	66.52	67.71	67.33	66.04	66.50	66.83	66.41	66.58	64.49	64.76	64.86
Al <sub>2</sub> O <sub>3</sub>	19.60	17.05	17.05	18.79	21.28	21.25	20.70	20.59	19.87	19.96	19.87
TiO <sub>2</sub>	0.04	0.00	0.01	0.03	0.00	0.00	0.00	0.02	0.03	0.01	0.00
Cr <sub>2</sub> O <sub>3</sub>	0.00	0.03	0.01	0.00	0.00	0.03	0.00	0.00	0.00	0.02	0.00
FeO	0.06	0.08	0.16	0.06	0.09	0.02	0.18	0.02	0.04	0.00	0.11
MnO	0.01	0.00	0.01	0.00	0.01	0.00	0.02	0.02	0.00	0.00	0.01
MgO	0.01	0.00	0.00	0.00	0.00	0.00	0.00	0.00	0.01	0.00	0.00
CaO	1.15	0.01	0.00	0.00	0.47	0.67	0.13	0.32	0.00	0.02	0.01
Na <sub>2</sub> O	11.87	0.32	0.35	1.88	11.90	11.23	11.83	11.30	0.46	1.11	0.35
K <sub>2</sub> O	0.05	15.51	15.35	13.49	0.09	0.08	0.10	0.89	15.40	14.36	15.35
F	0.00	0.00	0.00	0.00	0.00	0.00	0.00	0.00	0.00	0.00	0.00
Cl	0.01	0.00	0.00	0.00	0.00	0.00	0.01	0.00	0.00	0.00	0.00
Total	99.32	100.72	100.27	100.30	100.32	100.09	99.37	99.74	100.30	100.24	100.56
Calculated cation proportions (on the basis of 8 oxygen)											
Si	2.946	3.080	3.076	3.005	2.910	2.922	2.930	2.926	2.957	2.959	2.963
Al	1.023	0.914	0.918	1.008	1.097	1.095	1.076	1.066	1.074	1.075	1.070
Ti	0.001	0.000	0.000	0.001	0.000	0.000	0.000	0.001	0.001	0.000	0.000
Cr	0.000	0.001	0.000	0.000	0.000	0.001	0.000	0.000	0.000	0.001	0.000
Fe	0.002	0.003	0.006	0.002	0.003	0.001	0.006	0.001	0.002	0.000	0.004
Mn	0.000	0.000	0.000	0.000	0.001	0.000	0.001	0.001	0.000	0.000	0.000
Mg	0.001	0.000	0.000	0.000	0.000	0.000	0.000	0.000	0.000	0.000	0.000
Ca	0.055	0.000	0.000	0.000	0.022	0.031	0.006	0.015	0.000	0.001	0.000
Na	1.019	0.028	0.031	0.166	1.009	0.952	1.012	0.963	0.041	0.099	0.031
K	0.003	0.900	0.895	0.783	0.005	0.004	0.006	0.050	0.901	0.837	0.895
Total	5.051	4.927	4.927	4.965	5.046	5.006	5.037	5.022	4.976	4.971	4.964
An	5.07	0.05	0.00	0.00	2.13	3.17	0.58	1.46	0.00	0.09	0.05
Ab	94.65	3.04	3.35	17.47	97.41	96.41	98.86	93.66	4.32	10.54	3.38
Or	0.28	96.91	96.65	82.53	0.46	0.43	0.57	4.88	95.68	89.37	96.57

Perthite was found in syenitic rocks from both areas. The mineral chemistry of Feldspar pairs (K-feldspar and plagioclase) in perthite were summarized in Table 4.8 and 4.9. Atomic Ca-Na-K proportion of K-feldspar in perthite from Tha Takiap syenitic rocks range in 0.00-0.06% An, 3.55-20.76% Ab and 79.18-96.45% Or, while Mae Yan syenitic rocks range in 0.00-0.04% An, 3.84-9.95% Ab and 74.63-96.16% Or. Atomic Ca-Na-K proportion of plagioclase in perthite from Tha Takiap syenitic rocks range in 0.49-6.25% An, 84.85-97.72% Ab and 0.66-14.66% Or, while Mae Yan syenitic rocks range in 0.39-6.10% An, 92.60-98.99% Ab and 0.56-1.37% Or.

**Table 4.7** Mineral chemistry of feldspar in syenitic rocks from the Mae Yan area.

Analysis No.	MH 5-2-7	MH 5-2-8	MH 5-2-9	MH 5-2-10	MH 5-2-12	MH 5-2-13	MH 5-2-19	MH 5-2-20	MH 5-2-21	MH 5-2-25	MH 5-2-26
	Pl	Pl	Pl	Pl	Pl	Pl	Kfs	Kfs	Kfs	Kfs	Kfs
	Core	Core	Rim	Rim	Rim	Core	Core	Core	Core	Core	Core
SiO <sub>2</sub>	67.83	69.30	69.30	68.82	67.62	64.85	64.56	64.12	63.85	64.48	65.71
Al <sub>2</sub> O <sub>3</sub>	20.06	18.88	18.88	20.08	20.82	22.32	17.48	18.10	17.68	17.72	18.04
TiO <sub>2</sub>	0.00	0.02	0.02	0.00	0.00	0.00	0.02	0.03	0.01	0.02	0.05
Cr <sub>2</sub> O <sub>3</sub>	0.00	0.00	0.00	0.01	0.02	0.01	0.00	0.00	0.02	0.00	0.00
FeO	0.21	0.15	0.15	0.08	0.20	0.46	0.05	0.17	0.14	0.18	0.06
MnO	0.01	0.01	0.01	0.00	0.02	0.03	0.02	0.00	0.03	0.00	0.00
MgO	0.01	0.02	0.02	0.00	0.00	0.00	0.00	0.02	0.01	0.01	0.00
CaO	1.70	0.38	0.38	0.44	2.08	4.00	0.00	0.05	0.00	0.07	0.03
Na <sub>2</sub> O	9.25	8.82	8.82	9.17	8.29	7.42	0.66	2.60	0.33	1.23	1.03
K <sub>2</sub> O	0.27	2.11	2.11	0.06	0.19	0.38	15.25	12.24	15.27	13.73	14.40
F	0.00	0.00	0.00	0.00	0.00	0.00	0.00	0.00	0.00	0.00	0.00
Cl	0.00	0.00	0.00	0.01	0.00	0.01	0.00	0.00	0.01	0.00	0.00
Total	99.33	99.68	99.68	98.68	99.24	99.47	98.04	97.34	97.34	97.44	99.32
Calculated cation proportions (on the basis of 8 oxygen)											
Si	2.974	2.994	3.016	3.014	2.960	2.858	3.030	3.003	3.019	3.025	3.027
Al	1.037	1.028	0.968	1.037	1.074	1.159	0.967	0.999	0.985	0.980	0.979
Ti	0.000	0.000	0.001	0.000	0.000	0.000	0.001	0.001	0.000	0.001	0.002
Cr	0.000	0.000	0.000	0.000	0.001	0.000	0.000	0.000	0.001	0.000	0.000
Fe	0.008	0.005	0.005	0.003	0.007	0.017	0.002	0.007	0.005	0.007	0.002
Mn	0.000	0.000	0.000	0.000	0.001	0.001	0.001	0.000	0.001	0.000	0.000
Mg	0.000	0.000	0.001	0.000	0.000	0.000	0.000	0.001	0.000	0.001	0.000
Ca	0.080	0.056	0.018	0.020	0.098	0.189	0.000	0.003	0.000	0.004	0.001
Na	0.786	0.804	0.745	0.779	0.703	0.634	0.060	0.236	0.030	0.112	0.092
K	0.015	0.007	0.117	0.004	0.010	0.021	0.913	0.731	0.921	0.822	0.847
Total	4.900	4.894	4.871	4.857	4.854	4.879	4.973	4.980	4.964	4.951	4.951
An	9.07	6.41	2.02	2.54	12.04	22.37	0.00	0.28	0.00	0.40	0.16
Ab	89.23	92.72	84.65	97.01	86.69	75.08	6.13	24.31	3.19	11.91	9.80
Or	1.70	0.86	13.33	0.45	1.27	2.54	93.87	75.41	96.81	87.69	90.05

### Geobarometer and geothermometer

The crystallization condition (pressure and temperature) of plutonic rock can be estimated using composition of some mineral assemblages such as hornblende and feldspar which are typical mineral assemblages in the studied plutonic rocks.

In this study, geobarometer was calculated using the Al-in-hornblende as suggest by Schmidt (1992) which can determine an intrusion depth within the pressure range from 2.5 to 13 kbar with a precision of  $\pm 0.6$  kbar. The equation was described below.

$$P(\pm 0.6 \text{ kbar}) = -3.01 + 4.76Al^{\text{tot}} \text{ (Schmidt, 1992)}$$

Where  $Al^{\text{tot}}$  is the total Al content of hornblende in atoms per formula unit

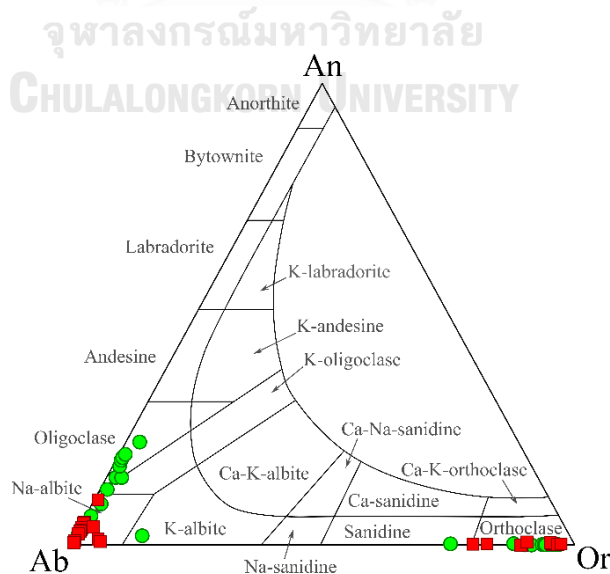


**Table 4.7** (continued)

Analysis No.	MH 5-2-27	MH 6-1	MH 6-2	MH 6-3	MH 14-23	MH 14-24	MH 14-26	MH 14-27	MH 14-28	MH 14-29
	Kfs	Kfs	Kfs	Kfs	Pl	Pl	Pl	Pl	Pl	Pl
	Core	Rim	Core	Core	Rim	Rim	Core	Rim	Rim	Core
SiO <sub>2</sub>	64.52	64.83	64.18	64.65	66.95	66.39	66.73	66.64	66.21	66.32
Al <sub>2</sub> O <sub>3</sub>	17.94	17.70	17.73	17.85	18.69	19.43	19.07	18.36	18.96	18.70
TiO <sub>2</sub>	0.00	0.00	0.02	0.02	0.01	0.00	0.00	0.02	0.01	0.01
Cr <sub>2</sub> O <sub>3</sub>	0.05	0.00	0.00	0.00	0.00	0.00	0.05	0.00	0.00	0.02
FeO	0.14	0.34	0.54	0.60	0.23	0.23	0.20	0.11	0.15	0.21
MnO	0.00	0.04	0.04	0.00	0.02	0.00	0.00	0.00	0.00	0.01
MgO	0.00	0.00	0.00	0.00	0.00	0.01	0.00	0.00	0.00	0.01
CaO	0.01	0.00	0.01	0.00	4.01	4.16	3.98	3.03	3.14	3.66
Na <sub>2</sub> O	0.92	0.48	0.68	0.64	9.38	9.37	9.68	9.44	9.94	9.54
K <sub>2</sub> O	14.57	15.44	14.83	14.90	0.13	0.18	0.15	0.50	0.34	0.23
F	0.00	0.00	0.00	0.00	0.00	0.00	0.00	0.00	0.00	0.00
Cl	0.00	0.00	0.01	0.00	0.01	0.00	0.00	0.00	0.01	0.01
Total	98.14	98.84	98.01	98.66	99.42	99.76	99.85	98.09	98.75	98.73

Calculated cation proportions (on the basis of 8 oxygen)

Si	3.016	3.023	3.015	3.016	2.964	2.933	2.946	2.980	2.951	2.957
Al	0.988	0.973	0.981	0.981	0.975	1.011	0.992	0.968	0.996	0.983
Ti	0.000	0.000	0.001	0.001	0.000	0.000	0.000	0.001	0.000	0.000
Cr	0.002	0.000	0.000	0.000	0.000	0.000	0.002	0.000	0.000	0.001
Fe	0.005	0.013	0.021	0.024	0.009	0.009	0.008	0.004	0.005	0.008
Mn	0.000	0.002	0.002	0.000	0.001	0.000	0.000	0.000	0.000	0.001
Mg	0.000	0.000	0.000	0.000	0.000	0.000	0.000	0.000	0.000	0.001
Ca	0.001	0.000	0.000	0.000	0.190	0.197	0.188	0.145	0.150	0.175
Na	0.083	0.044	0.061	0.057	0.805	0.802	0.828	0.818	0.859	0.825
K	0.869	0.919	0.888	0.887	0.007	0.010	0.008	0.029	0.019	0.013
Total	4.965	4.972	4.969	4.965	4.951	4.963	4.972	4.944	4.981	4.963
An	0.07	0.00	0.03	0.00	18.99	19.52	18.36	14.62	14.60	17.25
Ab	8.76	4.55	6.47	6.08	80.29	79.48	80.83	82.51	83.53	81.43
Or	91.17	95.45	93.50	93.92	0.73	1.00	0.80	2.88	1.87	1.31

**Fig. 4.10** Ternary classification diagram Ab-An-Or for feldspar (after Smith and Brown (1988)) showing compositional variation in K-feldspar and plagioclase of syenitic rocks from the Tha Takiap and Mae Yan areas (Rock type symbols are same as Fig. 4.1).

**Table 4.8** Mineral chemistry of feldspar pairs in perthite of syenitic rocks from the Tha Takiap area.

Sample No.	D11-4 (1)		D11-4 (2)		D11-20 (1)		D11-20 (2)		D12-6		D12-11	
Analysis No.	D11-4-6	D11-4-8	D11-4-8	D11-4-11	D11-20-20	D11-20-19	D11-20-21	D11-20-22	D12-6-26	D12-6-24	D12-11-2	D12-11-1
Perthite	Kfs	Pl	Kfs	Pl	Kfs	Pl	Kfs	Pl	Kfs	Pl	Kfs	Pl
SiO <sub>2</sub>	66.77	66.83	66.19	66.16	64.95	67.31	64.50	66.43	64.12	66.11	64.03	67.25
Al <sub>2</sub> O <sub>3</sub>	14.88	19.95	18.60	19.76	18.11	19.96	19.71	18.71	17.99	21.02	19.79	19.10
TiO <sub>2</sub>	0.00	0.03	0.00	0.02	0.00	0.00	0.00	0.02	0.02	0.03	0.00	0.02
Cr <sub>2</sub> O <sub>3</sub>	0.00	0.01	0.00	0.01	0.00	0.01	0.00	0.00	0.00	0.00	0.02	0.00
FeO	0.10	0.02	0.04	0.00	0.09	0.00	0.03	0.06	0.08	0.10	0.07	0.07
MnO	0.00	0.00	0.02	0.03	0.00	0.00	0.01	0.02	0.00	0.00	0.00	0.01
MgO	0.00	0.00	0.02	0.00	0.00	0.01	0.00	0.01	0.00	0.00	0.00	0.00
CaO	0.01	1.36	0.01	0.61	0.00	0.95	0.00	0.12	0.01	0.50	0.01	0.31
Na <sub>2</sub> O	2.71	11.17	1.05	11.25	0.37	11.10	0.51	11.48	1.08	11.47	0.59	11.98
K <sub>2</sub> O	15.68	0.12	15.38	0.61	15.20	0.12	15.19	3.02	15.11	0.66	15.23	0.16
F	0.00	0.00	0.00	0.00	0.00	0.00	0.00	0.00	0.00	0.00	0.00	0.00
Cl	0.00	0.00	0.01	0.00	0.01	0.00	0.00	0.00	0.01	0.00	0.01	0.02
Total	100.16	99.50	101.32	98.44	98.73	99.46	99.95	99.88	98.43	99.89	99.75	98.92
Calculated cation proportions (on the basis of 8 oxygen)												
Si	3.095	2.948	3.006	2.952	3.020	2.962	2.965	2.965	3.002	2.913	2.954	2.982
Al	0.813	1.037	0.995	1.039	0.993	1.035	1.067	0.984	0.993	1.092	1.076	0.998
Ti	0.000	0.001	0.000	0.001	0.000	0.000	0.000	0.001	0.001	0.001	0.000	0.001
Cr	0.000	0.000	0.000	0.000	0.000	0.000	0.000	0.000	0.000	0.000	0.001	0.000
Fe	0.004	0.001	0.002	0.000	0.004	0.000	0.001	0.002	0.003	0.004	0.003	0.003
Mn	0.000	0.000	0.001	0.001	0.000	0.000	0.000	0.001	0.000	0.000	0.000	0.000
Mg	0.000	0.000	0.001	0.000	0.000	0.001	0.000	0.000	0.000	0.000	0.000	0.000
Ca	0.001	0.064	0.000	0.029	0.000	0.045	0.000	0.006	0.000	0.024	0.000	0.015
Na	0.243	0.955	0.093	0.973	0.033	0.947	0.046	0.994	0.098	0.979	0.053	1.030
K	0.927	0.007	0.891	0.035	0.902	0.007	0.891	0.172	0.903	0.037	0.896	0.009
Total	5.084	5.014	4.989	5.031	4.951	4.997	4.970	5.125	5.001	5.049	4.983	5.038
An	0.06	6.25	0.04	2.81	0.00	4.51	0.00	0.49	0.04	2.27	0.04	1.41
Ab	20.76	93.07	9.43	93.85	3.55	94.84	4.89	84.85	9.82	94.19	5.55	97.72
Or	79.18	0.68	90.53	3.34	96.45	0.66	95.11	14.66	90.14	3.55	94.41	0.88
<i>T</i> (°C)	501		370		245		377		376		298	

Note: *T* is pre-exsolution temperature which were based on the calculation method of Elkins and Grove (1990) using the program SOLVCALC (Wen and Nekvasil, 1994).

**Table 4.9** Mineral chemistry of feldspar pairs in perthite of syenitic rocks from the Mae Yan area.

Sample No.	MH5-2 (1)		MH5-2 (2)		MH6		MH14	
Analysis No.	MH5-2-16	MH5-2-18	MH5-2-23	MH5-2-22	MH6-4	MH6-5	MH14-30	MH14-33
Perthite	Kfs	Pl	Kfs	Pl	Kfs	Pl	Kfs	Pl
SiO <sub>2</sub>	64.28	66.53	66.80	70.32	64.28	66.27	66.36	66.84
Al <sub>2</sub> O <sub>3</sub>	19.23	20.04	18.10	18.99	19.66	19.93	18.31	20.00
TiO <sub>2</sub>	0.06	0.03	0.01	0.00	0.02	0.00	0.03	0.00
Cr <sub>2</sub> O <sub>3</sub>	0.00	0.00	0.01	0.00	0.00	0.00	0.00	0.06
FeO	0.13	0.16	0.08	0.09	0.50	0.46	0.18	0.13
MnO	0.00	0.01	0.02	0.00	0.00	0.00	0.00	0.01
MgO	0.00	0.02	0.00	0.02	0.00	0.00	0.00	0.00
CaO	0.06	1.37	0.07	0.47	0.00	0.08	0.05	0.64
Na <sub>2</sub> O	0.62	11.51	2.56	9.88	0.41	11.69	1.08	11.12
K <sub>2</sub> O	15.26	0.25	11.65	0.09	15.40	0.11	14.85	0.24
F	0.00	0.00	0.00	0.00	0.00	0.00	0.00	0.00
Cl	0.00	0.00	0.01	0.01	0.00	0.01	0.00	0.00
Total	99.64	99.92	99.32	99.86	100.25	98.56	100.87	99.03
Calculated cation proportions (on the basis of 8 oxygen)								
Si	2.970	2.933	3.041	3.050	2.956	2.951	3.019	2.957
Al	1.047	1.041	0.971	0.970	1.065	1.046	0.982	1.043
Ti	0.002	0.001	0.000	0.000	0.001	0.000	0.001	0.000
Cr	0.000	0.000	0.001	0.000	0.000	0.000	0.000	0.002
Fe	0.005	0.006	0.003	0.003	0.019	0.017	0.007	0.005
Mn	0.000	0.000	0.001	0.000	0.000	0.000	0.000	0.000
Mg	0.000	0.001	0.000	0.001	0.000	0.000	0.000	0.000
Ca	0.003	0.065	0.004	0.022	0.000	0.004	0.002	0.030
Na	0.056	0.984	0.226	0.831	0.036	1.009	0.096	0.954
K	0.899	0.014	0.676	0.005	0.903	0.006	0.862	0.014
Total	4.982	5.045	4.924	4.882	4.981	5.034	4.968	5.005
An	0.28	6.10	0.40	2.55	0.00	0.39	0.25	3.03
Ab	5.80	92.60	24.97	96.89	3.84	98.99	9.95	95.60
Or	93.92	1.30	74.63	0.56	96.16	0.62	89.79	1.37
T (°C)	374		523		272		423	

Note:  $T$  is pre-exsolution temperature which were based on the calculation method of Elkins and Grove (1990) using the program SOLVICALC (Wen and Nekvasil, 1994).

In this study, geothermometer was calculated using the equilibrium relation of hornblende-plagioclase as suggest by Holland and Blundy (1994) which is suitable for samples in the range of 400-1,000 °C and 1-15 kbar. The equation was described below.

*Edenite-tremolite thermometer (for assemblages with quartz)*

$$T = \frac{-76.95 + 0.79P + Y_{ab} + 39.4X_{Na}^A + 22.4X_K^A + (41.5 - 2.89P) \cdot X_{Al}^{M2}}{-0.0650 - R \cdot \ln\left(\frac{27 \cdot X_{Si}^A \cdot X_{ab}^{plag}}{256 \cdot X_{Na}^A \cdot X_{Al}^{T1}}\right)} \quad (\text{Holland and Blundy, 1994})$$

Where the  $Y_{ab}$  term is given by: for  $X_{ab} > 0.5$  then  $Y_{ab} = 0$

$$\text{Otherwise } Y_{ab} = 12.0(1 - X_{ab})^2 - 3.0 \text{ kJ}$$

$$X_{Si}^{T1} = (\text{Si} - 4)/4$$

$$X_{Al}^{T1} = (8 - \text{Si})/4$$

$$X_{Al}^{M2} = (\text{Al} + \text{Si} - 8)/2$$

$$X_K^A = K$$

$$X_{\blacksquare}^A = 3 - \text{Ca} - \text{Na} - K - \text{cm}$$

$$X_{Na}^A = \text{Ca} + \text{Na} + \text{cm} - 2$$

Based on mineral chemistry of hornblende and plagioclase, the geobarometer of syenitic rocks from the Tha Takiap and the Mae Yan areas yield 3.10-4.00 kbar (average=3.4 kbar, rim= 3.16-3.85 kbar, core= 3.10-4.00 kbar) and 3.09-6.49 kbar (average=4.9 kbar, rim= 3.09-5.27 kbar, core= 4.17-6.49 kbar), respectively (Table 4.4 and 4.5). The geothermometer of syenitic rocks from the Tha Takiap and the Mae Yan areas yield 680-750 °C and 815-930 °C, respectively. The geothermobarometry indicates that syenite from the Mae Yan area was crystallized in higher pressure and temperature than the Tha Takiap area.

#### **Two-feldspar thermometry**

Mineral chemistry of feldspar pairs in perthite were used to determine minimum pre-exsolution temperatures. In this study, two-feldspar thermometry was calculated and illustrated using SOLVCALC program (Wen and Nekvasil, 1994) (Fig. 4.11). Isotherms of the solvus were calculated using the Margules parameters of Elkins and Grove (1990) which is suitable for low-pressure conditions. Syenitic rock from Tha Takiap area yields minimum pre-exsolution temperatures of 300-500 °C at 3.4 kbar, while Mae Yan area yields minimum pre-exsolution temperatures of 270-520 °C at 4.9 kbar.

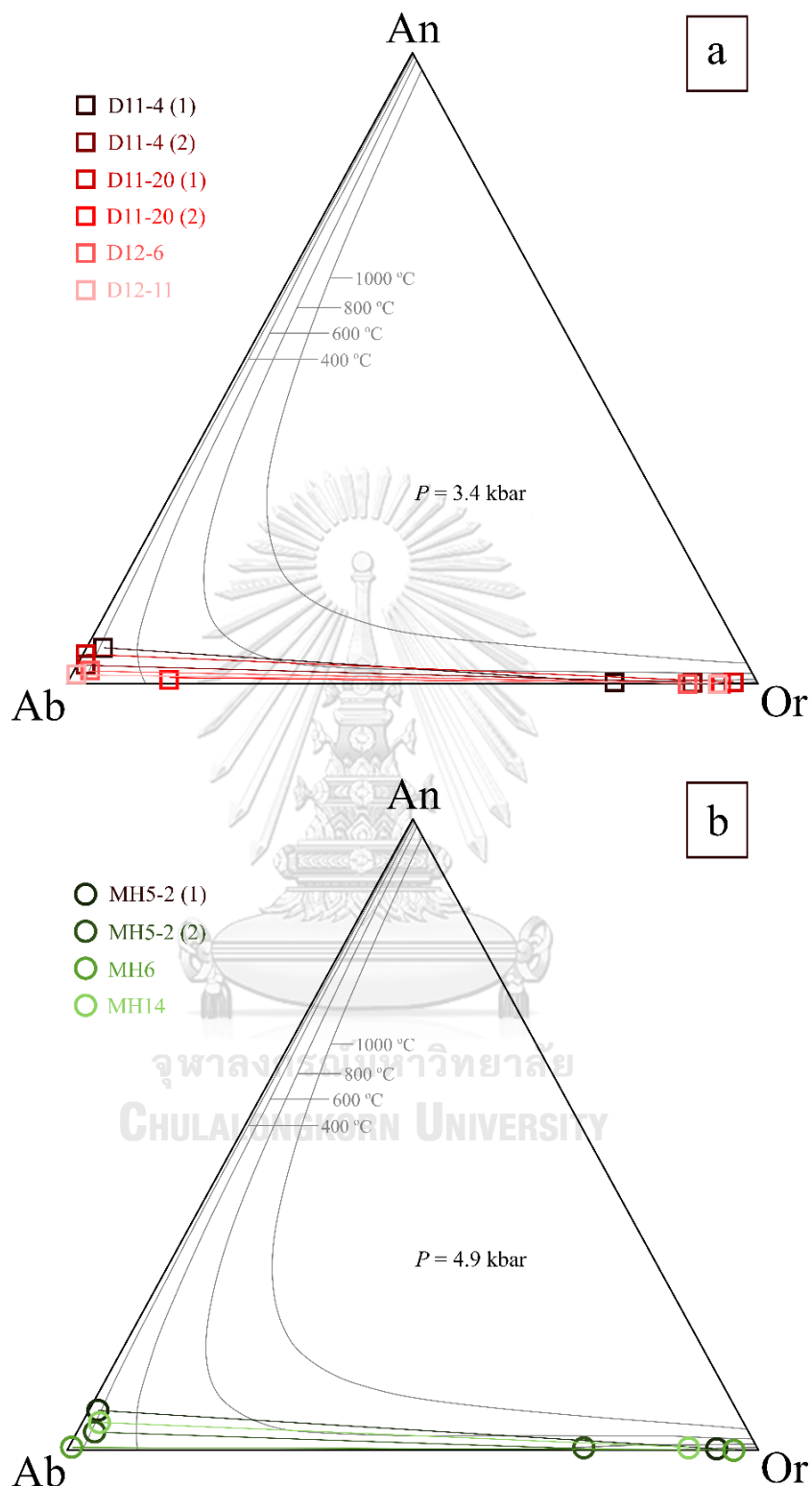


**Fig. 4.11** Ternary feldspar plot of feldspar pairs in perthite of syenitic rocks. Isotherms of the solvus were calculated with the Margules parameters of Elkins and Grove (1990) using SOLVCALC program (Wen and Nekvasil, 1994); **(a)** feldspar pairs in perthite of syenitic rocks from Tha Takiap area which were calculated by  $P=3.4$  kbar; **(b)** feldspar pairs in perthite of syenitic rocks from Tha Takiap area which were calculated by  $P=4.9$  kbar.

## CHAPTER 5

### DISCUSSION AND CONCLUSION

Base on the petrography and geochemistry that were described in Chapter 3 and Chapter 4, the petrogenesis and the tectonic implication of the studied syenites are discussed below.

#### 5.1 Petrogenesis

Alkaline plutons have been reported with limited exposures of small plutons in Thailand and Malaysia, and they are reported to occur in a few areas within the Central Granitic Belt in the Northern Thailand, and the Eastern Granitic Belt in the Eastern Malay Peninsula (Ng, Chung, et al., 2015; Ng, Whitehouse, et al., 2015). Alkaline plutonic rocks are unsuitable to be categorized by I- and S-type classification scheme (Bonin, 2007; Eby, 1990; Whalen et al., 1987), but they are generally classified into A-type granite (Litvinovsky et al., 2002; Litvinovsky, Jahn, and Eyal, 2015). Moreover, A-type granite can be separated into two subdivisions using chemical data which indicate different sources and tectonic settings. Eby (1990, 1992) reported that the subdivisions are, 1) A<sub>1</sub>-anorogenic; It was emplaced in continental rifts or during intraplate magmatism resulting of their chemical data near oceanic island basalt, and 2) A<sub>2</sub>-post-orogenic; It was emplaced after continental-continental collision or island arc magmatism resulting of their chemical data among continental crust to island arc basalt. Corresponding with geochemical composition-based classification for granite of Frost and Frost (2011) who proposed ferroan granite is congruent to A-type granite that can be divided into two originated models, partial melting of quartzo-feldspathic crust and differentiation of tholeiite.

Plutonic rocks in Tha Takiap and Mae Yan areas mainly consist of K-feldspar, hornblende, and a small amount of quartz, plagioclase and pyroxene that were plotted in QAPF diagram ranging from alkaline feldspar syenite to alkaline feldspar quartz syenite. Their characteristics are different from typical granitic rocks of the Eastern Granitic Belt which mainly comprises of medium- to coarse-grained equigranular crystals of various compositions ranging from syenogranite to gabbro (Department of Mineral Resources, 2014), and Central Granitic Belt which is medium- to coarse-grained with large K-feldspar megacryst, ranging in composition from syenogranite to

monzogranite and to quartz monzonite (Department of Mineral Resources, 2014). Riebeckite (Blue colored amphibole) is usually found as an accessory mineral in syenitic rock from the Mae Yan area that corresponds to geochemical data of major oxides in TAS diagram (Cox et al., 1979) (Fig. 4.2) and  $\text{Na}_2\text{O}+\text{K}_2\text{O}-\text{CaO}$  versus  $\text{SiO}_2$  (wt%) diagram (Frost et al., 2001) (Fig. 4.5b), which indicate that syenitic rocks from both areas are related with alkaline magmatism.

According to petrographic and geochemical results, the Tha Takiap and Mae Yan syenitic rocks were related to alkaline magmatism and were classified as A-type granite of A<sub>2</sub> subtype. However, based on petrographic study, the syenitic rock of both areas are slightly different. Pyroxene in syenitic rock from Tha Takiap area exhibits overgrowth of hornblende at the rim indicating magma evolve, and is related to negative anomalies of Eu which suggests that plagioclase and/or K-feldspar might retain in the source from the partial melting or removed during the magma evolution process. Syenitic rocks from Mae Yan area contains significant amount of accessory mineral, especially monazite that corresponded to the enrichment of Th, U and LREE as recognized in trace elements and REE spider diagrams.

Significant anomalies in primitive mantle normalized spider diagrams, such as positive anomalies of Ta that reflect upper oceanic crust magma source, positive anomalies of U and Pb that reflect continental crust magma source and flat chondrite-normalized REE patterns can be observed in syenitic rock from Tha Takiap that indicate the influence of both crust-derived and mantle-derived magmatism. In contrast, the strong influence of crust-derived magmatism, such as positive anomalies of Th, U and Pb in primitive mantle normalized spider diagrams, and the enrichment of LREE in chondrite-normalized REE patterns were observed in syenitic rock from the Mae Yan area.

Based on Rb versus Y+Nb plot (Fig. 5.1a) suggested by Pearce (1996), the Tha Takiap syenitic rocks show higher concentration of Y+Nb, as most of their plots are fallen into within-plate granite field which are typically associated to continental rift and/or ocean island setting. This result indicates that more enrichment of mantle source is involved in alkaline magma of the Tha Takiap syenitic rocks than Mae Yan syenitic rocks which fall on boundary of within post-collisional, syn-collisional and within-plate granite fields. However, post-collision related magmatism can be influenced by mantle-

derived and crustal assimilation depending on pre-collision history, and sometimes can be merged with within-plate granite (Pearce, 1996). Furthermore, Rb-Hf-Ta triangular plot (Fig. 5.1b) suggested by Harris, Pearce, and Tindle (1986) presents that most of the Tha Takiap syenitic rocks fall within within-plate field which is typically related to alkaline magmatism environment, might be caused by post-collision rift tectonics, while most of Mae Yan syenitic rocks fall within volcanic arc which could be derived from pre-collision volcanic arc.

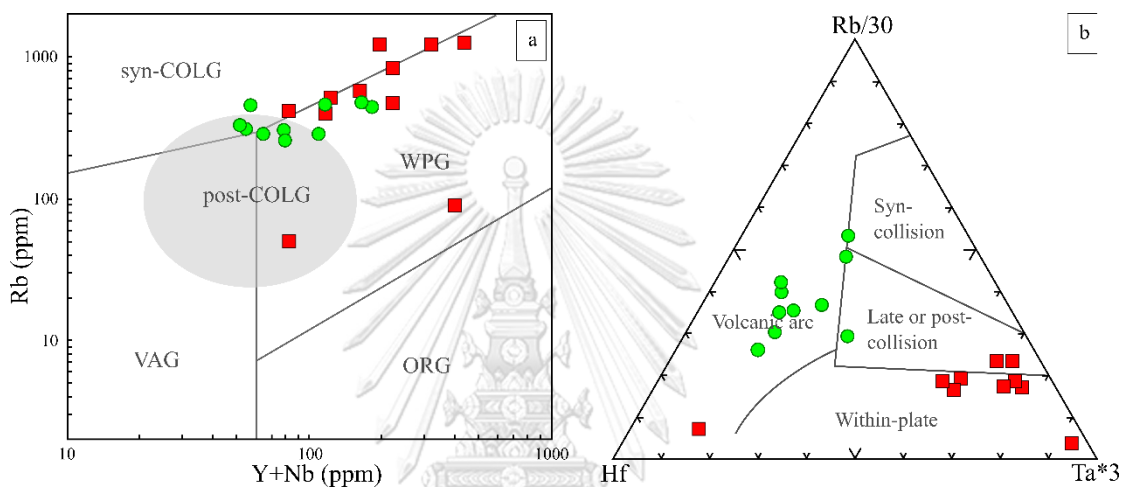


**Fig. 5.1** Discrimination diagrams for tectonic interpretation; (a) Rb versus (Y+Nb) bivariate plot after Pearce (1996) of Tha Takiap syenitic rocks and Mae Yan syenitic rocks; syn-COLG=syn-collisional granite; post-COLG=post-collisional granite; WPG=within-plate granite; VAG=volcanic arc granite; ORG=ocean ridge granite. (b) Rb-Hf-Ta triangular plot after Harris et al. (1986) of Tha Takiap syenite and Mae Yan syenite (Red square is syenitic rocks from Tha Takiap area, green circle is syenitic rocks from Mae Yan area).

The primitive mantle normalized and chondrite-normalized REE spider diagrams of syenitic rocks from both areas were compared with other research data to confirm magmatic source and related tectonic setting (Fig. 5.2). Similar trace element and REE spider diagrams of the Tha Takiap syenitic rocks have been observed in Xiaolonghe granite of the Tanchong-Lianghe tin belt, southwestern China (Fig. 5.2a-b) which is A-type granite and formed by the extensional regime after microplate collision or back-arc extension-related (Chen et al., 2015). On the other hand, similar trace element and REE spider diagrams of the Mae Yan syenitic rocks have been observed in post-collisional potassic rock in Xungba basin, southern Tibet (Fig. 5.2c-d) that was resulted from partial melting of the thickened lower crust and mixing with ancient Lhasa



basement rocks under the extensional tectonic condition (Liu et al., 2014). As a result, it is considered that the most suitable tectonic setting of Tha Takiap syenitic rocks are related to back-arc extension that is mainly influenced by mantle-derived magmatic sources. However, magma mixing between crust and mantle-derived origins is also found. In contrast, Mae Yan syenitic rocks are thought to be related to extension tectonic of post-collision that mainly influenced by crust-derived magmatic sources.

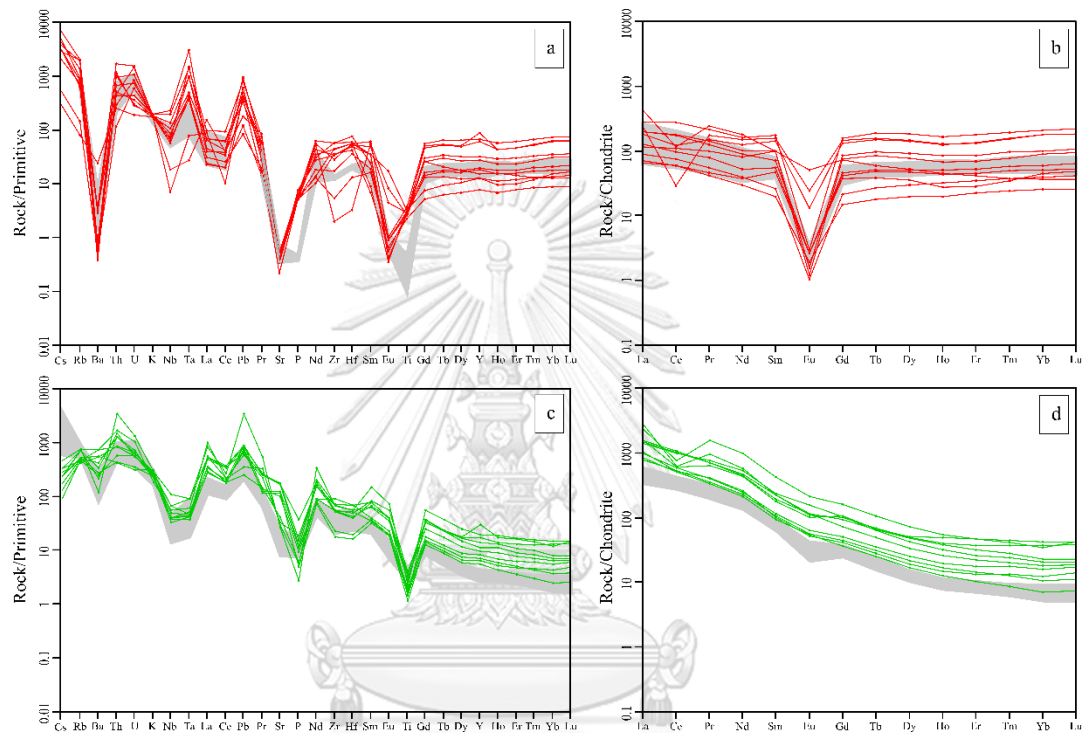


**Fig. 5.2** Spider diagrams of syenitic rocks in the study areas plotted using normalized values of Sun and McDonough (1989). **(a, b)** Primitive mantle-normalized spider diagrams and chondrite-normalized REE patterns of the Tha Takiap syenitic rocks, respectively, in comparison with data from Xiaolonghe granite which is extensional regime after microplate collision or back arc extension related A-type granite from Chen et al. (2015) presented as shade patterns. **(c, d)** Primitive mantle-normalized spider diagrams and chondrite-normalized REE patterns of the Mae Yan syenitic rocks, in comparison with data from post-collisional potassic rocks in southern Tibet from Liu et al. (2014) presented as shade patterns.

## 5.2 Tectonic Implication

This study's geochemical results suggest that syenitic rocks of Tha Takiap was formed in back-arc extension tectonic setting, and the age of syenitic rocks are Late Permian (ca. 260 Ma; Paipana (2014)). The extension tectonic and timing can be compared to tectonic setting in this region as back-arc extension of Nan-Uttaradit-Sa Kaeo Suture on the east of Sukhothai Arc. Nan-Uttaradit Suture in northern Thailand

was reported to have the oldest zircon U-Pb ages of  $311\pm 10$  and  $316\pm$  Ma from gabbro and meta-basalt representative of ophiolite (Yang et al., 2016), while amphibolites, metagabbro and plagiogranite of ophiolite suite at Pailin in West Cambodia suggest that Sa Kaeo Suture had formed as back-arc extension during 270-285 Ma. Besides, continental crust influence could be related to Sukhothai Arc that was active during 214-266 Ma (Gardiner et al., 2016; Ng, Whitehouse, et al., 2015; Wang et al., 2016; Khin Zaw et al., 2014). Schematic diagram of tectonic setting was shown in Fig. 5.3.

On the other hand, syenitic rocks from Mae Yan area were interpreted to have formed under post-collision condition. It is located on the western margin of Central Granitic Belt which is related to continental-continental collision under the closure of Paleo-Tethys during 198-225 Ma (Gardiner et al., 2016; Ng, Whitehouse, et al., 2015; Wang et al., 2016). However, the age of syenitic rocks are Late Cretaceous age (ca. 72 Ma; Duangkhamawat (2015)). Bonin (2007) suggested that post-collision A-type granite of Central Granite Belt should be ranged between 25-60 Ma, which is younger than collision evidence. Therefore, it is more reasonable to conclude that syenitic rocks from Mae Yan area is related to Western Granitic belt which had active orogenic event (arc subduction-collision) during 75-130 Ma (Gardiner et al., 2015; Nakapadungrat and Putthapiban, 1992) (Fig. 5.3).

### 5.3 REE Potential

Base on the petrography and geochemistry of syenitic rocks from Tha Takiap and Mae Yan areas were similar and classified as A-type syenitic rock of A<sub>2</sub> subtype. However, the variation of tectonic setting and magmatism source cause of the variation of REE concentration in syenitic rocks from the both areas.  $\Sigma\text{REE}+\text{Y}$  content of syenitic rocks from Tha Takiap ranges from 128 to 830 ppm with a ratio of LREE/HREE ranges from 1.56 to 6.57, and Mae Yan area range from 705 to 1,890 ppm with ratio of LREE/HREE ranges from 19.37 to 40.14. Consequently, syenitic rocks from Mae Yan area could be a better and good source for REE deposits. A significant amount of monazite could be a source of REE in Mae Yan syenitic rocks which show the enrichment of LREE and depletion of HREE. However, high ratio of LREE/HREE could decrease the interesting of them. Moreover, further study about REE-bearing minerals and the extraction of REE from REE-bearing minerals are necessary to confirm the potential of REE.

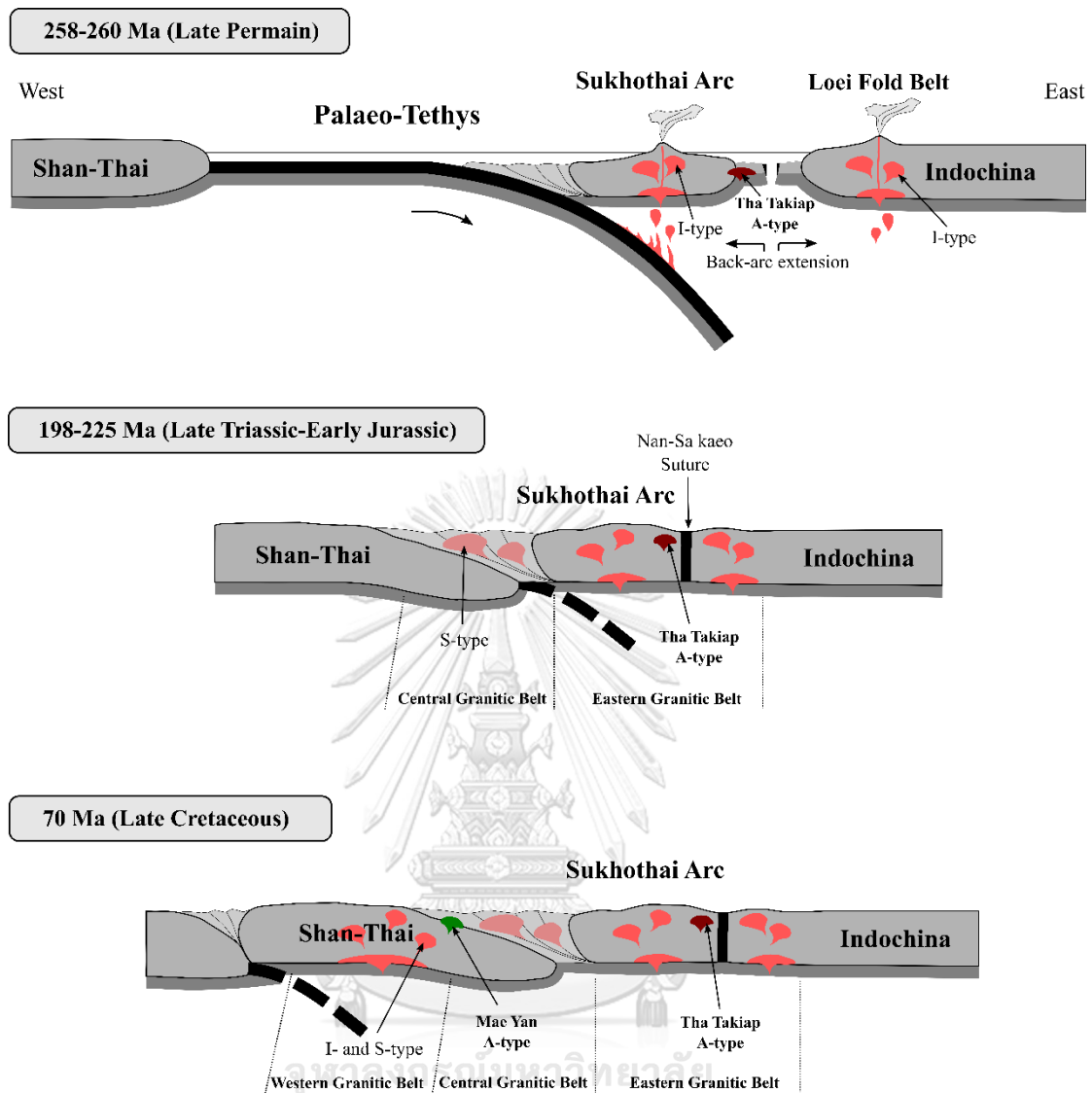


**Fig. 5.3** Schematic diagram showing reconstructed tectonic evolution and magmatism in the Tha Takiap and Mae Yan areas during Late Permian to Late Cretaceous (modified after Barber, Ridd, and Crow (2011); Salam et al. (2014); Sone and Metcalfe (2008)).

#### 5.4 Conclusion

1. Based on the petrographic and geochemical data collected in this study, the plutonic rocks in the Tha Takiap and Mae Yan areas were classified as syenitic rocks.
2. Both syenites of the Tha Takiap and Mae Yan areas can be assigned as A-type granite using I-, S- and A-type classification scheme of Whalen et al. (1987), and both syenites are further subdivided into A<sub>2</sub> subtype in classification diagrams of Eby (1992), suggesting that the alkaline magmatism responsible

for the syenites was formed as a result of post-orogenic event of continental collisions or island arc magmatism.

3. Trace element and REE spider diagrams reflect the different source of syenitic rocks in the Tha Takiap and Mae Yan area. Flat pattern of REE spider diagrams of Tha Takiap syenitic rocks reflect the possibility of mantle-derived magmatic source more than the arc-derived magmatic source. However, some positive anomalies of trace element related to continental crust were also found. In addition, Tha Takiap syenitic rocks share similarity of trace elements and REE spider diagrams of Xiaolonghe granite, and thus the most suitable origination of Tha Takiap syenitic rocks are related to back-arc extension tectonic. In contrast, Mae Yan syenitic rocks show steep pattern of REE spider diagrams and negative anomalies of Nb, Ta, and Ti and positive anomalies of Th, U, and Pb that are related to continental crust source and indicate subduction-related magmatism. Similarity of trace element and REE spider diagrams of post-collisional potassic rock in Xungba basin was also found. Therefore, the most suitable origination of Mae Yan syenitic rocks is the result from partial melting of the thickened lower crust and mixing with basement rocks under the extensional tectonic condition.
4. Incorporated with reported LA-ICP-MS zircon U-Pb age data of the syenites in the study areas and correlation with established regional tectonic setting, the syenite at the Tha Takiap area (260 Ma) is interpreted to have formed at back-arc of Late Permian east-dipping arc magmatism along the Sukhothai Arc, which was associated with the closure of Paleo-Tethys between the Sibumasu and Indochina Terranes. In contrast, Cretaceous syenite in the Mae Yan area (72 Ma) can be a part of the Western Granite Belt, and it is likely to have formed in post-collisional environment of collisional event between West Myanmar and Sibumasu Terrane.
5. Mae Yan syenitic rocks which are classified as A-type granite are enriched in REE and could be a good potential for REE deposits, while Tha Takiap syenitic rocks which are also classified as A-type granite show the low concentration of REE.

### 5.5 Recommendations for future works

1. Further study about the isotope could confirm the magmatic source and tectonic implication of both syenitic rocks in a part of petrogenesis.
2. The granitic rock in the adjacent area of Tha Takiap and Mae Yan area should be collected for further study to compare with syenitic rocks from Tha Takiap and Mae Yan area.
3. Advanced instrument such as SEM and LA-ICP-MS should be used to clarify REE-bearing mineral or REE deposits form in syenitic rocks from Mae Yan area to confirm the potential of REE.



## REFERENCES

- Bao, Z., and Zhao, Z. 2008. Geochemistry of mineralization with exchangeable REY in the weathering crusts of granitic rocks in South China. Ore Geology Reviews 33: 519-535.
- Barber, A. J., Ridd, M. F., and Crow, M. J. 2011. The origin, movement and assembly of the pre-Tertiary tectonic units of Thailand. In M. Ridd, A. Barber, and M. Crow (eds.), The Geology of Thailand, pp. 507-537. London: Geological Society.
- Barr, S. M., and Macdonald, A. S. 1991. Toward a Late Palaeozoic-Early Mesozoic tectonic model for Thailand. Journal of Thai Geosciences 1: 11-22.
- Beckinsale, R. D. 1979. Granite magmatism in the tin belt of South-east Asia. In M. P. Atherton, and J. Tarney (eds.), Origin of Granite Batholiths: Geochemical Evidence Based on a meeting of the Geochemistry Group of the Mineralogical Society, pp. 34-44. UK: Shiva Publishing Limited.
- Beckinsale, R. D., Suensilpong, S., Nakapadungrat, S., and Walsh, J. N. 1979. Geochronology and geochemistry of granite magmatism in Thailand in relation to a plate tectonic model. Journal of the Geological Society 136: 529-540.
- Bonin, B. 2007. A-type granites and related rocks: Evolution of a concept, problems and prospects. Lithos 97: 1-29.
- Bunopas, S. 1981. Paleogeographic history of Western Thailand and adjacent parts of Southeast Asia - A plate tectonics interpretation. Ph.D. thesis. Victoria University of Wellington, New Zealand.
- Bunopas, S., and Vella, P. Late Palaeozoic and Mesozoic structural evolution of northern Thailand a plate tectonic model. In P. Nutalaya (ed.), Bangkok, November, 1978. pp. 133-140.
- Bunopas, S., and Vella, P. 1983. Tectonic and geologic evolution of Thailand.
- Chappell, B. W., and White, A. J. R. 1974. Two contrasting granite types. Pacific Geology 8: 173-174.
- Charusiri, P., Clark, A. H., Farrar, E., Archibald, D., and Charusiri, B. 1993. Granite belts in Thailand: Evidence from the  $^{40}\text{Ar}/^{39}\text{Ar}$  geochronological and geological syntheses. Journal of Southeast Asian Earth Sciences 8(1-4): 127-136.
- Chauviroj, S., and Chaturongkawanich, S. 1985. Geology of Amphoe Pai, Technical report NO. T-07-2-0045-85/GEOL. Bangkok, Thailand: Department of Mineral Resources. [in Thai]
- Chen, X.-C., Hu, R.-z., Bi, X.-W., Zhong, H., Lan, J.-B., Zhao, C.-H., and Zhu, J.-J. 2015. Petrogenesis of metaluminous A-type granitoids in the Tengchong–Lianghe tin belt of southwestern China: Evidences from zircon U–Pb ages and Hf–O isotopes, and whole-rock Sr–Nd isotopes. Lithos 212-215: 93-110.
- Cobbing, E. J. 2011. Granitic rocks. In M. F. Ridd, Barber, A.J. and Crow, M. J. (ed.), The Geology of Thailand, pp. 441-457. London: Geological Society.
- Cobbing, E. J., Mallick, D. I. J., Pitfield, P. E. J., and Teoh, L. H. 1986. The granites of the Southeast Asian Tin Belt. Journal of the Geological Society 143: 537-550.

- Cobbing, E. J., Pitfield, P. E. J., Darbyshire, D. P. F., and Mallick, D. I. J. 1992. The Granites of the South-East Asian tin belt. Overseas Memoir 10. British Geological Survey.
- Cox, K. G., Bell, J. D., and Pankhurst, R. J. 1979. The Interpretation of Igneous Rocks. London: George Allen and Unwin.
- Darbyshire, D. P. F. 1988. South-east Asia granite project-Geochronology of Thai granite. London: National Environment Research Council, Isotope Geology Center.
- Department of Mineral Resources. 2003. Report of Mineral Resources Exploration and Evaluation Project: Area 4/2001 "Bo Thong". Bangkok, Thailand: Department of Mineral Resources. [in Thai]
- Department of Mineral Resources. 2014. Geology of Thailand. Bangkok, Thailand: Department of Mineral Resources, Ministry of Natural Resources and Environment.
- Duangkhamsawat, J. 2015. Petrochemistry and Mineralization of Doi Kio Lom Igneous Rocks, Pai District, Mae Hong Son Province. M.Sc. thesis. Department of Geology, Chiang Mai University.
- Duangkhamsawat, J., and Srichan, W. Petrography of Granitic Rocks from the Doi Kio Lom Area, Pai District, Mae Hong Son Province, Northern Thailand. In Chiang Mai University, Thailand, 20 December 2013, 2013. pp. 155-160.
- Eby, G. N. 1990. The A-type granitoids: A review of their occurrence and chemical characteristics and speculations on their petrogenesis. Lithos 26: 115-134.
- Eby, G. N. 1992. Chemical subdivision of the A-type granitoids: Petrogenetic and tectonic implications. Geology 20: 641-644.
- Elkins, L. T., and Grove, T. L. 1990. Ternary feldspar experiments and thermodynamic models. American Mineralogist 75: 544-559.
- Fanka, A., Tsunogae, T., Daorerk, V., Tsutsumi, Y., Takamura, Y., and Sutthirat, C. 2018. Petrochemistry and zircon U-Pb geochronology of granitic rocks in the Wang Nam Khiao area, Nakhon Ratchasima, Thailand: Implications for petrogenesis and tectonic setting. Journal of Asian Earth Sciences 157: 92-118.
- Frost, B. R., Barnes, C. G., Collins, W. J., Arculus, R. J., Ellis, D. J., and Frost, C. D. 2001. A Geochemical Classification for Granitic Rocks. Journal of Petrology 42(11): 2033-2048.
- Frost, C. D., and Frost, B. R. 2011. On Ferroan (A-type) Granitoids: their Compositional Variability and Modes of Origin. Journal of Petrology 52(1): 39-53.
- Gardiner, N. J., Searle, M. P., Morley, C. K., Robb, L. J., Whitehouse, M. J., Roberts, N. M. W., Kirkland, C. L., and Spencer, C. J. 2018. The crustal architecture of Myanmar imaged through zircon U-Pb, Lu-Hf and O isotopes: Tectonic and metallogenic implications. Gondwana Research 62: 27-60.
- Gardiner, N. J., Searle, M. P., Morley, C. K., Whitehouse, M. P., Spencer, C. J., and Robb, L. J. 2016. The closure of Palaeo-Tethys in Eastern Myanmar and Northern Thailand: New insights from zircon U-Pb and Hf isotope data. Gondwana Research 39: 401-422.

- Gardiner, N. J., Searle, M. P., Robb, L. J., and Morley, C. K. 2015. Neo-Tethyan magmatism and metallogeny in Myanmar – An Andean analogue? Journal of Asian Earth Sciences 106: 197-215.
- Gatinsky, Y. G., and Hutchison, C. S. 1986. Cathaysia, Gondwanaland, and the Paleotethys in the evolution of continental Southeast Asia. Bulletin of the Geological Society of Malaysia 20: 179-199.
- Gill, R. 2010. Igneous Rocks and Processes: A Practical Guide. Malaysia: Wiley-Blackwell.
- Guo, Z., Wilson, M., Zhang, M., Cheng, Z., and Zhang, L. 2015. Post-collisional Ultrapotassic Mafic Magmatism in South Tibet: Products of Partial Melting of Pyroxenite in the Mantle Wedge Induced by Roll-back and Delamination of the Subducted Indian Continental Lithosphere Slab. Journal of Petrology 56(7): 1365-1406.
- Hara, H., Tokiwa, T., Kurihara, T., Charoentitirat, T., Ngamnithiporn, A., Visetnat, K., Tominaga, K., Kamata, Y., and Ueno, K. 2018. Permian–Triassic back-arc basin development in response to Paleo-Tethys subduction, Sa Kaeo–Chanthaburi area in Southeastern Thailand. Gondwana Research 64: 50-66.
- Harris, N. B. W., Pearce, J. A., and Tindle, A. G. 1986. Geochemical characteristics of collision-zone magmatism. Geological Society, London, Special Publications 19: 67-81.
- Hofmann, A. W. 1988. Chemical differentiation of the Earth: the relationship between mantle, continental crust, and oceanic crust. Earth and Planetary Science Letters 90: 297-314.
- Holland, T., and Blundy, J. 1994. Non-ideal interactions in calcic amphiboles and their bearing on amphibole-plagioclase thermometry. Contributions to Mineralogy and Petrology 116(4): 433-447.
- Imai, A., Yonezu, K., Sanematsu, K., Ikuno, T., Ishida, S., Watanabe, K., Pisutha-Armond, V., Nakapadungrat, S., and Boosayasak, J. 2013. Rare Earth Elements in Hydrothermally Altered Granitic Rocks in the Ranong and Takua Pa Tin-Field, Southern Thailand. Resource Geology 63(1): 84-98.
- Jiang, H., Li, W.-Q., Jiang, S.-Y., Wang, H., and Wei, X.-P. 2017. Geochronological, geochemical and Sr-Nd-Hf isotopic constraints on the petrogenesis of Late Cretaceous A-type granites from the Sibumasu Block, Southern Myanmar, SE Asia. Lithos 268-271: 32-47.
- Khin Zaw, Meffre, S., Lai, C.-K., Burrett, C., Santosh, M., Graham, I., Manaka, T., Salam, A., Kamvong, T., and Cromie, P. 2014. Tectonics and metallogeny of mainland Southeast Asia — A review and contribution. Gondwana Research 26: 5-30.
- Leake, B. E., Woolley, A. R., Arps, C. E. S., Birch, W. D., Gilbert, M. C., Grice, J. D., Hawthorne, F. C., Kato, A., Kisch, H. J., Krivovichev, V. G., Linthout, K., Laird, J., Mandarino, J., Maresch, W. V., Nickel, E. H., Rock, N. M. S., Schumacher, J. C., Smith, D. C., Stephenson, N. C. N., Ungaretti, L., Whittaker, E. J. W., and Youzhi, G. 1997. Nomenclature of Amphiboles: Report of the Subcommittee on Amphiboles of the International Mineralogical Association Commission on New Minerals and Mineral Names. European Journal of Mineralogy 9: 623-651.



- Litvinovsky, B. A., Jahn, B.-m., Zanzilevich, A. N., Saunders, A., Poulain, S., Kuzmin, D. V., Reichow, M. K., and Titov, A. V. 2002. Petrogenesis of syenite–granite suites from the Bryansky Complex (Transbaikalia, Russia): implications for the origin of A-type granitoid magmas. Chemical Geology 189: 105-133.
- Litvinovsky, B. A., Jahn, B. M., and Eyal, M. 2015. Mantle-derived sources of syenites from the A-type igneous suites — New approach to the provenance of alkaline silicic magmas. Lithos 232: 242-265.
- Liu, D., Zhao, Z., Zhu, D.-C., Niu, Y., DePaolo, D. J., Harrison, T. M., Mo, X., Dong, G., Zhou, S., Sun, C., Zhang, Z., and Liu, J. 2014. Postcollisional potassic and ultrapotassic rocks in southern Tibet: Mantle and crustal origins in response to India–Asia collision and convergence. Geochimica et Cosmochimica Acta 143: 207-231.
- Metcalf, I. 1984. Stratigraphy, palaeontology and palaeogeography of the Carboniferous of Southeast Asia. Memoirs of the Geological Society of France 147: 107-118.
- Metcalf, I. 1993. Southeast Asian terranes: Gondwanaland origins and evolution. In pp. 181-200.
- Metcalf, I. 2002. Permian tectonic framework and palaeogeography of SE Asia. Journal of Asian Earth Sciences 20: 551-566.
- Metcalf, I. 2011. Tectonic framework and Phanerozoic evolution of Sundaland. Gondwana Research 19: 3-21.
- Metcalf, I. 2017. Tectonic evolution of Sundaland. Bulletin of the Geological Society of Malaysia 63: 27-60.
- Metcalf, I., Henderson, C. M., and Wakita, K. 2017. Lower Permian conodonts from Palaeo-Tethys Ocean Plate Stratigraphy in the Chiang Mai-Chiang Rai Suture Zone, northern Thailand. Gondwana Research 44: 54-66.
- Middlemost, E. A. K. 1975. The basalt clan. Earth-Science Reviews 11: 337-364.
- Mitchell, A. H. G. 1977. Tectonic settings for emplacement of Southeast Asian tin granites. Geol. Soc. Malaysia 9: 123-140.
- Mitchell, A. H. G. 1981. Phanerozoic plate boundaries in mainland SE Asia, the Himalayas and Tibet. Journal of the Geological Society 138: 109-122.
- Nakapadungrat, S., and Putthapiban, P. Granites and Associated Mineralization in Thailand. In C. Piancharoen (ed.), Proceeding of National Conference on Geologic Resources of Thailand: Potential for Future Development, Department of Mineral Resources, Bangkok, Thailand, 17-24 November, 1992. pp. 153-171.
- Nesbitt, H. W., and Young, G. M. 1982. Early Proterozoic climates and plate motions inferred from major element chemistry of Intites. Nature 299: 715-717.
- Ng, S. W.-P., Chung, S.-L., Robb, L. J., Searle, M. P., Ghani, A. A., Whitehouse, M. J., Oliver, G. J. H., Sone, M., Gardiner, N. J., and Roselee, M. H. 2015. Petrogenesis of Malaysian granitoids in the Southeast Asian tin belt: Part 1. Geochemical and Sr-Nd isotopic characteristics. Geological Society of America Bulletin 127(9/10): 1209-1237.
- Ng, S. W.-P., Whitehouse, M. J., Searle, M. P., Robb, L. J., Ghani, A. A., Chung, S.-L., Oliver, G. J. H., Sone, M., Gardiner, N. J., and Roselee, M. H. 2015. Petrogenesis

- of Malaysian granitoids in the Southeast Asian tin belt: Part 2. U-Pb zircon geochronology and tectonic model. Geological Society of America Bulletin 127(9/10): 1238-1258.
- Niu, Y., and O'Hara, M. J. 2009. MORB mantle hosts the missing Eu (Sr, Nb, Ta and Ti) in the continental crust: New perspectives on crustal growth, crust–mantle differentiation and chemical structure of oceanic upper mantle. Lithos 112: 1-17.
- Nualkhao, P., Takahashi, R., Imai, A., and Charusiri, P. 2018. Petrochemistry of Granitoids Along the Loei Fold Belt, Northeastern Thailand. Resource Geology 68(4): 395-424.
- Paipana, S. 2014. Geology and mineralisation characteristics of Bo Thong antimony±gold deposit, Chonburi Province, Eastern Thailand. B.Sc. (Hons) thesis. ARC Center of Excellence in Ore Deposits (CODES), University of Tasmania.
- Pearce, J. 1996. Sources and Settings of Granitic Rocks. Episodes 19(4): 120-125.
- Pitfield, P. E. J. 1988. Report on the geochemistry of the granites of Thailand, BGS Report WC/88/6. Nottingham, United Kingdom: British Geological Survey.
- Qian, X., Feng, Q., Wang, Y., Zhao, T., Zi, J.-W., Udchachon, M., and Wang, Y. 2017. Late Triassic post-collisional granites related to Paleotethyan evolution in SE Thailand: Geochronological and geochemical constraints. Lithos 286-287: 440-453.
- Rice, T. D. 1982. Determination of iron(II) in silicates by gravimetric titration. Analyst 107(1270): 47-52.
- Ridd, M. F. 2015. East flank of the Sibumasu block in NW Thailand and Myanmar and its possible northward continuation into Yunnan: a review and suggested tectono-stratigraphic interpretation. Journal of Asian Earth Sciences 104: 160-174.
- Rudnick, R. L., and Gao, S. 2003. Composition of the Continental Crust. In R. L. Rudnick (ed.), The Crust, pp. 1-64. New York: Elsevier.
- Salam, A., Zaw, K., Meffre, S., McPhie, J., and Lai, C.-K. 2014. Geochemistry and geochronology of the Chatree epithermal gold–silver deposit: Implications for the tectonic setting of the Loei Fold Belt, central Thailand. Gondwana Research 26: 198-217.
- Salvi, S., and Williams-Jones, A. E. 2005. Alkaline granite-syenite deposits. In R. L. Linnen, and I. M. Samson (eds.), Rare Element Geochemistry and Mineral Deposits, GAC Short Course Notes 17, pp. 315-341. Geological Association of Canada.
- Sanematsu, K., Kon, Y., Imai, A., Watanabe, K., and Watanabe, Y. 2013. Geochemical and mineralogical characteristics of ion-adsorption type REE mineralization in Phuket, Thailand. Miner Deposita 48: 437-451.
- Schmidt, M. W. 1992. Amphibole composition in tonalite as a function of pressure: an experimental calibration of the Al-in-hornblende barometer. Contributions to Mineralogy and Petrology 110(2): 304-310.
- Shand, S. J. 1943. Eruptive Rocks: Their Genesis, Composition, Classification, and Their Relation to Ore-Deposits with a Chapter on Meteorite. New York: John Wiley & Sons.

- Smith, J. V., and Brown, W. L. 1988. Feldspar Minerals: Volume 1 Crystal Structures, Physical, Chemical, and Microtextural Properties. New York: Springer-Verlag.
- Sone, M., and Metcalfe, I. 2008. Parallel Tethyan sutures in mainland Southeast Asia: New insights for Palaeo-Tethys closure and implications for the Indosinian orogeny. Comptes Rendus Geoscience 340: 166-179.
- Sone, M., Metcalfe, I., and Chaodumrong, P. 2012. The Chanthaburi terrane of southeastern Thailand: Stratigraphic confirmation as a disrupted segment of the Sukhothai Arc. Journal of Asian Earth Sciences 61: 16-32.
- Streckeisen, A. 1976. To each plutonic rock its proper name. Earth-Science Reviews 12(1): 1-33.
- Sun, S.-s., and McDonough, W. F. 1989. Chemical and isotopic systematics of oceanic basalts: implications for mantle composition and processes. Geological Society, London, Special Publications 42: 313-345.
- Tiyapiract, S. 1996. Geological map of Amphoe Tha Takiap (5335 IV)–1:50,000 Scale[Bangkok, Thailand: Bureau of Geological Survey, Department of Mineral Resources.
- Wang, Y., He, H., Cawood, P. A., Srithai, B., Feng, Q., Fan, W., Zhang, Y., and Qian, X. 2016. Geochronological, elemental and Sr-Nd-Hf-O isotopic constraints on the petrogenesis of the Triassic post-collisional granitic rocks in NW Thailand and its Paleotethyan implications. Lithos 266-267: 264-286.
- Wen, S., and Nekvasil, H. 1994. SOLVALC: An interactive graphics program package for calculating the ternary feldspar solvus and for two-feldspar geothermometry. Computers & Geosciences 20(6): 1025-1040.
- Whalen, J. B., Currie, K. L., and Chappell, B. W. 1987. A-type granites: geochemical characteristics, discrimination and petrogenesis. Contributions to Mineralogy and Petrology 95: 407-419.
- Wilson, M. 1989. Igneous Petrogenesis: A global Tectonic Approach. London: Unwin Hyman.
- Wu, C. 2008. Bayan obo controversy: Carbonatites versus Iron Oxide-Cu-Au-(REE-U). Resource Geology 58: 348-354.
- Yang, W., Qian, X., Feng, Q., Shen, S., and Chonglakmani, C. 2016. Zircon U-Pb geochronological evidence for the evolution of the Nan-Uttaradit suture in northern Thailand. Journal of Earth Science 27(3): 378-390.
- Zhang, P., Mei, L., Hu, X., Li, R., Wu, L., Zhou, Z., and Qiu, H. 2017. Structures, uplift, and magmatism of the Western Myanmar Arc: Constraints to mid-Cretaceous-Paleogene tectonic evolution of the western Myanmar continental margin. Gondwana Research 52: 18-38.

## VITA

**NAME** THANAZ WATCHARAMAI

**DATE OF BIRTH** 19 August 1984

**PLACE OF BIRTH** Bangkok

**INSTITUTIONS ATTENDED** Bachelor of Science in Geology, Chiang Mai University, Thailand

**HOME ADDRESS** 59/67 Moo 5, Khlong Song Sub-District, Khlong Luang District, Pathum Thani, Thailand 12120



จุฬาลงกรณ์มหาวิทยาลัย  
CHULALONGKORN UNIVERSITY